工 學 博 士 學 位 論 文

Mass spectrometry-based glycomic profiling and its applications to α1,3-galactosyltransferase gene-knockout pig in xenotransplantation

질량 분석 기반의 당 프로파일링 및 이종장기이식에서 알파갈 합성효소 유전자 제거 돼지에의 응용

2014 년 8 월

서울大學校 大學院

化學生物工學部

朴 海 珉

Abstract

Glycans are expressed on surface of mammalian cells and tissues, and play important roles in diverse biological functions including cell-cell interaction, signal transduction, metastasis, etc. In xenotransplantation, a galactose-alpha-1,3-galactose epitope, namely α-Gal, is the major carbohydrate xenoantigen that triggers hyperacute rejection (HAR) by the interaction of natural antibodies. Nevertheless, despite of production of α1,3-galactosyltransferase gene-knock out (GalT-KO) pigs as donors, there are still other antigens (e.g., non-Gal antigens) such as Hanganutziu-Deicher (H-D) antigen that induce acute vascular rejection (AVR) or delayed xenograft rejection (DXR) and subsequence xenograft failure.

Mass spectrometry (MS) is a powerful tool for identification and structural elucidation of diverse and complex oligosaccharides. In addition, MS-based quantitative technologies for the oligosaccharide analysis have been developed in recent years. More recently, the improvement of mass spectrometry-based glycomics techniques (i.e. highly sensitive, quantitative and high-throughput analytical tools) has enabled us to obtain a large dataset of glycans.

Cell-based glycomic analysis of WT and GalT-KO pig fibroblasts was performed by using matrix-assisted laser desorption/ionization time-of-flight (MALDI-TOF) MS and MALDI- quadrupole ion trap (QIT)-TOF MS/MS. Total 47 N-glycans from WT and GalT-KO pig fibroblasts were identified and quantified. These results revealed that the level of overall sialylated glycans was higher in GalT-KO pig fibroblasts than WT, and relative quantity of N-glycolylneuraminic acid (NeuGc) antigen, which has been considered as one of non-Gal antigens,

slightly increased in GalT-KO. The result proposed that the targeted knockout of α1,3-galactosyltransferase gene not only result in the removal of Galα1,3Gal residue but also influence sialylated glycan expression including NeuGc antigen.

In the case of the pig tissue, the integrated MS-based glycomic analysis of GalT-KO pig kidney was carried out by MALDI-TOF MS, MALDI-QIT-TOF MS/MS, and electrospray ionization (ESI)-MS and MS/MS. The *N*-glycome derived from GalT-KO pig kidney was identified and quantified, and the result allowed an in-depth comparison of the total N-glycomic profiles between wild-type (WT) and GalT-KO. MS analysis revealed that the relative abundance of sialic acid-containing glycans increased in GalT-KO. The current analysis also enabled a priori identification of N-glycolylneuraminic acid (NeuGc) regarded as one of non-Gal antigens in both WT and GalT-KO, and showed that the NeuGc level was higher in GalT-KO pig relative to WT.

In addition, based on these glycome profiles of pig cells and tissues, a pig glycome database was developed here. The database contains cell- or tissue-specific pig glycomes analyzed with mass spectrometry-based techniques, including the comprehensive pig glycan information on chemical structures, mass values, types and relative quantities. It was designed as a user-friendly web-based interface that allows users to query the database according to pig tissue/cell types or glycan masses. This database provides qualitative and quantitative information on glycomes characterized from various pig cells/organs in xenotransplantation.

Finally, the study on pig glycome-human immune cell interactions was performed by fluorescence-activated cell sorting (FACS) and LC-MS/MS analysis. The *in-vitro* experiment of human immune cell activation against pig glycans, and

the screening and identification of their surface proteins using glycan-immobilized beads were carried out. The results showed no difference associated with human immune cells between WT and GalT-KO pig. However, the more complete characterization of the interaction between pig glycans and human immune cells remained to be improved for the xenotransplantation research.

Key words: Xenotransplantation, GalT-KO pig, N-linked glycan, NeuGc xenoantigen, Pig glycome database, Human immune cell, Mass spectrometry

Student number: 2007-21191

CONTENTS

LIST OF TABLES

LIST OF FIGURES

Chapter 1. Introduction

1.1 Overview of glycosylation in mammalian cells

1.1.1 Glycan structure

Glycan are abundantly expressed on the surface of mammalian cells, and constitute a large complex and diverse repertoire of structures collectively known as the 'glycome' **(Figure 1.1)**. These glycans are classified into three major classes, which are N-linked glycan, O-linked glycan, and glycosphingolipid-derived glycan. The N-linked glycan (abbreviated to N-glycans) is covalently attached to the amine group in the asparagine (Asn) residue side chain. The N-glycosylation site on polypeptides or proteins is determined to the sequon Asn-Xaa-Ser/Thr, where Xaa is any amino acid residue except proline and aspartic acid [1, 2]. N-linked glycans are synthesized and processed as follows. The lipid-linked oligosaccharide precursor is synthesized in the endoplasmic reticulum (ER), and the precursor oligosaccharide ($Glc_3Man_9GlcNAc_2$) is transferred from the lipid donor to the amine group in the protein Asn residue side chain. The core structure of N-linked glycan is composed of $Man_3GlcNAc_2$. Subsequently, N-linked glycans are processed by diverse enzymes (e.g. glycosylhydrolases and glycosyltransferases) in the ER and Golgi apparatus. The assembled N-linked glycan structures are classified into three different types: high-mannose type, complex type, and hybrid type N-linked glycan.

O-linked glycan is most commonly attached to the hydroxyl group of the serine (Ser) or threonine (Thr) residues on proteins. The mucin-type O-glycan, which is the extended structure from a core *N*-acetylgalactosamine (GalNAc) α-linked to the protein, is one of the predominant glycan types. Unlike N-

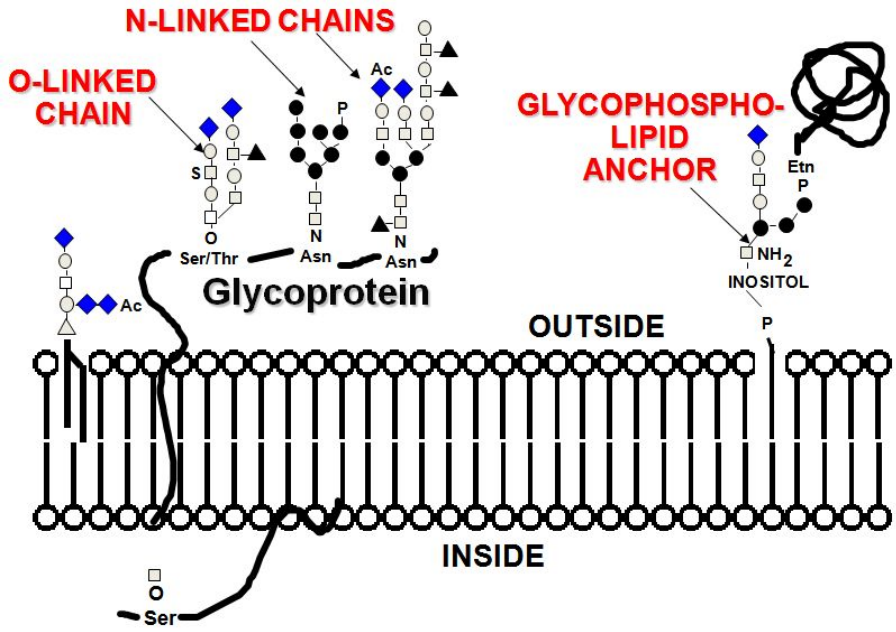

Figure 1.1 Three major glycan classes presented on the surface of mammalian cells: N-linked glycan, O-linked glycan, and glycosphingolipid-derived glycan [3]

glycosylation, there is no consensus sequence at O-glycosylation site on proteins. Protein O-glycosylation takes place in the secretory pathway after N-glycosylation. O-linked glycans are synthesized in a stepwise process, which is initiated by the transfer of N-acetylgalactosamine (GalNAc) to a peptide substrate by specific polypeptide GalNAc transferases (ppGalNAcTs). There are several different core structures of O-linked glycans based on differential monosaccharide linkage reactions **(Figure 1.2)**. Core 1 subtype structure is Galβ1,3GalNAc formed by the transfer of Gal in a β1,3-linkage to the GalNAc. Core 2 subtype structure is GlcNAcβ1,6(Galβ1,3)GalNAc extended from the Core 1 structure by the addition of GlcNAc in β1,6-linkage. Core 3 subtype structure is GlcNAcβ1,3GalNAc formed by the addition of GlcNAc in β1,6-linkage to the GalNAc. Core 4 subtype structure is GlcNAcβ1,6(GlcNAcβ1,3)GalNAc extended from the Core 3 structure by the transfer of GlcNAc in β1,6-linkage. Most O-linked glycans contain a Galβ1,3GalNAc (Core 1) subtype structure.

Glycolipids are synthesized in a stepwise process, similar to the O-linked glycan synthesis. The glycolipid synthesis is initiated by addition of a monosaccharide residue (glucose or galactose) to the sphingosineceramide though a glycolipid-specific glycosyltransferase. The core globoside, ganglioside, and lactoside structures are subsequently synthesized from glucosphingolipids. In contrast, galactosphingolipids form sulfate glycolipids which are attached to one or two additional monosaccharide residues.

1.1.2 Biological functions of glycosylation on cell surface

Protein glycosylation is one of largest and most important post-translational

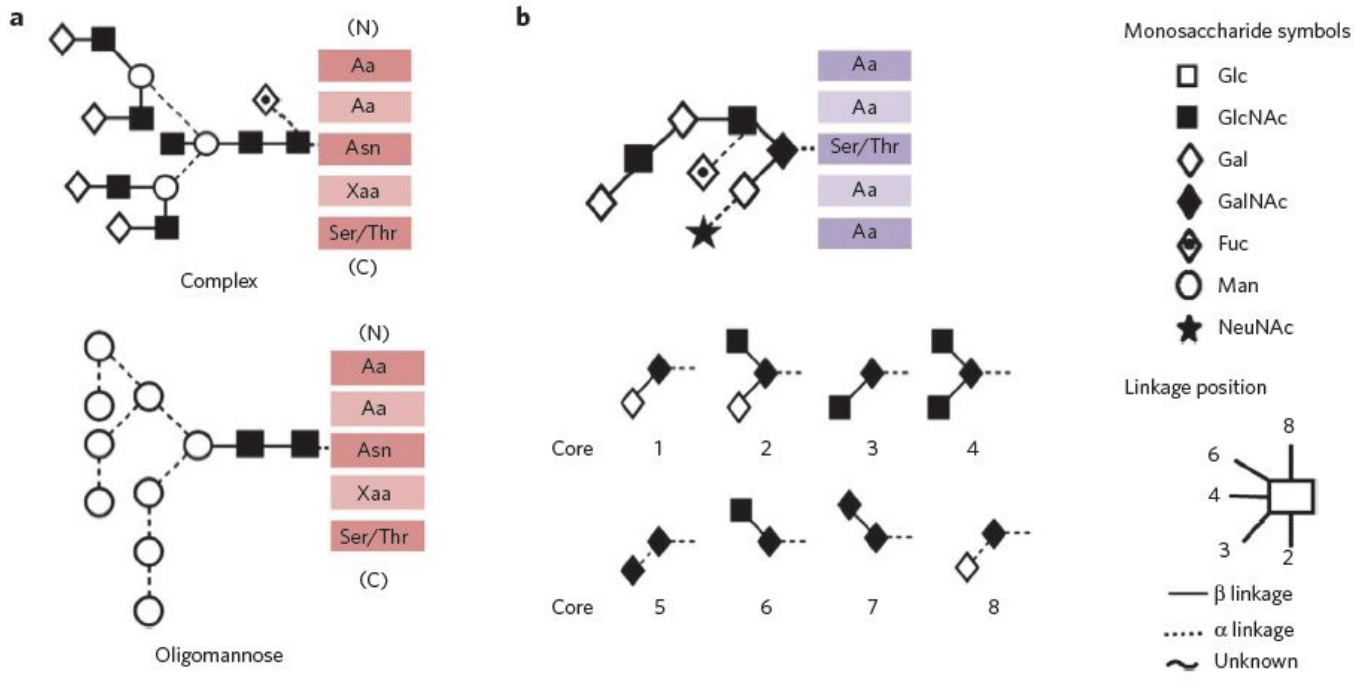

Figure 1.2 Mammalian glycan structures. (a) N-linked glycans attached to Asn of polypeptides or proteins (sequon Asn-Xaa-Ser/Thr), (b) O-linked glycans covalently attached to Ser/Thr of polypeptides or proteins. There are eight different core structures of O-glycans [4]

modifications. The glycosylation plays significant roles in numerous biological processes such as cell development, cell-cell interactions and signaling [5-7], immune response [8, 9], and tumor growth and metastasis [10, 11] etc,. Within the immune system, the interaction between carbohydrate and proteins serve various functions in cell activation, differentiation, and homing **(Figure 1.3)**. There are diverse glycan-binding proteins (GBPs) that recognize specific glycan structures expressed on the surface of mammalian cells **(Figure 1.4)**. Many of GBPs are members of C-type lectin receptor (CLR) family, which are calcium-dependent carbohydrate-binding proteins. These CLRs such as dendritic cell-Specific intercellular adhesion molecule-3-grabbing non-integrin (DC-SIGN), macrophage galactose-specific lectin (MGL), langerin, and mannose receptor recognize fucose-linked glycans (Lewis antigens), GalNAc or GlcNAc epitope, and high-mannose type glycans [12-15]. C-type lectins have functions as pathogen recognition, cell adhesion and signaling receptors [16]. Galectins are a family of proteins that have a specificity for N-acetyllactosamine (Galβ1,4GlcNAc) epitope of carbohydrates by a conserved carbohydrate-recognition domain (CRD) [17, 18] Activated B cells and T cells express these soluble galectins, which participate in the modulation of activated macrophages and regulatory T cells, and thereby produce cytokines [19, 20]. Siglecs are a member of sialic acid-binding immunoglobulin-like lectins, which control cell functions in immune systems. These siglecs are classified into two types based on sequence similarity and evolutionary conservation, which are CD33-related siglecs and siglecs common to mammals [e.g., Sialoadhesin, CD22, myelin-associated glycoprotein (MAG), Siglec-15] [21]. The siglecs are abundantly presented on the surface of various immune cells such as monocytes,

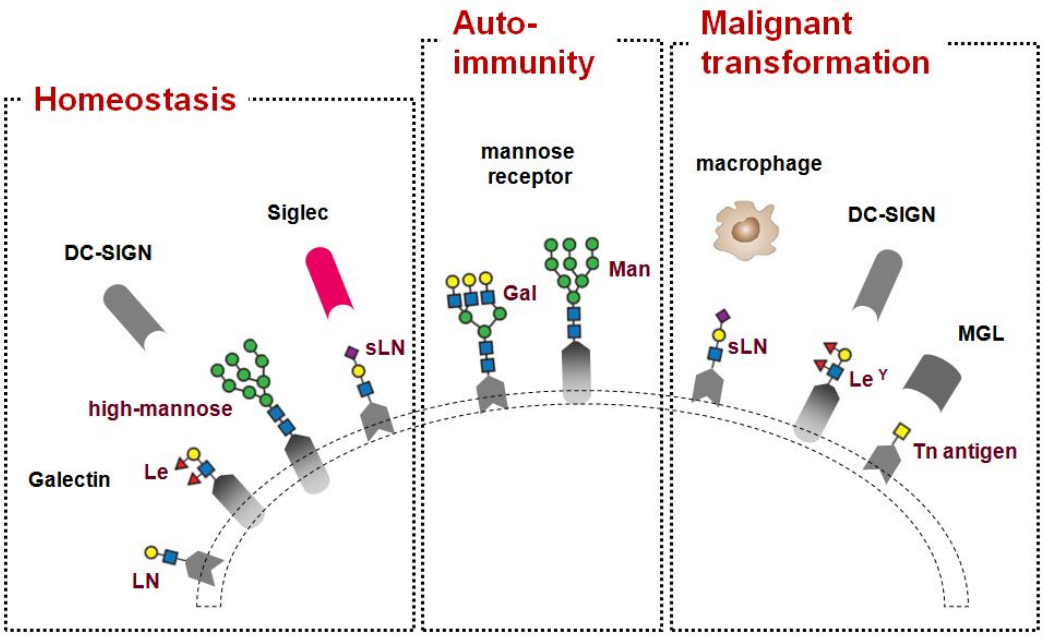

Figure 1.3 The interaction between specific glycans and protein receptors associated with immune system.

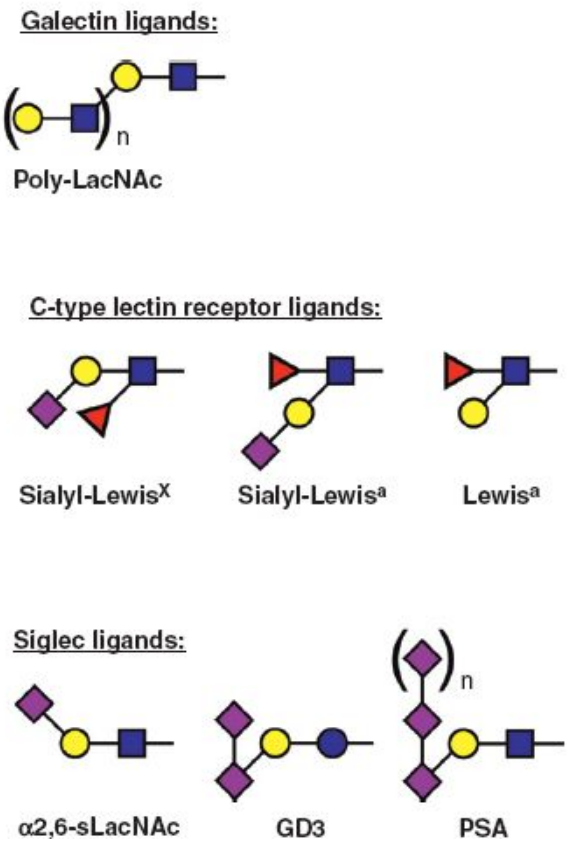

Figure 1.4 Oligosaccharide ligands against the three major lectins (C-type lectins, galectins, and siglecs) in the immune system [22]. The oligosaccharide structures expressed on either host cells or pathogens are recognized by their specific lectins.

dendritic cells, and neutrophils, etc. It has been commonly demonstrated that these glycan-binding proteins have a specificity for sialic acids but can distinguish among sialic acid linkages (α2,3-, α2,6-, and α2,8-linkage) by which the sialic acid residues are linked to the oligosaccharide structure. The molecular interactions between the sialic acid and siglec lead to communication of immune cells. In addition, the siglecs involve in pathogen recognition because sialic acid-terminated sugars are also reported on pathogenic microorganisms including *Helicobacter pylori*, *Campylobacter jejuni*, *Haemophilues influenza*, and *Escherichia coli* [21].

1.2 Glycobiology in xenotransplantation

1.2.1 Xenotransplantation in GalT-KO era

Due to shortage of human donor organs, it has increased the interest in xenotransplantation. The pig, of non-human primates, has been a preferred source as donor because of anatomic and physiologic similarity and ethical acceptance. However, there is strong immune response in pig-to-human xenotransplantation **(Figure 1.5)**. A galactose-alpha-1,3-galactose epitope (α-Gal) is the major carbohydrate xenoantigen expressed on surface of non-human cells and tissues, and triggers HAR to xenograft through the interaction with natural anti-α-Gal antibodies. To solve this problem, GalT-KO pigs, which do not express the α-Gal antigen, have been produced [23-25]. This approach, deletion of α-Gal expression in donors, is one of efficient approaches as a solution to antibody-mediated xenotransplantation rejection **(Table 1.1)**.

However, even after the production of GalT-KO pigs as donors, there still remains non-Gal antigens present on pig cell surfaces. These antigens react with anti-non-Gal antibodies in human sera, and therefore induce AVR or DXR in xenotransplantation [26, 27]. The NeuGc-terminated carbohydrate antigen (e.g. H-D antigen), of non-Gal antigens, has been considered as an important xenoantigen in GalT-KO pig era. Anti-HD antibodies account for a large proportion of total anti-non-Gal antibodies in human sera [28]. Moreover, the targeted disruption of α1,3-galactosyltransferase gene leads to the perturbation of other genes and consequently results in unknown phenotypic effects such as increase or decrease of other xenoantigen levels [29, 30].

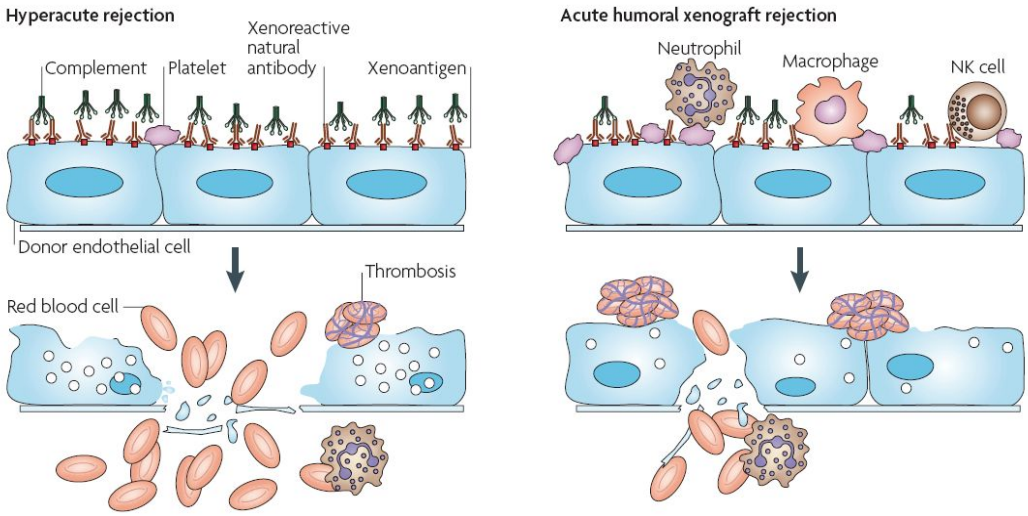

Figure 1.5 Humoral rejection. Immune rejection responses such as HAR and AHXR occured via the interaction between xenoantigens and xenoreactive natural antibodies, and subsequence xenograft failure [31]

Table 1.1 Strategies to overcome antibody-mediated xenotransplantation rejection [31]

Approach	Strategy	Efficacy (short term/long term)
Inhibition of complement activation	Recipient: cobra-venom factor, soluble complement receptor	High/low
	Donor: expression of human complement regulatory protein (CRP) transgenes	High/low
Depletion of α-Gal-specific antibody in recipients	*Ex vivo* haemoperfusion and injection of soluble xenoantigen conjugates	High/low
Accommodation*	Transient depletion of xenoreactive natural antibody or complement	High/unknown
Antithrombosis and/or	Recipient: anticoagulants or antiplatelet agents	Low/low

anticoagulation	Donor: expression of human CD39 and natural anticoagulants	Unknown/ unknown
Reduction or deletion of α-Gal expression in donors	Transgenic expression of human α1,2-fucosyltransferase	Low/low
	α1,3-galactosyltransferase deficiency	High/high
B-cell tolerance*	Induction of mixed chimerism	High/high

*Based on studies in rodent xenotransplantation models.

1.2.2 Immune system in xenotransplantation

In addition to the function of natural antibodies, it has been recently demonstrated that several other elements in innate immune system play an important role in AVR/DXR [32] as shown in **Figure 1.6**. Human natural killer (NK) cells have a direct interaction with non-human cells (e.g. pig cells), and hence mediate xenograft rejection. The NK cells also indirectly participate in xenograft rejection. Li et al. have demonstrated that the NK cells contribute to the production of T-cell independent xenoantibody [33], and Xu et al. have demonstrated that the activated NK cells increase T cell xenoreactivity [34]. A recent study on human macrophage provided evidence that the macrophage recognizes xenogeneic cells via the interaction between human signal-regulatory protein-α (SIRPα) and CD47 (integrin-associated protein), and lead to inhibition of phagocytosis. Monocytes are also one of the most significant inflammatory cells and involve in DXR. It has recently been reported that the α-Gal antigen activates human monocytes via the interaction with human monocyte receptor Galectin-3 [35], suggesting that human macrophage also recognizes the α-Gal antigen because Galectin-3 is expressed on the human macrophage as well as the monocyte. Some studies indicated that human neutrophils can recognize porcine endothelial cells but not allogeneic endothelial cells, and subsequently that express high levels of adhesion molecules. The porcine endothelial cells were previously reported to produce a secreted molecule promoting the adhesion of human neutrophils [36]. This interaction results in NK cell lysis [37, 38], and occurs regardless of α-Gal epitope [39].

1.2.3 Carbohydrate antigens in xenotransplantation

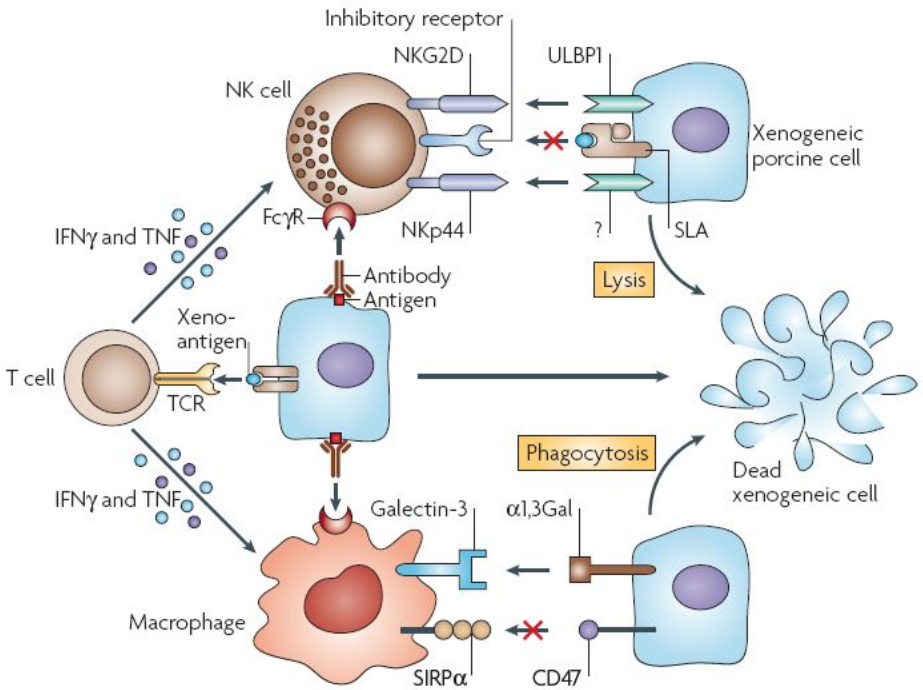

Figure 1.6 Cellular rejection. NK cells and macrophages play a central role in regulation of cellular responses through stimulatory and inhibitory receptors [31].

1.2.3.1 α-Gal antigen in pig tissues

There are several carbohydrate antigens that may be relevant in pig-human xenotransplantation **(Table 1.2)**. As illustrated above, α-Gal antigen (Galα1,3Galβ1,4GlcNAc residue) is regarded as the most vital xenoantigenic carbohydrate expressed on surface of non-human primates, which have the enzyme α1,3-galactosyltransferase (GGTA1) that synthesize the α-Gal antigen. This carbohydrate antigen on xenograft endothelium binds to natural anti-α-Gal antibodies in the sera, and subsequently the interaction activates complement system and coagulation cascades followed by triggering HAR within minutes to hours [40-42].

Although GalT-KO non-human primates were produced for preventing the HAR on xenograft, there has been a controversy over the elimination of α-Gal antigens. A previous study reported that GalT-KO pigs expressed low levels of α-Gal antigen and other α1,3-galactosyltransferase, GGTA2 was reported to synthesize isoglobotriaosylceramide (iGb3; Galα1,3Galβ1,4Glcβ1-ceramide) as an alternative α-Gal antigen candidate in GalT-KO non-human primates [43, 44] suggesting that there are two different glycan processing pathway for the synthesis of Galα1,3Gal disaccharide [45]. Therefore, it is essential to confirm the complete absence of the α-Gal antigen in GalT-KO animals for pre-clinical trial in xenotransplantation.

1.2.3.2 non-Gal antigens

1.2.3.2.1 *N*-glycolylneuraminic acid

The sialic acid is one the most common epitopes of oligosaccharide attached

Table 1.2 Xeno-antigenic carbohydrate structures (α-Gal and non-Gal antigens) found on the cell surface of non-human primates.

xeno-angtigen		structure
α-Gal antigen		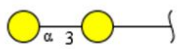
non-Gal antigen	H-D antigen (Hanganutziu-Deicher)	
	Forssman antigen	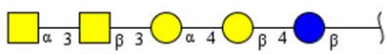
	Tn antigen	
	Sialosyl-Tn antigen	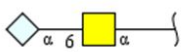

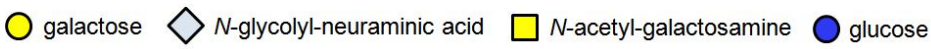

to proteins and lipids. These sialic acids are divided into two major classes, which are N-acetylneuraminic acid (NeuAc) and N-glycolylneuraminic acid (NeuGc). In stark contrast to the NeuAc, which is ubiquitously expressed, the NeuGc antigen is presented in mammalian species such as pigs and monkeys, but absent in human and birds [46-48]. O-acetylated sialic acids were also found in non-human primates such as cow and horse [49], which can be positioned at C4,C7, C8 or/and C9 of the sialic acid structure.

The Hanganutziu-Deicher antigens (H-D antigens), which are glycolids containing the NeuGc xenoantigen, has been regarded as one of the non-Gal antigens in pig organs [50]. NeuGc is mainly synthesized via hydroxylation of NeuAc by CMP-N-actetylneuraminic acid hydroxylase (CMAH) with cytochrome b5 and NADH cofactors [51, 52] **(Figure 1.7)**. Bouhours et al. first identified H-D antigens in pig endothelial cells, and recognized by anti-H-D antibodies in the human serum [53]. Recently, N- and O-linked glycans as well as glycolipids have been reported to contain NeuGc residues on the surface of pig cells and tissues [54-58]. In addition, some studies showed the various expression levels of NeuGc antigens according to the pig organ [29, 59].

In spite of the importance of NeuGc antigenecity, the quantitative measurement of the NeuGc antigens is a difficult task because there is no available lectin which specifically binds to the NeuGc epitope. A recent study reported that quantification of NeuGc was performed by 1,2-diamino-4,5-methylenedioxybenzene (DMB) derivatization of sialic acids [29], but not distinguished the major glycan type such as N- and O-glycans and glycolipid-derived glycans.

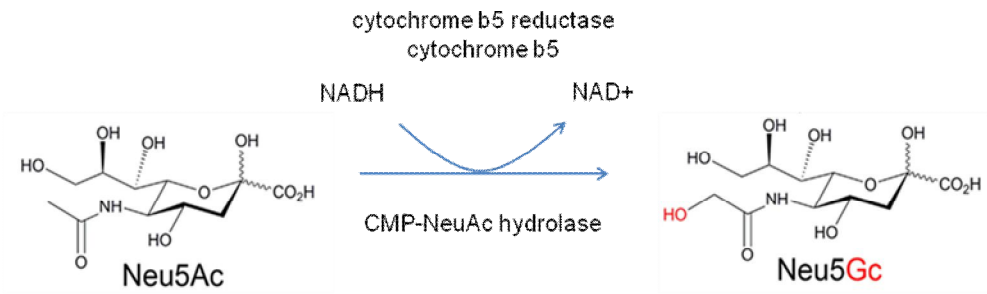

Figure 1.7 Biosynthesis of NeuGc. Hydroxylation of NeuAc by CMP-N-actetylneuraminic acid hydroxylase (CMAH) with cytochrome b5 and NADH cofactors

1.2.3.2.2 Other non-Gal antigens

Some other carbohydrate constituents have been suggested as potential xenoantigens, which may play a role in human immune system on xenotransplantation [60]. Swanson et al. identified Tn (GalNAcα-R) and sialyl-Tn (NeuAcα2-6GalNAcα-R) antigens in porcine red blood cells [61], and Kirkeby et al. characterized Tn antigen in pig kidney [62]. A recent study also detected the Tn antigen expressed on GalT-KO pig endothelial cells as well as fibroblasts [63]. These antigens have been extensively reported to involve in humoral and cellular immune response in human cancer [64, 65]. The preformed natural antibodies specific for these antigens have been found in some humans [65].

Forssman antigen (GalNAcα1-3GalNAcβ1-3Galα1-4Galβ1-4Glcβ1-R) is an non-Gal antigen candidates on pig to human xenograft, which is presented on the cell surface of Forsmann positive species such as pigs, sheep, and hamsters [66]. Although this antigen was expressed on human cancer [67, 68], and anti-Forsmann antibodies were found in normal human sera [69], human has been considered as one of Forsmann positive primates.

1.3 Analytical methodologies in glycobiology

1.3.1 Qualitative glycomic analysis

As described above, the glycosylation plays roles in many cellular processes including cell adhesion, immune response, and signal transduction, etc. Therefore, the analysis of glycan structures is important issue for understanding molecular mechanisms involved in these events. Analytical technology for oligosaccharide sequencing has been developed based on exoglycosidase sequencing and tandem mass spectrometric analysis

1.3.1.1 Exoglycosidase sequencing

Enzymatic glycan analysis using exoglycosidases has been a powerful analytical approach for determination of glycan sequence because the enzyme(s) remove specific terminal monosaccharides (**Figure 1.8)** [70]. Furthermore, the simultaneous digestion of oligosaccharide can be rapidly carried out using various enzyme arrays [71], and subsequently the oligosaccharide fragment products from the sequential exoglycosidases are analyzed by HPLC or MS instruments [55, 56, 72]. To detect oligosaccharides in the HPLC instrument, the reducing end of the oligosaccharides is chemically labeled with fluorescent molecules such as 2-aminobezamide (2-AB) [73]. Structural assignment can be determined by elution positions of the glycan because incremental values are calculated for individual carbohydrate residue from oligosaccharide core structures [72] (**Figure 1.9)**. More recently, a HPLC technology coupled with glycan database which contains glucose unit (GU) values for 2-AB labeled glycans allowed a rapid and structural

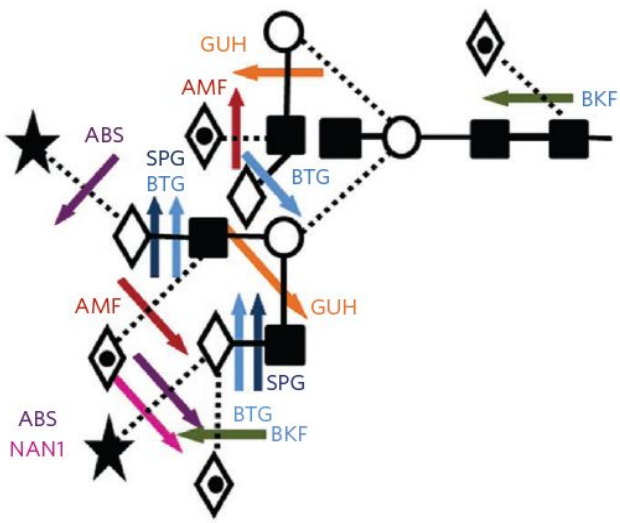

Figure 1.8 Specificities of exoglycosidase digestion for identify glycan structures. ABS: *Arthrobacter ureafaciens* sialidase (EC 3.2.1.18); NAN1: *Streptococcus pneumoniae* sialidase (EC 3.2.1.18); BTG: bovine testes β-galactosidase (EC 3.2.1.23); SPG: *S. pneumoniae* β-galactosidase (EC 3.2.1.23); AMF: almond meal α-fucosidase (EC 3.2.1.51); BKF: bovine kidney alpha-fucosidase (EC 3.2.1.51); GUH: β-*N*-acetylglucosaminidase (EC3.2.1.30). [4]

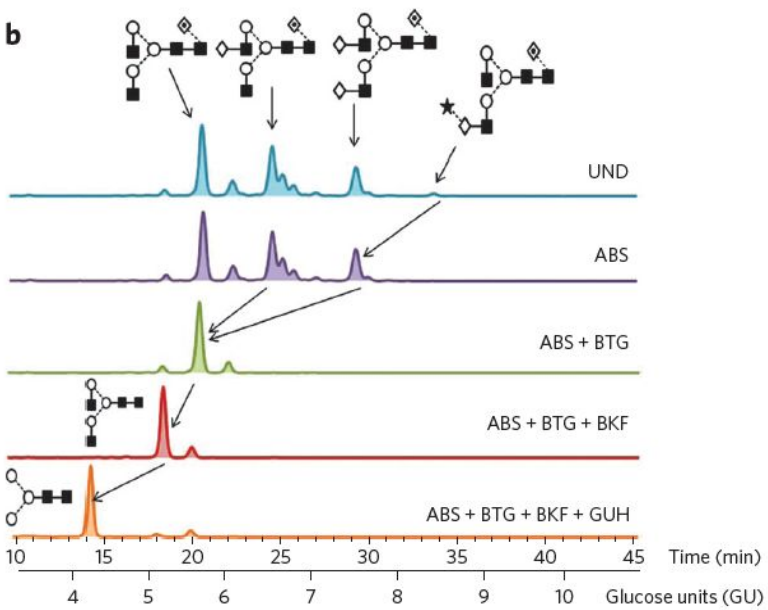

Figure 1.9 HPLC profiles before/after sequential exoglycosidase digestion of N-linked glycans [4]

identification of N-linked glycans as well as quantitation [74]. However, such an HPLC-based analysis has a limitation for the characterization of unknown or unique glycan structures.

1.3.1.1 Tandem mass spectrometric analysis

MS has lead to recent advances in the field of structural glycomics because of its high-performance in mass range, resolution, and sensitivity. Moreover, MS/MS (or MS^n) analysis allowed simultaneous sequencing of oligosaccharides through ion fragmentation processes such as collision induced dissociation (CID) in ESI-MS/MS and MALDI-in source decay (ISD) or post source decay (PSD). Most tandem mass spectrometric analyses have been used by CID, which technique makes precursor ions into a collision cell fragmented by collision with a neutral gas such as Helium (He) and Argon (Ar). The nomenclature for carbohydrate fragment ions [75] is shown in **Figure 1.10**. The fragment ions containing the non-reducing end in oligosaccharides are labeled as A-, B-, C-ions while those containing reducing terminus are indicated as X-, Y-, Z-ions. In contrast to MALDI-TOF MS/MS, which produces more complicated cleavage ions, ESI-MS/MS or MALDI-QIT-TOF MS/MS equipped with ion trap instrumentation yields simple product ions. The mass fragmentation pattern represents predominant B- and Y-ions, which are generated from glycosidic bond cleavage, while cross ring fragment ions (A- and X-ions) are weak or absent. Unlike HPLC analysis, this tandem mass spectrometric analysis allowed the elucidation of unknown or unique oligosaccharide sequences. The alternative fragmentation methods of electron capture dissociation (ECD) and electron transfer dissociation (ETD) have been

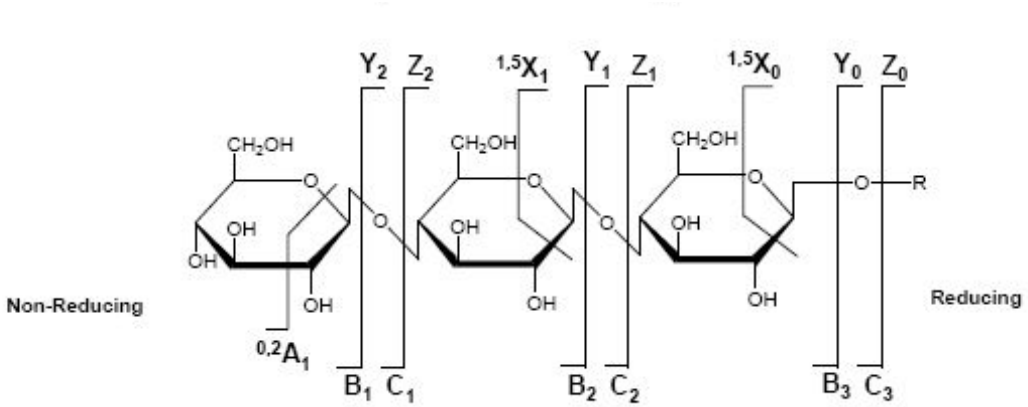

Figure 1.10 Nomenclature for carbohydrate fragmented ions (A-, B-, C- and X-, Y-, Z-ions) proposed by Domon and Costello [75]

recently demonstrated for glycopeptide and other PTM analysis [76-78]. However, these MS/MS techniques generated dissociation resulting in the production of relatively abundant cross-ring cleavage ions that are highly informative for detailed structural identification of sialylated and neutral glycans [79]. A previous study also reported application to glycan analysis using alkali, alkaline earth, and transition metals for increasing ionization efficiency of oligosaccharides [80].

1.3.2 Quantitative glycomic analysis

1.3.2.1 Lectin-based assay and HPLC analysis

A number of studies for oligosaccharide identification of prokaryotic and eukaryotic cells/tissues have used a lectin-based approach [81-83] **(Figure 1.11)**. However, such an approach has a limitation for qualitative and quantitative analysis of glycomes. For example, there are a limited number of lectins which are available, and these lectin-based methods enable the classification of structural oligosaccharide motifs but not the elucidation of the entire chemical structures of oligosaccharides. Furthermore, the quantitative evaluation of glycomes by these methods might be less reliable compared with other analytical methods.

High-performance liquid chromatography (HPLC) analysis combined with fluorescent oligosaccharide labeling is the conventional method for identification and quantification of glycans. Because the carbohydrate has no UV absorbing or fluorophore group, the fluorophore such as 2-aminobenzoic acid (2-AA) and 2-AB [73, 84] was introduced on the reducing end of oligosaccharides as described above, and resulted in sensitive detection of oligosaccharides at the femtomole level [85, 86]. Hydrophilic interaction chromatography (HILIC) provided improved resolution for complex glycan mixtures. Moreover, this analytical technique enabled the separation of oligosaccharide structural isomers which is challenging to other techniques. Nonetheless, these HPLC-based glycan analyses are difficult to identify large and diverse glyconjugates isolated from mammalian cells and tissues because a limited number of oligosaccharide standards are available.

In recent years, mass spectrometry is widely used for analysis of glycans.

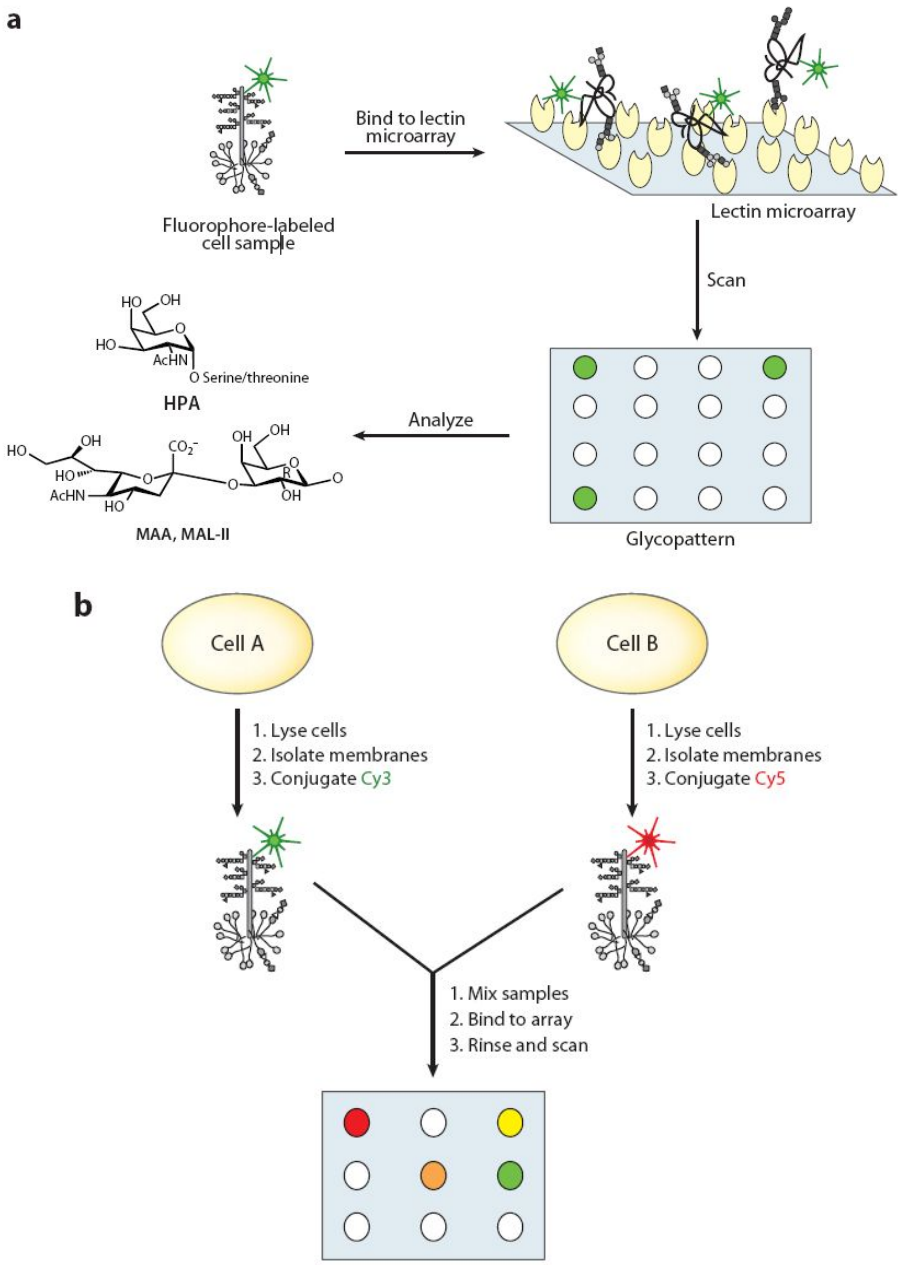

Figure 1.11 Scheme of lectin-based (a) single-color and (b) dual-color microarray for relative oligosaccharide quantification [87, 88]

However, in spite of wide application to structural analysis as described above, MS has a limitation for quantitation of oligosaccharides because the oligosaccharide mixture in biological samples (e.g. human serum) has various ionization efficiencies resulting from the complexity and diversity of glycan structure. MS has been also used in the identification of GalT-KO pig glycans in recent years. Diswall et al. and Puga Yung et al. recently reported on the glycolipids-derived glycans isolated from GalT-KO pig tissues and cells [89, 90]. However, there are no previous both structural and quantitative glycomic studies regarding GalT-KO pig glycomes using MS-based approach.

1.3.2.2 MS-based glycomic analysis

1.3.2.1 Girard reagent's T derivatization

The previous study presented relative and absolute quantitative analysis of neutral oligosaccharides by derivatization with carboxymethyl trimethylammonium hydrazide (also called Girard's reagent T) [91] (**Figure 1.12)**. A permanent cationic charge was introduced on the reducing end of oligosaccharides, and consequently MALDI-TOF MS spectra showed that $[M+GT]^+$ was mainly produced from heterogeneous metal adduct ions such as $[M+H]^+$, $[M+Na]^+$, and $[M+K]^+$. As a result, peak ion intensities in the MALDI-TOF MS spectra revealed a good linearity with the concentration (or amount) of glycan samples. However, this method is impossible to quantify sialic acid-containing glycans due to the negative charge state occurred in the sialic acid residue.

1.3.2.3 Solid-phase permethylation

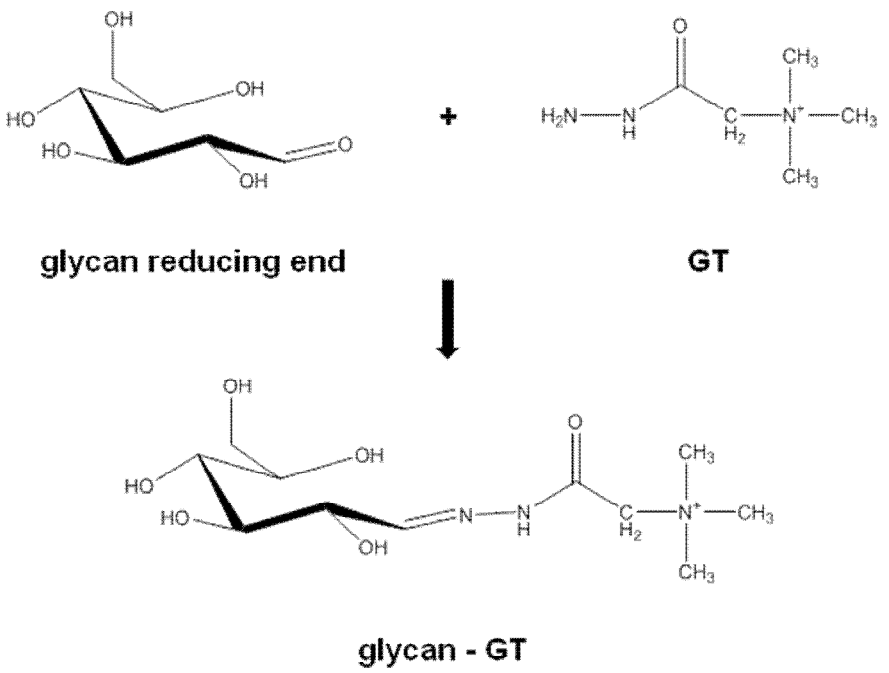

Figure 1.12 Derivatization of the glycan reducing end with carboxymethyl trimethylammonium hydrazide (GT) for the introduction of a permanent positive charge

Permethylation method has been commonly used in many glycomic studies [92]. The permethylation of oligosaccharides allows for significantly increasing MS detection sensitivity compared to other oligosaccharide derivatization methods, and simplifying interpretation of tandem mss spectra for structural identification of oligosaccharides. This derivatization is resulted from the chemical reaction of oligosaccharides with iodomethane in sodium hydroxide solution (NaOH). However, the problem of this conventional permethylation is believed to be dependent on oxidative degradation and peeling reactions under harsh basic conditions by NaOH solution. To overcome this shortcoming, Kang et al. pioneered solid-phase permethylation technique prior to MS analysis for micro-scale determination [93]. The MALDI-TOF MS analysis combined with the solid-phase permethylation approach permits comprehensive identification of both neutral and acidic glycans and therefore simultaneous quantitation of total glycans on biological samples because the solid-phase permethylation stabilized labile sialic acids by minimizing oxidative degradation and peeling reactions. Recently, permethylation coupled with commercially available stable isotope reagents has been used for comparative glycomic mapping [94]. **(Figure 1.13)**

1.3.2.4 Acetohydrazide amidation for sialylated glycan analysis

Although the introduction of a permanent charge on oligosaccharides result in provide reliable quantitation through MS instruments as mentioned above, this approach has a difficulty to apply for acidic oligosaccharide analysis. A previous study developed the neutralization of the sialic acid in oligosaccharides using methyl-esterification chemistry and showed significant difference of sialylated *N*-

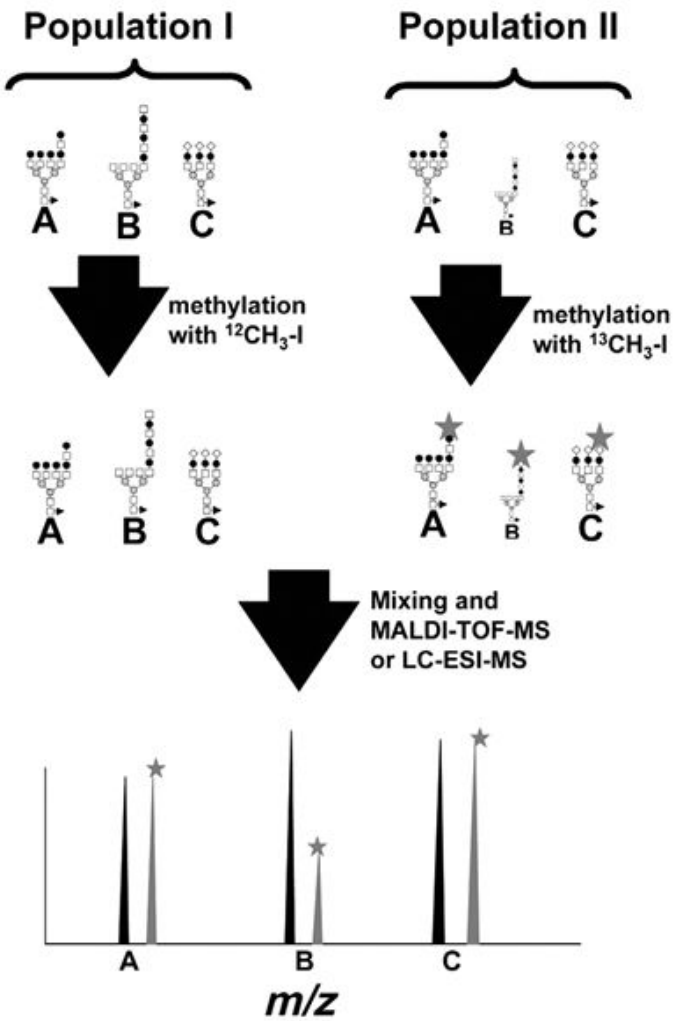

Figure 1.13 Comparative quantitation of the oligosaccharide by $^{13}CH_3I$ isotope permethylation [95]

glycans from the recombinant therapeutic glycoproteins [96]. However, incomplete modification of α2,3-linked sialylated glycans as well as the loss of sialic acids were occurred in the methyl-esterification reaction. Unlike methyl-esterification, amidation using acetohydrazide reagent under mild acidic condition has been reported to prevent the sialic acid of glycans from degradation and incomplete modification [97]. A recent study on quantitative glycomic analysis have reported on neutralization of sialic acids of oligosaccharides in combination with labeling of permanent charges on the reducing end [98] (**Figure 1.14**). This result showed that quantitative analysis using MALDI-TOF MS is in good agreement with the HPLC analytical method.

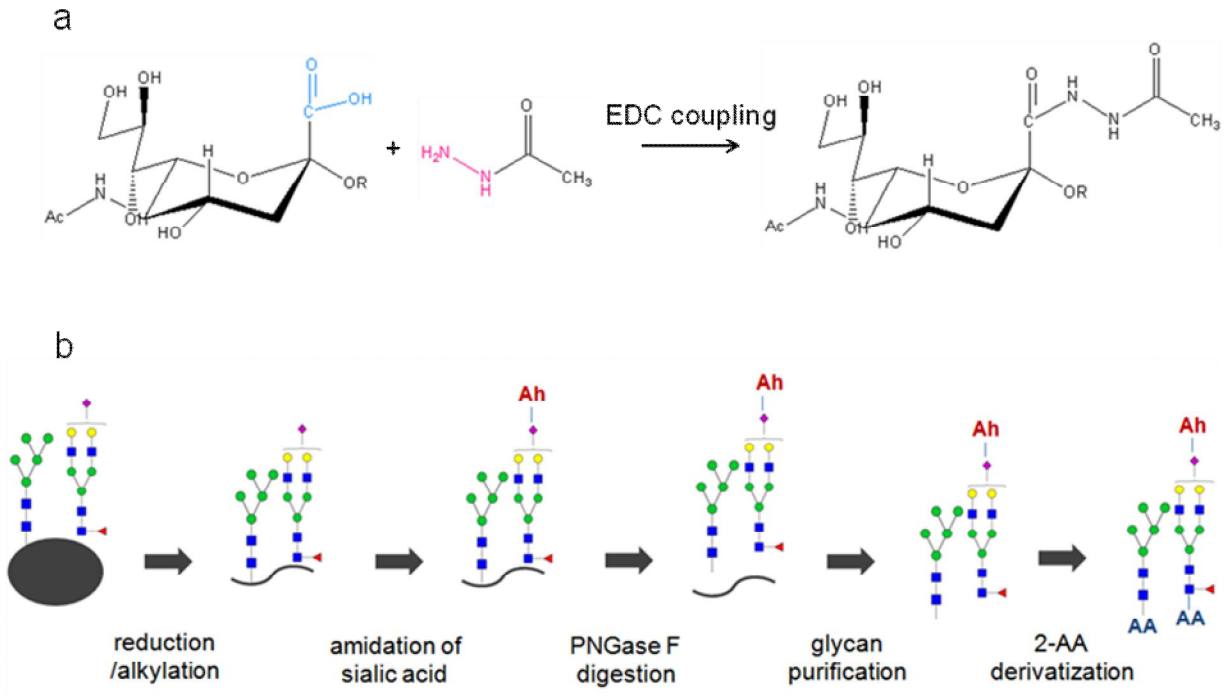

Figure 1.14 An approach for MS-based quantitation of sialylated glycans. (a) acetohydrazide amidation for neutralization of the sialic acid, (b) a scheme of oligosaccharide preparation from glycoproteins using acetohydrazide amidation.

1.4 Database in glycobiology

1.4.1 Importance of big data processing and current status in glycobiology

Because there is a need for researchers to access what is already known in their field, databases are invaluable bioinformatics tools for scientific research. In genomics and proteomics field, database has become an indispensable tool for research, but the application of databases for glycomics is less frequent than genomics and proteomics. However, as it increases in the availability of glycan analytical technologies and quantity of data, it becomes more important to data collection for glycans, and thus actually requires glycome data repositories and their processing software tools. To this end, during the past decades, several databases have been developed to assist the assignment, annotation and interpretation of glycan and glycoconjugates datasets [74, 99-103] **(Table 1.3)**. However, none of them systematically classify and update the pig glycans according to the specific pig tissues and cells. Qualitative and quantitative information on the glycan antigens, which play an important role in immune rejection, is also lacking.

Table 1.3 Glycan data management: glycan database and its resources [4]

	Database	URL
Integrated databases	GlycomeDB	http://www.glycome-db.org
	EuroCarbDB	http://www.ebi.ac.uk/eurocarb
	CFG	http://functionalglycomics.org
	GlycoSuiteDB	http://glycosuitedb.expasy.org/glycosuite/glycodb
	Glycosciences DE	http://www.glycosciences.de/index.php
	JCGGDB	http://jcggdb.jp
Glycan biosynthetic and catabolic pathways	KEGG-Glycan	http://www.genome.jp/kegg/glycan
	CazyDB	http://www.cazy.org
	GGDB	http://riodb.ibase.aist.go.jp/rcmg/ggdb
Structural glycan characterization	GlycoBase (Dublin/NIBRT)	http://glycobase.nibrt.ie/glycobase.html
	Glycobase (Lille)	http://glycobase.univ-lille1.fr/base
	CCSD (CarbBank)	http://boc.chem.uu.nl/sugabase/carbbank.html

	GMDB (Glycan Mass Spectra Database)	http://riodb.ibase.aist.go.jp/rcmg/glycodb/Ms_ResultSearch
	BCSDB (Bacterial Carbohydrate Structural Database)	http://www.glyco.ac.ru/bcsdb3
Tridimensional structure	Glycoconjugate databank	http://www.glycoconjugate.jp

Chapter 2. Materials and methods

2.1 Structural analysis and quantitation of pig cell and tissue glycomes using mass spectrometry

2.1.1 Isolation of homozygous GalT KO pig fibroblast cells

Fibroblasts were cultured from ear skin biopsies of the heterozygous GalT KO piglets as previously reported [104]. Selection of homozygous GalT KO cells derived from loss of heterozygosity was performed as described elsewhere [105]. Briefly, 5 x 10^5 heterozygous GalT KO cells were washed twice with Dulbecco's phosphate buffered saline (DPBS), resuspended with 1 ml of DPBS containing 4 μg biotin-conjugated IB4-lectin (EY Laboratories, San Mateo, CA, USA) in a 1.5-ml tube, and incubated for 1 hr on ice with tapping the tube to prevent precipitation of the cells. After washing cells twice with DPBS by centrifugation, 4 mg of Dynabeads M-280 Streptavidin (Invitrogen, Carlsbad, CA, USA) was added to the pellet and the resulting mixture was again incubated same as the IB4-lectin treatment. Then, the tube was placed on a magnet for 2-3 min, and the supernatant was transferred to a new tube on a magnet. This procedure was repeated three times. The final supernatant was cultured in Dulbecco's modified Eagle medium (DMEM) containing 10% (v/v) fetal bovine serum (FBS) in 60-mm culture dish for 10-14 days until colonies reached approximately 2 mm in diameter. The culture dish containing fibroblast colonies was washed twice with DPBS and covered with dimethylpolysiloxane (DMPS). Colonies were dissociated by injecting 30 μl of 0.25% trypsin-EDTA on top of each colony underneath DMPS using micropipette. After incubation for 5 min at 39°C, fibroblasts dissociated from each colony were

transferred onto 0.1% gelatin-coated 24-well culture dish for clonal culture. Clones of homozygous GalT KO were analyzed by PCR as previously reported (Ahn *et al*., 2011). Briefly, genomic DNA was prepared from fibroblasts using DNeasy Tissue Kit (Qiagen, Valencia, CA) according to the manufacturer's protocol. Using Maxime PCR premix kit (Intron Biotechnology, Seongnam, Korea) in 20 μL reaction volume, amplification of the target gene was carried out using forward 5'-AGAGGTCGTGACCATAACCAGAT-3' and reverse 5'-AGCCCATGCTGAACATCAAGTC-3' primers. Conditions for PCR were as follows: 30 cycles of 15 s at 94°C, 30 s at 65°C, 10 min + 20 s increase/cycle at 68°C; and one final cycle of 7 min at 68°C. Amplification products (9.2 kb GalT gene-targeted and/or 7.4-kb wild type allele,) were analyzed by 0.4% agarose gel electrophoresis. Fibroblasts confirmed to be GalT KO were used for subsequent experiments.

2.1.2 Preparation of membrane fractions from pig fibroblasts

Cell membrane fractionation procedure was performed following a previously described study [56], with minor modifications. Briefly, pig fibroblasts (wild-type and GalT-KO, respectively) consisting of 1 x 10^6 ~ 1 x 10^7 cells were washed with twice with 1 x phosphate buffered saline (PBS) by centrifugation at 90 x g for 5 min. The washed cell pellets were homogenized by sonication followed by centrifugation at 3,500 rpm for 10 min to remove cell debris and nuclear fraction. The supernant was centrifuged at 100,000 x g for 1 h and then precipitates (membrane fraction) were washed with 1 x PBS three times to remove cytosol

fraction. The washed precipitates were dissolved in 50 mM sodium phosphate buffer (pH 7.5) for further enzyme reaction.

2.1.3 Preparation of membrane fraction from GalT-KO pig kidney

Centrifugation and incubation were carried out at 4 ℃ and all fractions were stored at -20 °C until further use. Membrane fractionation protocol was performed according to our previous studies [106, 107]. Briefly, the fresh GalT-KO pig kidney tissue was sliced and homogenized in 1 x Tris-buffered saline (TBS) (50 mM Tris, 150 mM NaCl, pH 7.5) containing protease inhibitor cocktail tablets (Roche, Germany) using a motor-driven homogenizer. The tissue homogenate was centrifuged at 3,500 rpm for 10 min to remove cell debris and nuclear fractions. Membrane proteins were fractionated through centrifugation at 40,000 rpm for 2 h using an ultracentrifuge (Beckman Ti 70 rotor), and then the precipitates were washed with 1 x phosphate buffered saline (PBS) three times to remove residual cytosol fractions. The washed precipitates were resuspended in 50 mM sodium phosphate buffer (pH 7.5) for further N-deglycosylation enzyme reaction. Membrane protein concentration (6.6 mg/mL) was determined by the Bradford assay using a BSA standard.

2.1.4 Glycan release form pig fibroblasts and kidney membrane fractions

The membrane proteins were denatured at 95 ℃ for 3 min. After cooling to room temperature, the proteins were deglycosylated by treatment with peptide *N*-

glycosidase F (PNGase F; Roche, Germany) (5 U) followed by incubation at 37 ℃ for 16 h. After *N*-deglycosylation, ethanol precipitation was performed by the addition of a 4-fold volume of cold ethanol and incubation for 2 h at -20 °C, and supernants containing *N*-linked glycans and precipitants (*N*-deglycosylated proteins) were separated by centrifugation at 13,500 rpm for 15 min at 4 °C. Collected supernants were carefully transferred to new tubes and dried with a centrifugal vacuum concentrator for further purification.

2.1.5 Purification of released glycans

For purification of *N*-linked glycans from salts and other contaminants, porous graphitic carbon (PGC) cartridge (HyperSep Hypercarb SPE, Thermo Scientific, Bellefonte, PA, USA) was used. The purification protocol was as follows: First, the cartridge was washed with 30% (v/v) acetic acid/water followed 50% (v/v) acetonitrile (ACN)/water containing 0.1% trifluoroacetic acid (TFA). Next, the cartridge was equilibrated with 5% (v/v) ACN/water containing 0.1% TFA and then the released *N*-linked glycans dissolved in water were loaded onto the cartridge. Subsequently, the cartridge was washed with water followed by 5% (v/v) ACN/water containing 0.1% TFA. The *N*-linked glycans were eluted with 50% (v/v) ACN/water containing 0.1% TFA, and then the collected eluent was dried completely with a centrifugal vacuum concentrator for further steps.

2.1.6 Exoglycosidase digestion of purified glycans

The purified *N*-linked glycans were treated with exoglycosidases (Prozyme, Hayward, CA, USA) according to manufacturer's protocol. The exoglycosidases used in this study are as follows: *Arthrobacter ureafaciens* sialidase (EC3.2.1.18, specificity for α(2-6/3/8)-linked nonreducing terminal *N*-acetylneuraminic acid (NeuAc) and *N*-glycolylneuraminic acids (NeuGc)), bovine testes β-galactosidase (EC3.2.1.23, specificity for nonreducing terminal galactose with β(1-3/4) linkages). β-*N*-acetylhexosaminidase cloned from *S. pneumoniae*, expressed in *Escherichia coli* (EC3.2.1.30, specificity for β(1-2/3/4/6)-linked *N*-acetyl-glucosamine), and green coffee bean α-galactosidase (EC 3.2.1.22, specificity for α(1-3/4/6)-linked galactose). Deglycosylated glycans were purified from exoglycosidase enzyme(s) using Amicon®Ultra Centrifugal Filters (Millipore, Billerica, MA, USA) for further MS analysis.

2.1.7 Solid-phase permethylation of purified glycans

The purified *N*-glycans were permethylated using the solid-phase permethylation method [93]. Briefly, micro spin column (Harvard Apparatus, Holliston, MA, USA) were first filled with sodium hydroxide (NaOH) beads. Next, the spin column was washed dimethyl sulfoxide (DMSO) and then the *N*-glycans, which are dissolved in 141.6 μL of DMSO, 52.8 μL of iodomethane (CH_3I), and 5.6 μL of water, was applied to the NaOH-packed spin column. Subsequently, the sample was passed for at least eight times through the spin column by centrifugation at 1,200 rpm for 15 sec. The spin column was washed with 100 μL of ACN followed by centrifugation at 10,000 rpm for 1 min for complete collection

prior to two-phase extraction. The collected *N*-glycans were extracted from the sample solution with 200 μL of chloroform and 200 μL of water and neutralized with water until pH 6-7. Chloroform layer containing permethylated *N*-glycans was then dried prior to for further MS analyses.

2.1.8 Matrix-assisted laser desorption/ionization time-of-flight mass spectrometry (MALDI-TOF MS) analysis

0.5 μL of the sample solutions were mixed with 0.5 μL of 2,5-dihydroxybenzoic acid (DHB) solution (30 mg/mL in 30/70 (v/v) water/ACN). 1 μL of the mixture was spotted on stainless steel MALDI plate and dried at R.T. MS analysis was performed using a MALDI-TOF (matrix-assisted laser desorption/ionization time-of-flight) MS instrument with an Autoflex system from Bruker Daltonics (Bruker, Breman, Germany) and controlled by FlexControl 3.0 software (Bruker, Breman, Germany) according to manufacturer's protocols. The analysis parameters were as follows: positive-ion and reflectron mode, detector gain = 5.4 and laser power = 70%. Peptide calibration standard II (Bruker, Breman, Germany) of Angiotensin II (*m/z* 1046.54), Angiotensin I (*m/z* 1296.68), Substance P (*m/z* 1347.74), Bombesin (*m/z* 1619.82), ACTH1-17 (*m/z* 2093.09), ACTH18-39 (*m/z* 2465.20), Somatostatin (*m/z* 3147.47) was used for mass accuracy. 10,000 different spots were scanned to acquire a mass spectra data. The intensity of each peak was obtained by integrating from first to third isotopic peaks intensity. Data acquisition and processing were performed with flexAnalysis 3.3 software (Bruker, Breman, Germany). The GlycoMod (http://web.expasy.org/glycomod) was used for

determination of glycan compositions from measured masses.

2.1.9 Electrospray ionization mass spectrometry (ESI-MS) analysis

Dissolved in 4 μL water and 1 μL samples cleaned with a Nafion membrane [108]. Samples were diluted with 4 μL 0.1 M ammonium phosphate (to ensure that all neutral glycans formed $[M+(H_2PO_4)]^-$ ions) and 5 μL methanol and spun at 10,000 rpm (9503 x g) in a bench centrifuge for 1 min. Samples were infused through Waters thin-wall nanospray capillaries into a Waters Synapt G2 travelling wave ion mobility mass spectrometer (Waters MS-technologies, Manchester UK) [109] fitted with an electrospray (ESI) ion source. The instrument was operated in negative ion mode. The ESI capillary voltage was 1.2 kV, the cone voltage was 20-180 V and the ion source temperature and desolvation temperature were maintained at 80°C and 120°C respectively. The T-wave velocity and peak height voltages were 450 m/sec and 40 V respectively. Instrument calibration was performed with released *N*-glycans from bovine fetuin. The T-wave mobility cell (nitrogen) was operated at a pressure of 0.55 mbar. Fragmentation was performed after mobility separation in the transfer cell with argon as the collision gas. Data acquisition and processing were carried out using the Waters Driftscope (version 2.1) software and MassLynx™ (version 4.1). The scheme devised by Domon and Costello [110] was used to name the fragment ions and the structures were drawn with the scheme devised by Harvey *et al*. [111].

2.1.10 MALDI-quadrupole ion trap (QIT)-TOF MS/MS analysis

0.5 μL of The sample solutions were mixed with 0.5 μL of DHB solution (10 mg/mL in 30/70 (v/v) water/ACN) and subsequently subjected to MALDI-TOF MS/MS analysis. MS/MS analysis was performed using an Axima Resonance MALDI-quadrupole ion trap-TOF instrument (Shimadzu, Manchester, UK). The analysis parameters were as follows: positive-ion and reflectron mode. The TOF detector was calibrated as described above. Fragment ions generated by collision-induced dissociation (CID) of the precursor ions were analyzed after passing through the ion reflector. Data acquisition and processing were performed with Launchpad 2.9.3 software (Kratos Analytical Ltd, Manchester, UK).

2.1.11 Statistical analysis

Student's *t* tests were calculated using Microsoft Excel.

2.2 Development of qualitative and quantitative pig glycome database

2.2.1 Design and implementation

XDB is based on open-source technology, developed in jruby 1.7.0 and trinidad1.4.4 Tomcat 7.0.37 and tested on Debian. The database was used in SQLite version 3.0 as a data storage program. The HTML-based web interface has been tested using Safari 6 and Chrome 22. The updated version of web browsers is recommended for the usage of the XDB. The flow chart for development of 'Mass spectrometry-based glycan searching', which is one of major query options implemented in pig glycome database, is shown in **Figure 2.1**.

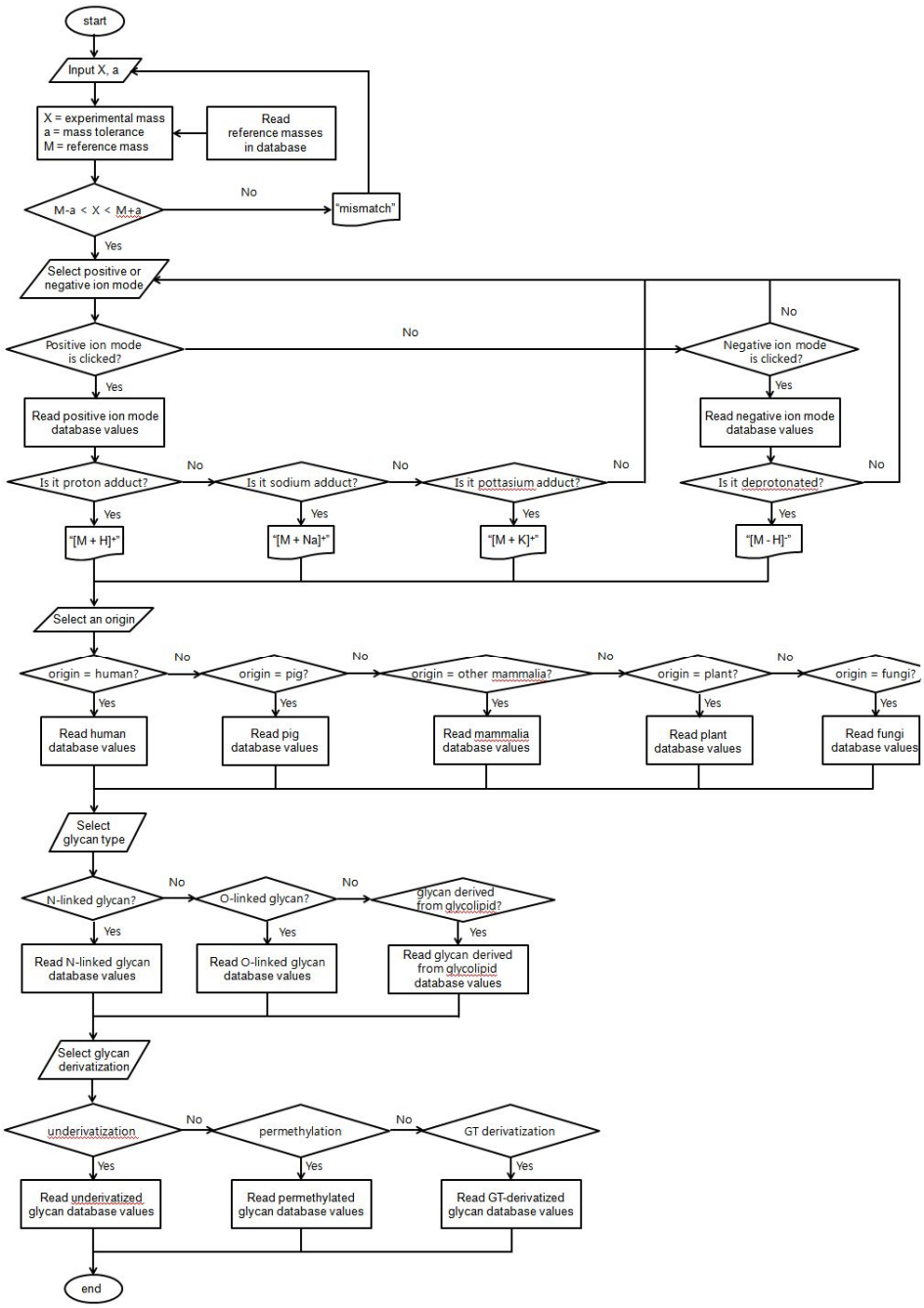

Figure 2.1 A flow chart for construction of 'Mass spectrometry-based glycan searching' in pig glycome database.

2.3 Pig glycome-human immune cell interaction study

2.3.1 Preparation of WT and GalT-KO pig kidney glycans

The protocol for the preparation of N-linked glycans derived from pig kidney is as chapter from 2.1.3 to 2.1.5.

2.3.2 Isolation and culture of human immune cells

Isolation and culture of human monocytes protocol was carried out following a previously described study [112] with minor modifications. Human mononuclear cells were isolated from buffy coats obtained from healthy donors using Ficoll-Hypaque™ PLUS (GE Healthcare), followed by anti-CD14 microbeads magnetic cell sorting, according to the manufacturer's instruction (Miltenyi Biotec/CLB, Amsterdam, The Netherlands). The CD14+ cells were seed in plastic six-well culture plates (3 x 10^6 cells/well) at 37°C in 10% FBS RPMI. For macrophage differentiation, GM-CSF (500 unit/mL) was added to the medium and incubated for 6 days. The cells were sub-cultured in 3 mL of 10% FBS RPMI culture media with treatment of pig glycans (WT and GalT-KO, respectively) from membrane fraction (2 mg) every 2 days. For mature macrophages, immature macrophages were incubated followed by stimulation with LPS (100 ug/mL) for one additional day. Dendritic cells were provided from Prof. Kyeong-Cheon Jung of Seoul National University College of Medicine.

2.3.3 FACS (Fluorescence-activated cell sorting) analysis

Human immune cells were washed with PBS, and then incubated with PBS containing 5 mM EDTA for 5 min at 37°C to detachment from six-well culture plates and washed with 10% FBS RPMI. The washed cells then were stained with conjugated antibodies at 4°C for 30min. Intracellular expression of CD86, CD80, CD14, CD40, CD11b, and CD11c were access according to the manufacturer's protocol. Data acquisition and processing was carried out using a FACSCalibur (BD Biosciences) and mean fluorescence intensities (MFI) were analyzed using FlowJo 7.5.5 software (Tree Star, Inc).

2.3.4 Pig glycan-binding membrane protein screening from human immune cells

Membrane proteins derived from dendritic cells were fractionated by the same method described in chapter 2.1.3. The glycan-immobilization protocol was carried out according to a previous study [106]. The prepared pig glycan and hydrazide core-shell beads (20 mg) were resuspended with 30% acetic acid, and then incubated at room temperature for 4 h. After the coupling reaction, pig glycan-immobilized beads were washed with water five times The membrane fraction solution was incubated mock bead to prevent non-specific binding, and then the supernant was mixed with WT and GalT-KO pig kidney N-glycan-immobilized beads, respectively, at 37°C for 1 h. After washing with PBS three times, the

proteins were eluted with 0.2 M glycine-HCl buffer (pH 2.2). The eluted protein solution was neutralized with 1 M Tris-HCl buffer (pH 9.1). The proteins were denatured at 95°C for 3 min. After cooling down, the samples were mixed with 10 μL of trypsin (1 μg/μL, Promega, Madison, WI, USA), and then incubated at 37°C for 16 h. Finally, the tryptic digested peptides were dried prior to proteomic analysis using MS.

2.3.5 LC-MS/MS analysis

MS/MS analysis was performed using LTQ FT Orbitrap mass spectrometer (Thermo Electron Corp, USA) equipped with a nano-electrospray ionization (NSI) source in positive mode at an ion spray voltage of 1.50 kV. 35% of normalized collisional energy and 2 Da of isolation width were used for tandem mass spectrometric fragmentation. The trypsin-digested protein fragments were injected into the nano LC (LC packing, Netherland)-MS/MS system. The loaded sample was eluted with gradient from 2% to 35% solvent B for 30 min, then from 35% to 90% for 10 min, followed by 90% solvent B for 5 min, and finally 5% solvent B for 15 min at a flow rate of 300 nL/min. Solvent A was constituted in water/acetonitrile (98/2 [v/v]) and 0.1 % formic acid, and solvent B was constituted in water/acetonitrile (2/98 [v/v]) and 0.1 % formic acid. Data acquisition and processing were performed with BioWorks 3.2 software based on the SEQUEST and the generated MS/MS data were compared to Swiss-Prot human databases from NCBI.

Chapter 3. Comparative glycome analysis of WT and GalT-KO pig cells and tissues

3.1 Qualitative and quantitative N-linked glycan analysis of WT and GalT-KO pig fibroblasts

3.1.1 Isolation of homozygous GalT KO cells

Fibroblasts with biallelic disruption of GalT gene due to LOH in heterozygous KO were obtained by the selection using IB4-Dynabead. As shown in **Figure 3.1**, PCR analysis confirmed that fibroblasts from the selected colony contained only GalT gene-targeted allele (9.2 kb) without having wild type allele (7.4 kb), demonstrating that homozygous KO fibroblasts were successfully isolated.

3.1.2 MS profiling of N-linked glycans using MALDI-TOF MS

This study sought to identify N-glycans on the cell surface of WT and GalT-KO pig fibroblasts using MS-based approaches. The scheme of the approach used in this study is described as **Figure 3.2**. Cell membrane proteins were fractionated from pig fibroblast lysate by ultracentrifugation separation, and then *N*-linked glycans were released from the cell membrane proteins by peptide *N*-glycosidase F (PNGase F) digestion. Next, the released *N*-linked glycans were desalted using porous graphitic carbon (PGC) for solid-phase extraction. Finally, the purified *N*-linked glycans were permethylated, and subsequently analyzed by MALDI-TOF MS and MS/MS.

The representative mass spectra obtained from the WT and GalT-KO pig fibroblasts are shown in **Figure 3.3**, respectively. The N-glycan profile showed

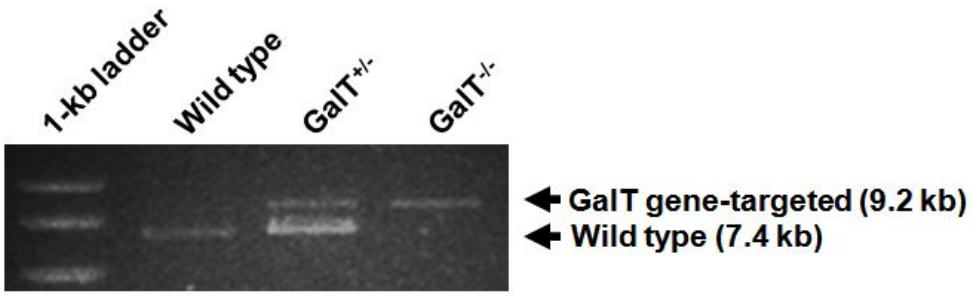

Figure 3.1 PCR analysis of homozygous GalT KO fibroblasts. Note that GalT-/- fibroblasts contain only GalT gene-targeted alleles, whereas wild type alleles remain in both wild type and GalT+/- cells.

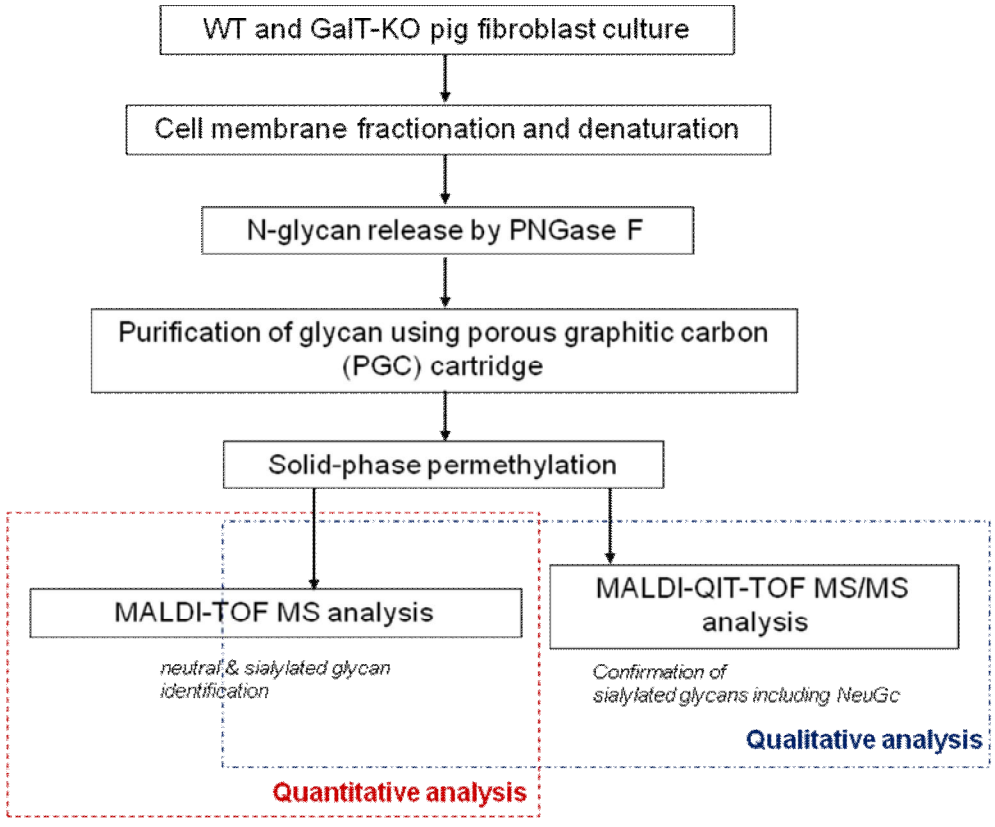

Figure 3.2 Streamlined process outline for N-glycan analysis from pig fibroblasts

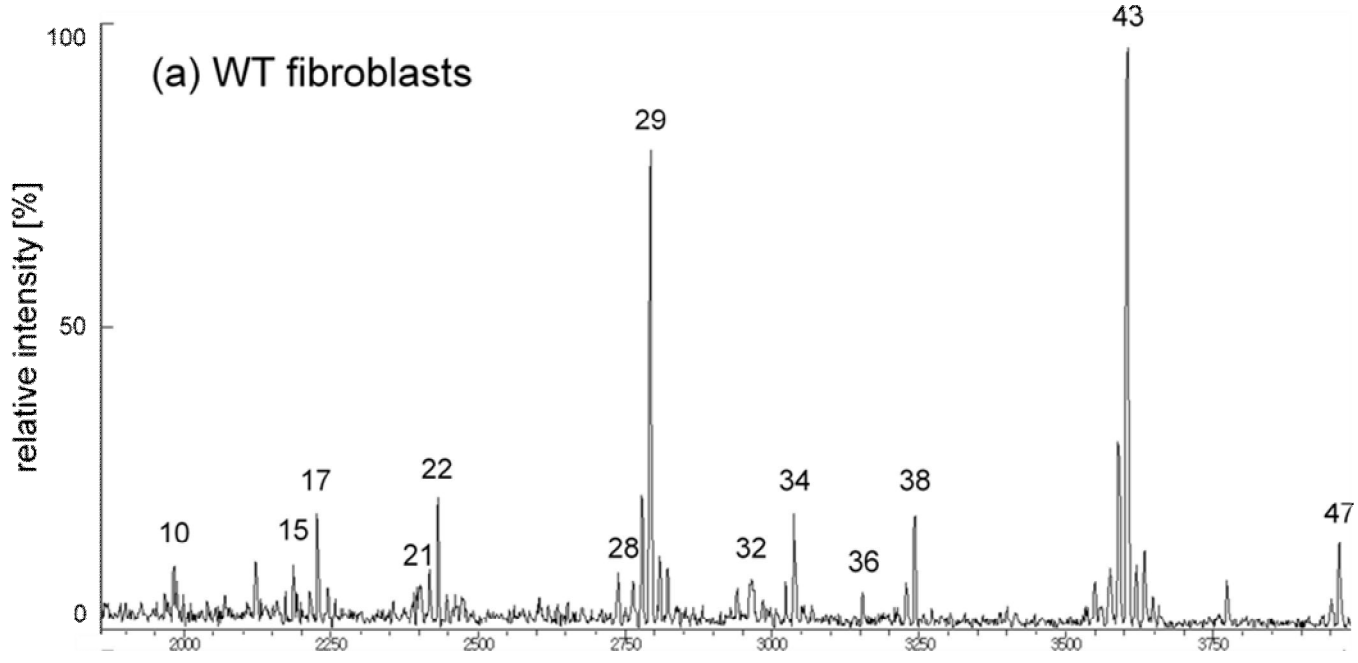
(a) WT fibroblasts
relative intensity [%]
100
50
0
2000
2250
2500
2750
3000
3250
3500
3750
10
15
17
21
22
28
29
32
34
36
38
43
47

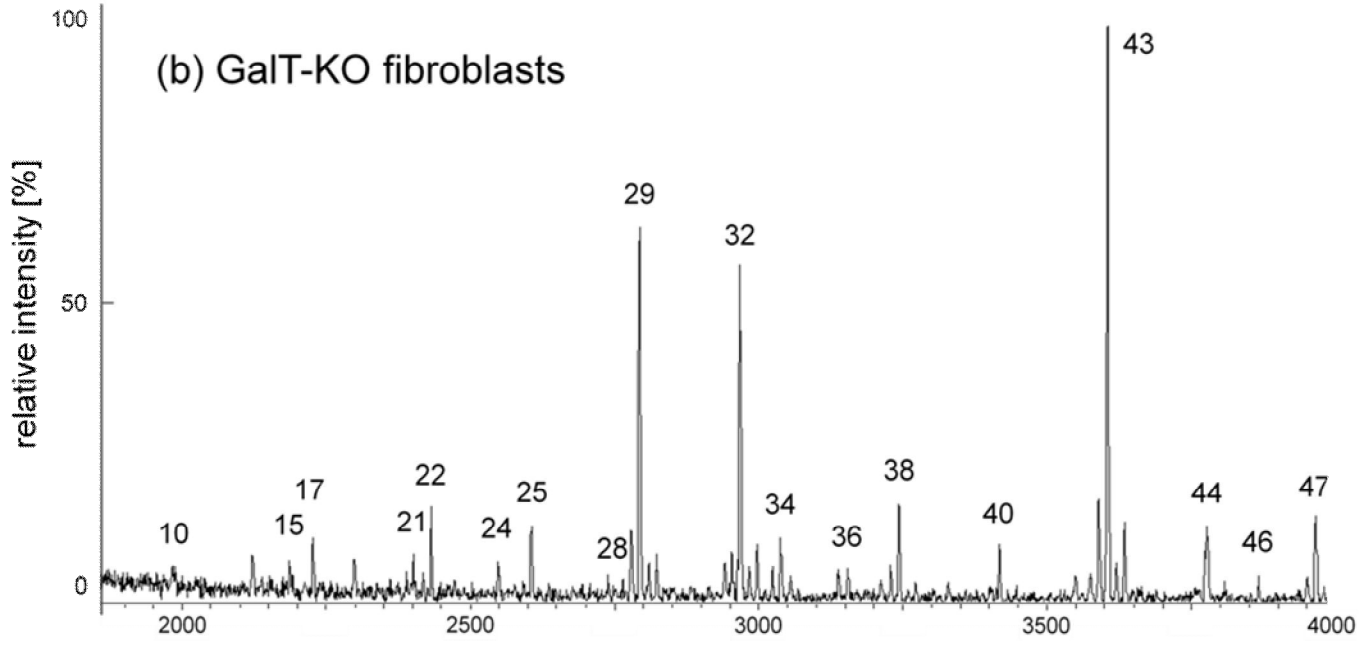

Figure 3.3 Positive ion MALDI-TOF mass spectrum of the *N*-glycans isolated from pig (a) wild-type and (b) GT-KO fibroblasts

totally 47 N-glycan including high-mannose type glycans and complex type glycans with bi-, tri-, and tetra-antennary structures on pig fibroblasts as summarized in **Table 3.1**. The predicted structures were proposed according to the structural information in our previous studies [55, 107]. The MS results also indicated that sialylated glycans as well as fucosylated glycans were the abundant components for complex type glycans. Notably, the α-Gal antigen considered as the major xenoantigen was not detected in Gal-KO pig fibroblasts, whereas this antigen (*m/z* 2652.4) was observed as a trace in WT. This α-Gal xenoantigen was deduced as two α-galactosylated bi-antennary glycan according to its molecular weight. It was also confirmed here that α-Gal-terminated N-glycan was absent on GalT-KO pig fibroblasts using MS. On the other hand, five N-linked glycans (observed at *m/z* value of 2186.2, 2822.5, 2996.6, 3445.8, and 3806.7) proposed as NeuGc-containing glycans were detected in both WT and GalT-KO pig fibroblasts.

3.1.3 Quantitative analysis of N-linked glycans using solid-phase permethylation and MALDI-TOF MS

To quantify N-linked glycan array on pig fibroblasts, MS-based quantitative analysis using solid-phase permethylation was carried out. As results, the relative quantities of and sialylated (92.3%) glycans in GalT-KO pig fibroblasts were higher than those in WT (69.9%) **(Figure 3.4a)**. In addition, each N-glycan among total glycans using MS-based analysis combined with solid-phase permethylation is quantified. Most notably, a sialylated glycan composed of $Hex_5HexNAc_4Fuc_1NeuAc_2$ was dramatically elevated in the GalT-KO (14.2%)

Table 3.1 Identification of *N*-linked glycans derived from WT and GalT-KO pig fibroblasts

peak no.	$[M+Na]^+$ *m/z*		compositions					proposed structure	% total MALDI[a]	
	Cal[c]	Exp[d]	Hex	HexNAc	Fuc	NeuAc	NeuGc		WT	GT-KO
1	1579.8	1579.9	5	2	0	0	0	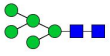	13.3 (±0.60)	3.6 (±0.35)
2	1590.8	1590.9	3	3	1	0	0	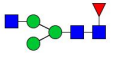	2.1 (±0.15)	0.5 (±0.19)
3	1620.8	1620.9	4	3	0	0	0	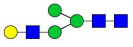	1.1 (±0.28)	trace
4	1661.8	1661.9	3	4	0	0	0	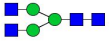	0.9 (±0.21)	0.6 (±0.23)
5	1783.9	1784.0	6	2	0	0	0	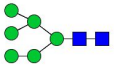	3.4 (±0.10)	0.5 (±0.31)
6	1794.9	1795.0	4	3	1	0	0	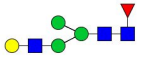	0.5 (±0.08)	trace
7	1824.9	1825.0	5	3	0	0	0	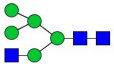	0.6 (±0.09)	trace

8	1835.9	1836.0	3	4	1	0	0	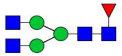	1.6 (±0.15)	0.4 (±0.18)
9	1865.9	1866.0	4	4	0	0	0	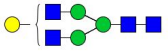	0.4 (±0.12)	trace
10	1982.0	1982.1	4	3	0	1	0	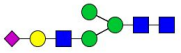	1.5 (±0.09)	1.0 (±0.35)
11	1988.0	1988.1	7	2	0	0	0	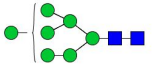	0.9 (±0.13)	0.3 (±0.08)
12	1999.0	1999.1	5	3	1	0	0	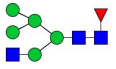	0.6 (±0.21)	0.1 (±0.05)
13	2040.0	2040.1	4	4	1	0	0	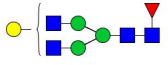	0.4 (±0.05)	0.2 (±0.02)
14	2070.0	2070.1	5	4	0	0	0	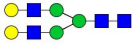	0.4 (±0.15)	trace
15	2186.2	2186.2	4	3	1	0	1	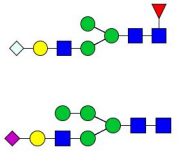	1.9 (±0.03)	1.2 (±0.18)
			5	3	0	1	0			
16	2192.1	2192.2	8	2	0	0	0	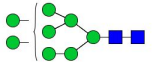	0.7 (±0.19)	0.4 (±0.04)

17	2227.1	2227.2	4	4	0	1	0	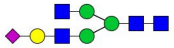	3.7 (±0.19)	2.0 (±0.31)
18	2244.2	2244.3	5	4	1	0	0	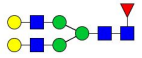	0.9 (±0.05)	0.3 (±0.02)
19	2360.2	2360.3	5	3	1	1	0	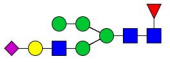	trace	0.4 (±0.10)
20	2390.2	2390.3	6	3	0	1	0	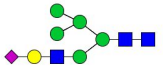	0.7 (±0.17)	0.3 (±0.24)
21	2401.2	2401.3	4	4	1	1	0	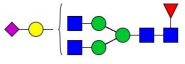	1.4 (±0.28)	1.4 (±0.09)
22	2431.2	2431.3	5	4	0	1	0	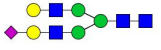	4.3 (±0.11)	3.5 (±0.22)
23	2472.2	2472.4	4	5	0	1	0	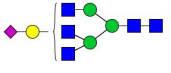	1.1 (±0.22)	0.7 (±0.04)
24	2547.3	2547.4	5	3	0	2	0	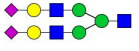	ND[b]	1.3 (±0.15)
25	2605.3	2605.4	5	4	1	1	0	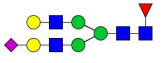	0.3 (±0.08)	2.9 (±0.13)

26	2652.3	2652.4	7	4	1	0	0	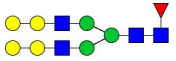	0.6 (±0.14)	ND
27	2676.3	2676.4	5	5	0	1	0	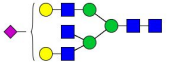	0.4 (±0.19)	0.2 (±0.23)
28	2764.4	2764.4	6	6	0	0	0	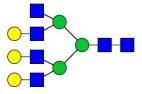	1.4 (±0.26)	0.4 (±0.38)
29	2792.4	2792.4	5	4	0	2	0	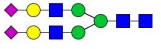	17.2 (±0.42)	15.3 (±0.36)
30	2822.4	2822.5	5	4	0	1	1	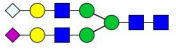	1.8 (±0.36)	1.7 (±0.07)
31	2880.4	2880.5	6	5	0	1	0	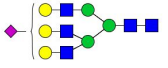	0.3 (±0.04)	0.2 (±0.20)
32	2966.5	2966.6	5	4	1	2	0	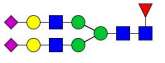	1.5 (±0.10)	14.3 (±0.46)
33	2996.5	2996.6	5	4	1	1	1	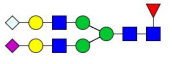	0.2 (±0.17)	2.2 (±0.04)
34	3037.5	3037.6	5	5	0	2	0	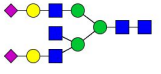	3.6 (±0.25)	2.3 (±0.12)

35	3054.5	3054.5	6	5	1	1	0	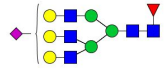	0.4 (±0.01)	0.9 (±0.11)
36	3153.6	3153.6	5	4	0	3	0	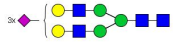	0.9 (±0.06)	0.8 (±0.34)
37	3211.6	3211.7	5	5	1	2	0	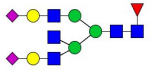	0.3 (±0.11)	0.4 (±0.38)
38	3241.6	3241.7	6	5	0	2	0	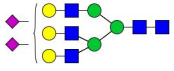	4.3 (±0.36)	3.9 (±0.03)
39	3327.7	3327.7	5	4	1	3	0	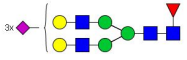	0.1 (±0.09)	0.4 (±0.00)
40	3415.7	3415.7	6	5	1	2	0	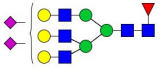	0.1 (±0.21)	2.5 (±0.49)
41	3445.7	3445.8	6	5	1	1	1	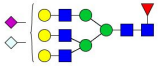	0.2 (±0.05)	0.2 (±0.16)
42	3503.7	3503.7	7	6	1	1	0	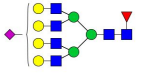	0.1 (±0.09)	trace
43	3602.8	3602.8	6	5	0	3	0	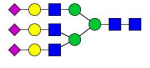	20.9 (±0.26)	24.2 (±1.25)
44	3776.8	3776.7	6	5	1	3	0	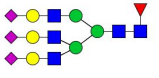	ND	2.9 (±0.17)

45	3806.9	3806.8	6	5	1	2	1	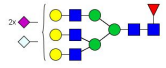	0.1 (±0.08)	0.5 (±0.07)
46	3864.9	3864.8	7	6	1	2	0	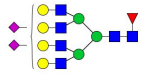	trace	0.7 (±0.06)
47	3964.0	3963.9	6	5	0	4	0	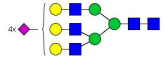	2.9 (±0.11)	3.3 (±0.14)

[a] Quantitative sialylated and neutral N-glycan percentages measured by MALDI-TOF MS combined with solid-phase permethylation.

[b] ND = not detected

fibroblasts compared with WT (1.5%). In addition, $Hex_5HexNAc_4Fuc_1NeuAc_1$ (2.9%) and $Hex_6HexNAc_5Fuc_1NeuAc_{2-3}$ (2.5% and 2.9%, respectively) glycans were also only observed or increased in the GalT-KO fibroblasts. This result indicated that $Hex_5HexNAc_4Fuc_1NeuAc_2$ bi-antennary N-linked glycan leads to an increase of total sialylation in GalT-KO pig fibroblasts. This study showed that these increased sialic acid-containing glycans, which contain a fucose monosaccharide, lead in an increase of the overall fucosylation level as well as sialylation on the pig GalT-KO as shown in **Figure 3.4b**. The current analysis also revealed that the quantity of NeuGc-containing N-linked glycan was slightly higher in the GalT-KO (6.1%) relative to the WT (4.5%) in **Figure 3.4c**.

3.1.4 Qualitative analysis of N-linked glycans using MALDI-QIT-TOF MS/MS

To validate N-linked glycan structures in pig fibroblasts, tandem mass spectrometry analysis was carried out using MALDI-QIT TOF MS. Above mentioned $Hex_5HexNAc_4Fuc_1NeuAc_{1-2}$ and $Hex_6HexNAc_5Fuc_1NeuAc_{2-3}$ glycans, the relative quantities of which are higher in GalT-KO pig fibroblasts than WT, were analyzed. As shown in **Figure 3.5**, the chemical structures of the glycans were elucidated through peak assignment of fragment ions in mass spectra and were therefore confirmed to be N-linked glycans which contain both sialic acid and fucose residues. For example, fragment ions at *m/z* 2230.2, 2591.4, 3040.3, and 3401.4 were generated from parent ions at *m/z* 2605.4, 2966.6, 3415.7, and 3776.6, respectively, by the loss of an *N*-acetylneuraminic acid residue (375.2 Da) present in the N-linked glycans. The parent ions also produced a fragment ion at *m/z*

(a) sialylated glycan

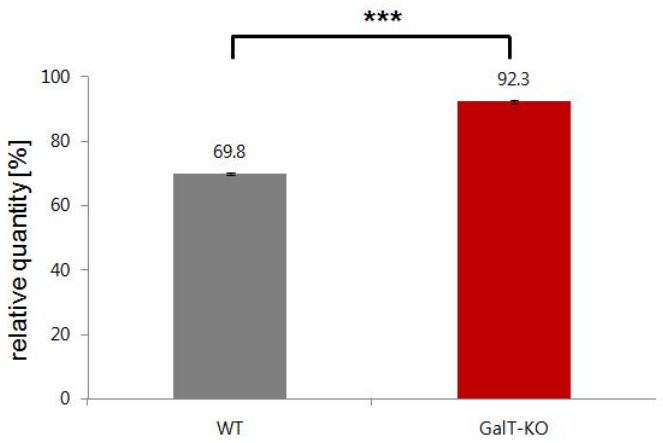

(b) fucosylated glycan

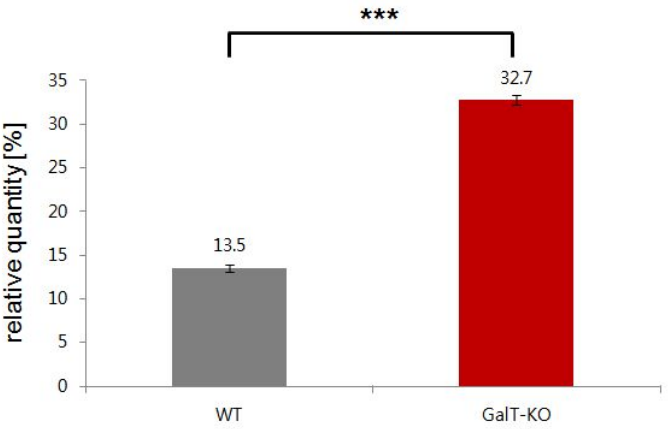

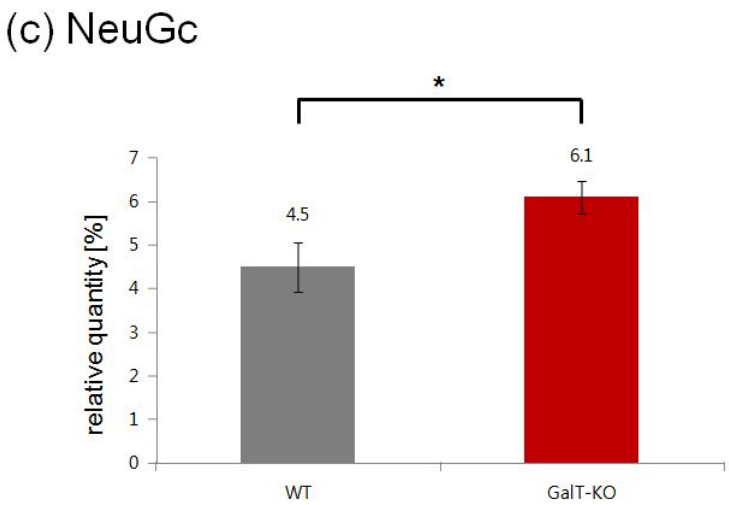

Figure 3.4 Relative quantitative comparison of (a) sialylated N-glycans, (b) fucosylated N-glycans, and (c) NeuGc-containing N-glycan derived from pig fibroblasts using MALDI-TOF MS combined with solid-phase permethylation. The annotations with asterisks in this figure are as follows: *: $p < 0.05$, ***: $p < 0.001$

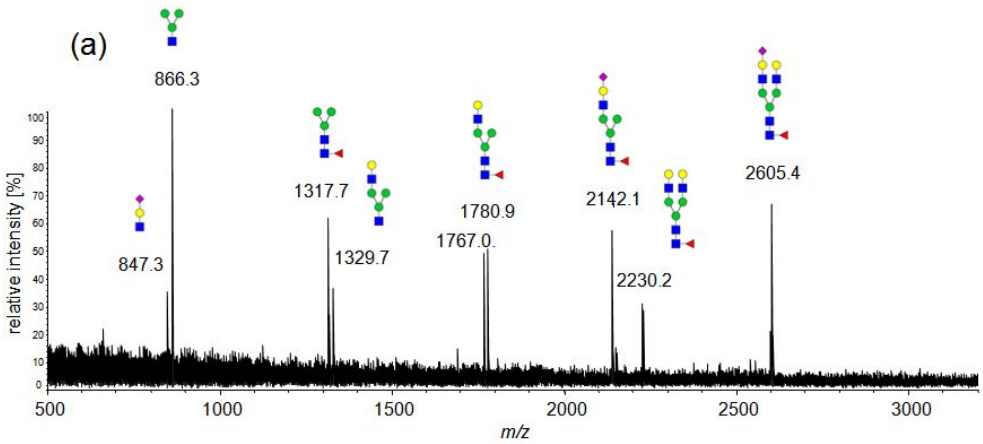
(a)
866.3
847.3
1317.7
1329.7
1780.9
1767.0
2142.1
2230.2
2605.4
relative intensity [%]
m/z

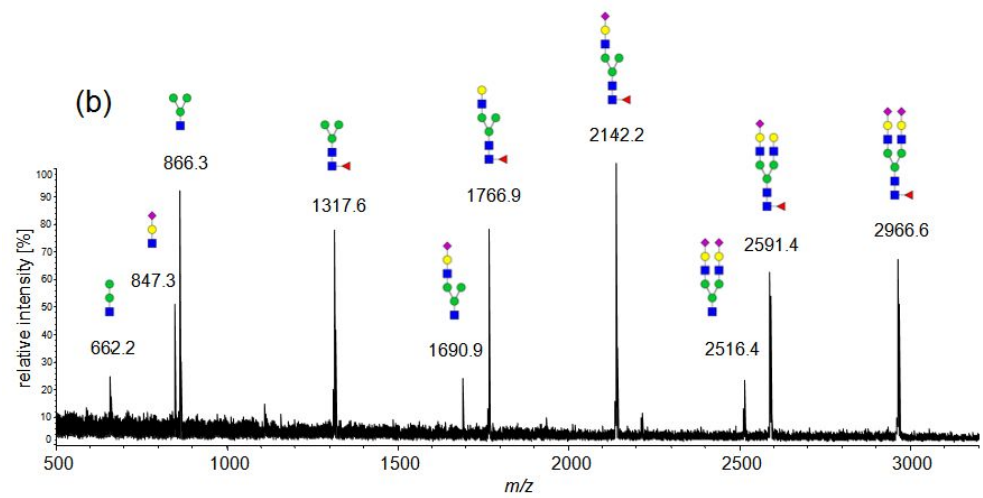
(b)
866.3
847.3
662.2
1317.6
1766.9
1690.9
2142.2
2516.4
2591.4
2966.6
relative intensity [%]
m/z

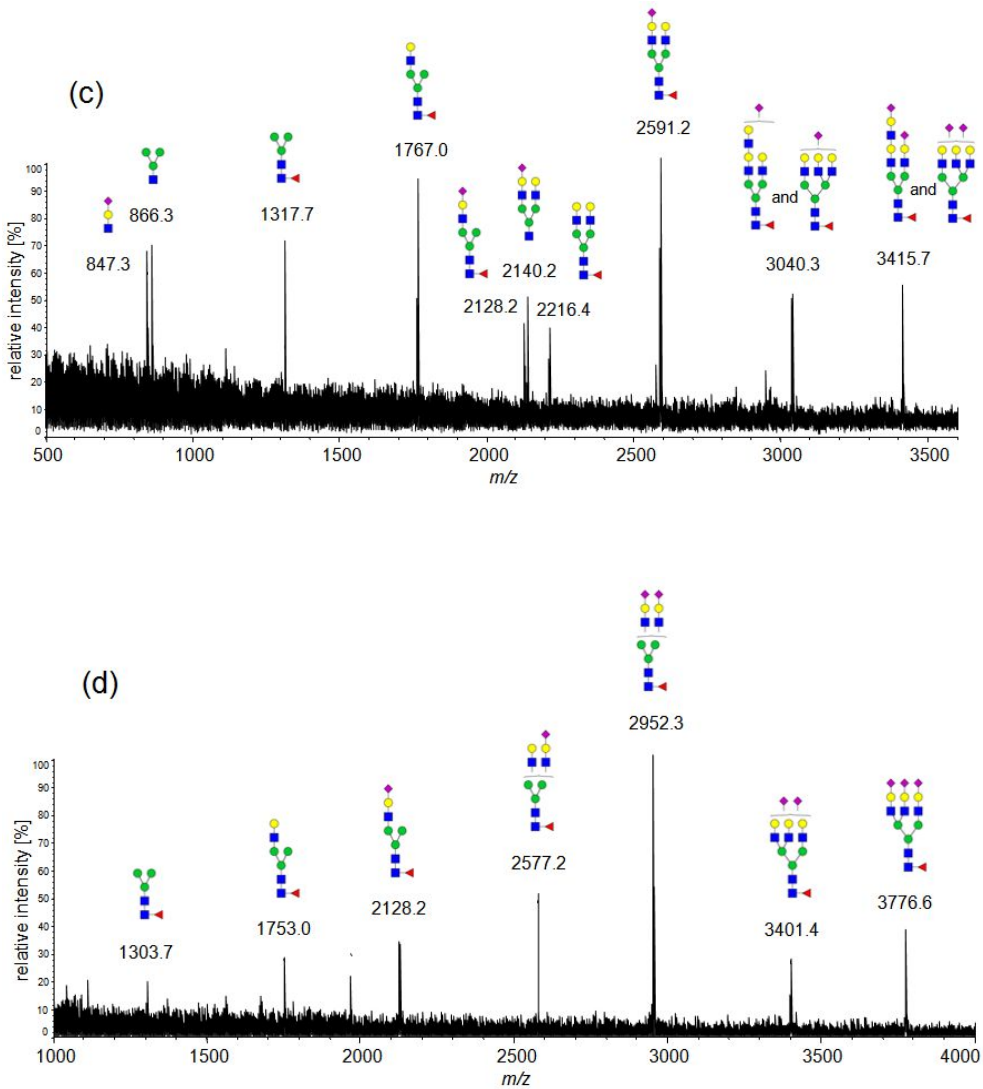

Figure 3.5 Positive ion MS/MS spectra of permethylated sialylated N-linked glycans observe at m/z values of (a) 2605.4, (b) 2966.6, (c) 3415.7, and (d) 3776.6

1303.7 or 1317.7 corresponding to a fucosylated *N*-glycan core structure. In addition, NeuGc-containing *N*-glycans ($Hex_5HexNAc_4NeuAc_1NeuGc_1$ and $Hex_5HexNAc_4Fuc_1NeuAc_1NeuGc_1$) were confirmed by MS/MS analysis **(Figure 3.6)**. For instance, fragment ions at *m/z* 2417.4 and 2591.3 were resulted from parent ions at *m/z* 2822.5 and 2996.6 by cleavage of a NeuGc residue (405.1 Da).

3.1.5 Discussion

The α-Gal antigen considered as the major xenoantigen was not observed in Gal-KO pig fibroblasts, whereas this antigen was found as a trace in WT. The quantitative study on pig glycan showed that two α-Gal-terminated glycan with a core fucose ($Hex_7HexNAc_4Fuc_1$) was identified as the most abundant α-Gal antigen among total α-Gal antigens on WT pig by both MS and HPLC analyses [106]. This study therefore suggested that this α-Gal antigen may be the major α-Gal antigen structure of N-linked glycans expressed on WT pig organs. On the other hand, five N-linked glycans proposed as NeuGc-containing glycans were detected in both WT and GalT-KO pig fibroblasts, indicating that NeuGc are still present on cell surface of pig fibroblasts after deletion of α-galactosyltransferase gene. Therefore, this NeuGc antigen may be the second major hurdle for further studies on pig-to-human as described previously [50]. For quantitation of N-linked glycan array on pig fibroblasts, MS-based quantitative analysis using solid-phase permethylation was performed in this study. MALDI-TOF MS combined with permethylation was reported as a good quantitative method in excellent correlation to the HPLC of reductive amination derivatization [113]. Moreover, solid-phase permethylation

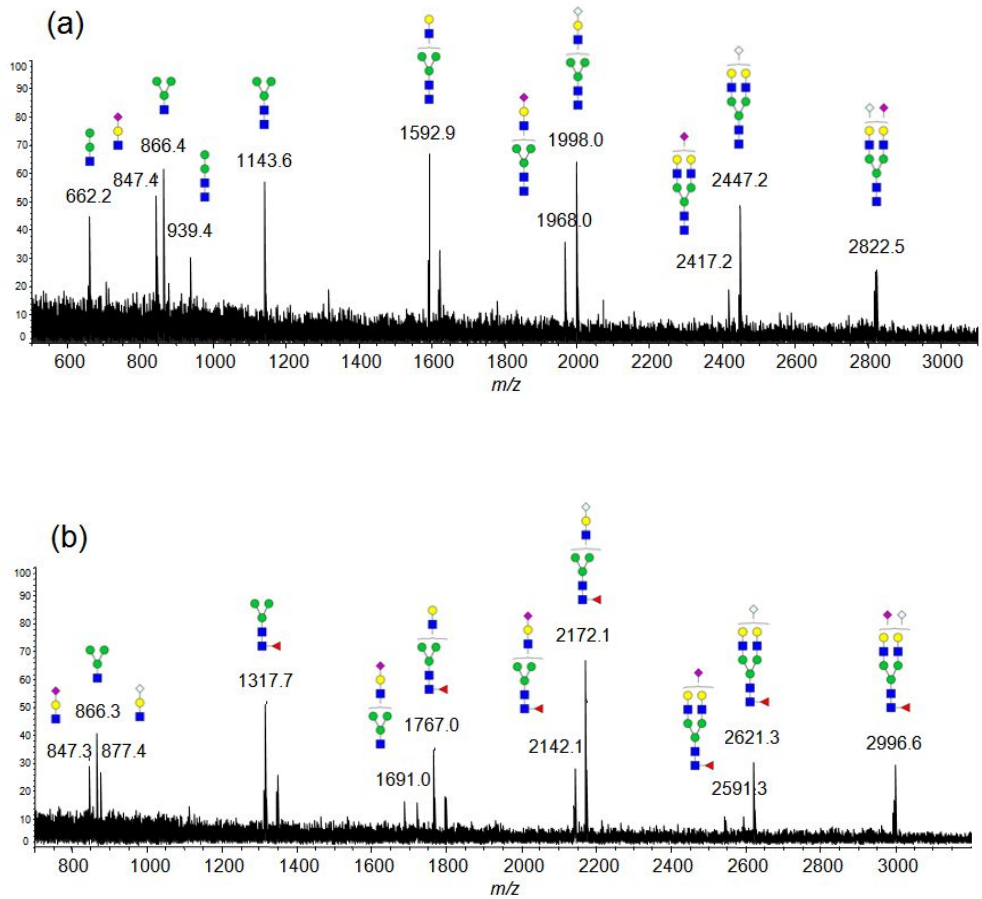

Figure 3.6 Positive ion MS/MS spectra of permethylated NeuGc-containing N-glycans observe at m/z values of (a) 2822.5 and (b) 2996.6

minimize sialic acid loss by oxidative degradation and peeling reaction and thus are more quantitative and efficient compared to conventional permethylation [114]. This study revealed that the relative quantities of and sialylated glycans in GalT-KO pig fibroblasts were higher than those in WT, and therefore corresponded with recent studies on different organs of the GalT-KO pig [29, 106]. Park et al. reported that α1,3-galactosyltransferase deficiency in pigs increases sialic acid-terminated glycoconjugates epitopes using enzyme-linked lectinosorbent assay. This lectin-based method was able to analyze on specific carbohydrate epitopes expressed on the cell surface, but did not provide quantitative information on individual glycans as well as these glycan structures of the GalT-KO pig.

The current analysis revealed that a sialylated glycan composed of $Hex_5HexNAc_4Fuc_1NeuAc_2$ was dramatically elevated in the GalT-KO fibroblasts compared with WT. This result indicated that this N-linked glycan leads to an increase of total sialylation in GalT-KO pig fibroblasts. Interestingly, this study also showed that these increased sialylated glycans contains a fucose monosaccharide, and consequently these glycans took the lead in an increase of the overall fucosylation level as well as sialylation on the pig GalT-KO. A previous report showed there is no significant difference of fucose level between GalT-KO and WT pig fibroblasts [63]. However, in that study, overall cellular glycoconjugates include O-glycans and glycolipid-derived glycans as well as N-glycan were measured by the lectin-based method.

Some studies have reported to delineate various glycoconjugates in GalT-KO pig organs using lectin-based array [63, 115]. However, the detection and quantitative measurement of NeuGc has not been carried out because there is no

available lectin which specifically binds to the NeuGc epitope. Recently, Park et al. reported that quantification of NeuGc was performed by 1,2-diamino-4,5-methylenedioxybenzene (DMB) derivatization of sialic acids, but did not distinguished the major glycan type such as N- and O-glycans and glycolipid-derived glycans [29]. In the present study, glycan-specific analysis was performed using a glycan release method by enzyme, and thus it was possible to obtain the more detailed information regarding NeuGc-terminated N-glycans structure by MS analysis. The MS analysis revealed that the quantity of NeuGc-containing N-linked glycan was slightly higher in the GalT-KO relative to the WT. The increase of the NeuGc quantity on fibroblasts matched previous results on GalT-KO pig organs [29, 106], which showed that heart, liver, and kidney of the GalT-KO pigs had a higher level of NeuGc than the WT. Taken together, we concluded that sialic acid-containing glycoconjugates including NeuGc antigen expression in pigs increase by deletion of α-galactosyltransferase gene.

For validation of N-linked glycan structures in pig fibroblasts, tandem mass spectrometry analysis was carried out using MALDI-QIT TOF MS in this study, and consequently N-glycan structures were characterized. However, unfortunately, other N-glycans, which were expected to contain NeuGc residues, were difficult to be assigned because their peak intensities are too low to be isolated for MS/MS. Nevertheless, this study showed here that MS-based approach enabled qualitative and quantitative analysis of cellular N-glycan including xenoantigens from pig WT and GalT-KO cells.

3.2 Comprehensive N-linked glycan analysis of GalT-KO pig kidney and comparative N-linked glycan profiling of WT and GalT-KO pig kidneys

3.2.1 Strategy for N-linked glycan analysis

The analytical scheme for N-glycome analysis used in this study is described as **Figure 3.7**. Cell membrane fractions were isolated from GalT-KO pig kidney tissues and then *N*-linked glycans were released from the membrane fractions by enzymatic *N*-deglycosylation. Ethanol precipitation was performed to remove *N*-deglycosylated proteins and enzymes. After PGC purification, N-linked glycans were analyzed by multi-mass spectrometric analyses using MALDI-TOF MS and ESI-MS. This comprehensive MS-based glycomic approach allowed structural characterization and quantitation of total N-linked glycans on GalT-KO pig kidney. Both MALDI-TOF MS coupled with exoglycosidase sequencing, and ESI-MS/MS analysis enabled to elucidate N-linked glycan structures. MALDI-TOF MS analysis combined with solid-phase permethylation method permits comprehensive identification of both neutral and acidic glycans and therefore simultaneous quantitation of total N-linked glycans on GalT-KO pig kidney because the solid-phase permethylation stabilized labile sialic acids by minimizing oxidative degradation and peeling reactions [93].

3.2.2 MS profiling of N-linked glycans using MALDI-TOF MS

The representative MALDI-TOF mass spectra obtained from the GalT-KO pig kidney are shown in **Figure 3.8** and **Table 3.2** represents the total N-glycome

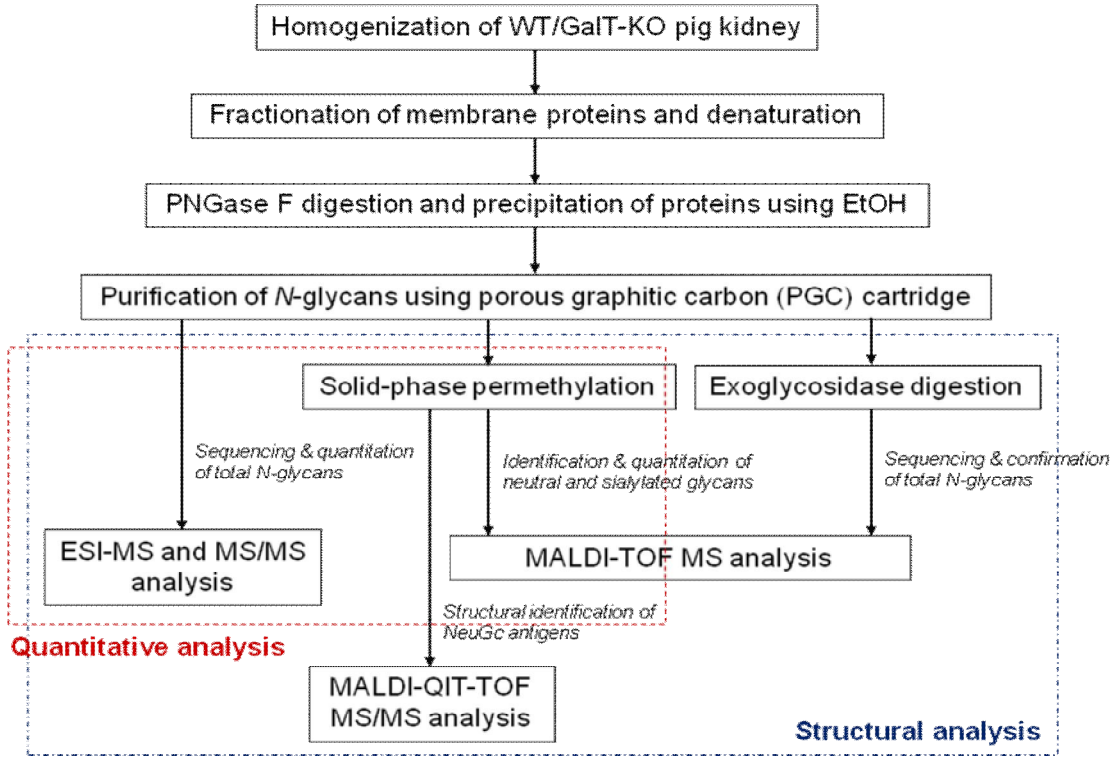

Figure 3.7 The comprehensive analytical scheme for N-glycome derived from GalT-KO pig kidney

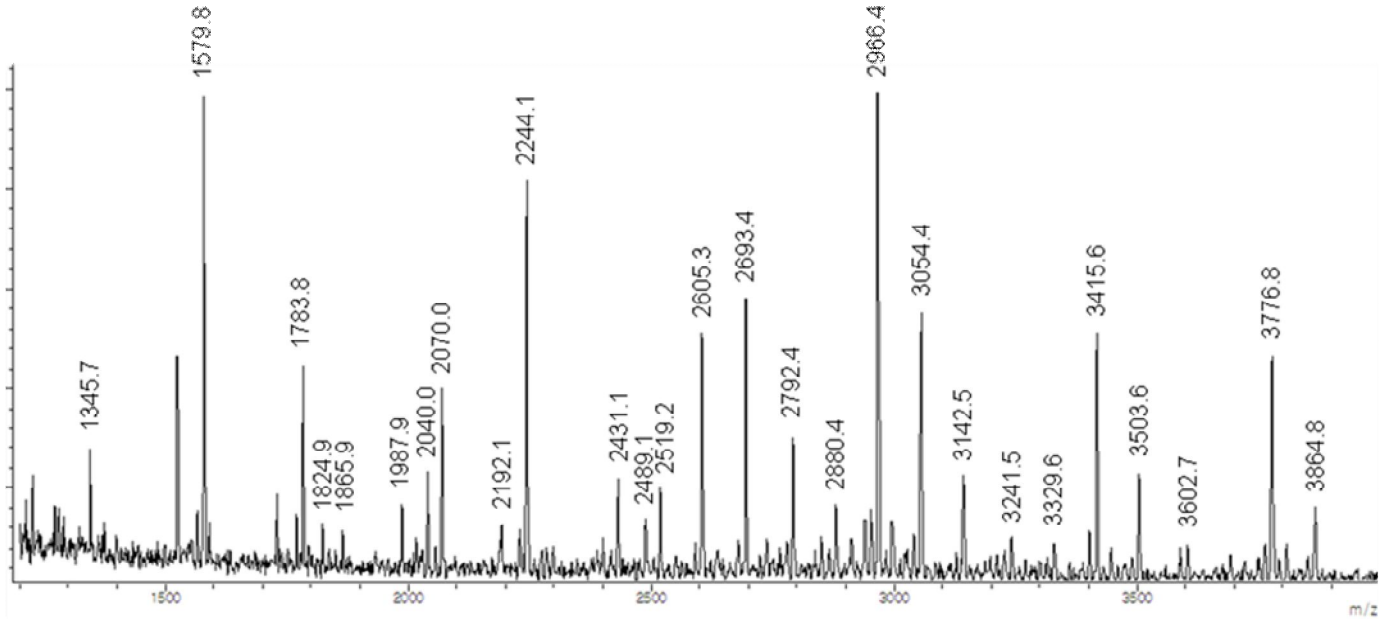

Figure 3.8 Positive-ion mode MALDI-TOF mass spectrum of *N*-linked glycans isolated from the GalT-KO pig kidney tissue

Table 3.2 Identification and characterization of total N-linked glycan structures derived from GalT-KO pig kidney tissue

m/z				Composition					Ion on ESI		Structure	Relative quantity (%)		evidence
ESI-MS		MALDI-TOF MS		H	HN	F	NA	NG	Ion[a]	Na		ESI-MS	MALDI-TOF MS	
Found	Calc.	Found	Calc.											
-	-	1345.7	1345.7	3	2	1	0	0			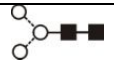	-	1.4 (±0.22)	MALDI-TOF MS
1169.3	1169.3	-	-	4	2	0	0	0	a	0	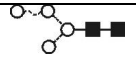	1.4	-	ESI-MS/MS
-	-	1416.7	1416.7	3	3	0	0	0			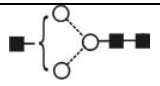	-	0.7 (±0.15)	MALDI-TOF MS
1331.4	1331.4	1579.8	1579.8	5	2	0	0	0	a	0	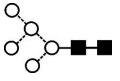	11.4	4.3 (±0.16)	MALDI-TOF MS ESI-MS/MS
1356.4	1356.4	1590.8	1590.8	3	3	1	0	0	a	0	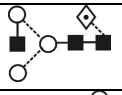	2.2	0.8 (±0.20)	MALDI-TOF MS ESI-MS/MS
1372.4	1372.4	1620.8	1620.8	4	3	0	0	0	a	0	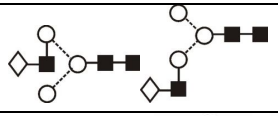	1.0	0.4 (±0.17)	MALDI-TOF MS ESI-MS/MS
-	-	1982.0	1982.0	4	3	0	1	0	-	-	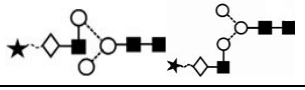	-	0.3 (±0.11)	MALDI-TOF MS

1413.5	1413.5	-	-	3	4	0	0	0	a	0	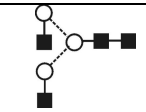	0.5	-	ESI-MS/MS
1493.5	1493.5	1783.9	1783.9	6	2	0	0		a	0	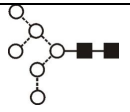	5.0	2.7 (±0.09)	MALDI-TOF MS ESI-MS/MS
1518.5	1518.5	1794.9	1794.9	4	3	1	0		a	0	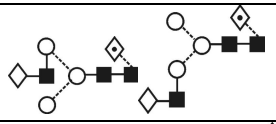	0.9	0.6 (±0.05)	MALDI-TOF MS ESI-MS/MS
1711.6	1711.6	2156.0	2156.0				1		b	1	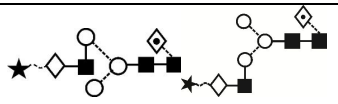	0.7	0.5 (±0.19)	MALDI-TOF MS ESI-MS/MS
1534.5	1534.5	1824.9	1824.9	5	3	0	0		a	0	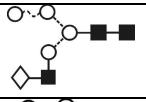	0.9	0.7 (±0.07)	MALDI-TOF MS ESI-MS/MS
1727.6	1727.6	2186.1	2186.1	5	3	0	1		b	0	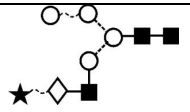	0.7	0.6 (±0.18)	MALDI-TOF MS ESI-MS/MS
1559.5	1559.5	1835.9	1835.9	3	4	1	0		a	0	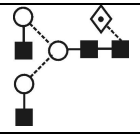	0.8	0.4 (±0.22)	MALDI-TOF MS ESI-MS/MS
1575.5	1575.5	1865.9	1865.9	4	4	0	0		a	0	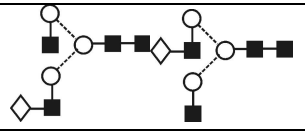	0.9	0.8 (±0.09)	MALDI-TOF MS ESI-MS/MS

1768.6	1768.6	-	-	4	4	0	1		b	0	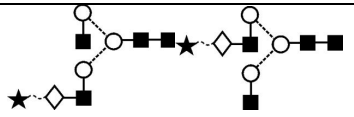	0.5	-	ESI-MS/MS
1655.5	1655.5	1988.0	1988.0	7	2	0	0		a	0	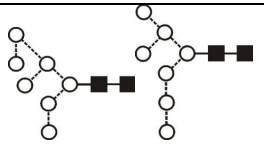 Major	1.9	1.2 (±0.18)	MALDI-TOF MS ESI-MS/MS
1680.5	1680.5	1999.0	1999.0	5	3	1	0		a	0	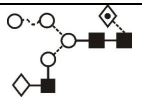	0.2	0.2 (±0.23)	MALDI-TOF MS ESI-MS/MS
1696.5	1696.5	2029.0	2029.0	6	3	0	0		a	0	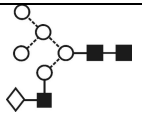	0.5	0.6 (±0.04)	MALDI-TOF MS ESI-MS/MS
-	-	2390.2	2390.2	6	3	0	1				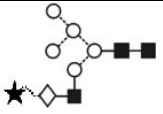		0.6 (±0.17)	MALDI-TOF MS
1721.6	1721.6	2040.0	2040.0	4	4	1	0		a	0	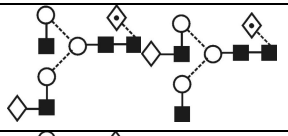	1.3	1.6 (±0.03)	MALDI-TOF MS ESI-MS/MS
1914.7	1914.7	2401.2	2401.2	4	4	1	1		b	0	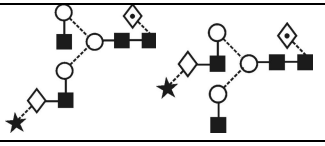	0.6	1.0 (±0.16)	MALDI-TOF MS ESI-MS/MS

1737.6	1737.6	2070.0	2070.0	5	4	0	0		a	0	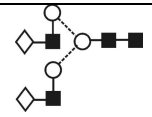	1.6	2.8 (±0.12)	MALDI-TOF MS ESI-MS/MS
1930.7	1930.7	2431.2	2431.2	5	4	0	1		b	0	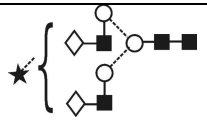	1.3	1.8 (±0.07)	MALDI-TOF MS ESI-MS/MS
2243.8	2243.8	2792.4	2792.4	5	4	0	2		b	1	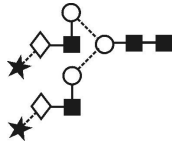	8.5	2.9 (±0.05)	ESI-MS/MS
1110.4	1110.4								c	0				
1762.6	1762.6	-	-	3	5	1	0		a	0	-	0.1	-	ESI-MS/MS
1817.6	1817.6	2192.1	2192.1	8	2	0	0		a	0	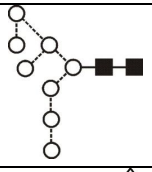	0.8	0.9 (±0.06)	MALDI-TOF MS ESI-MS/MS
1873.7	1873.7	-	-	5	3	1	1		b	0	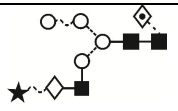	0.3	-	ESI-MS/MS
1883.6	1883.7	2244.1	2244.1	5	4	1	0		a	0	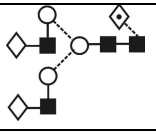	2.2	6.0 (±0.11)	MALDI-TOF MS ESI-MS/MS

2076.7	2076.7	2605.3	2605.3	5	4	1	1		b	0	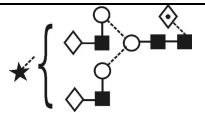	1.5	4.5 (±0.05)	MALDI-TOF MS ESI-MS/MS
-	-	2635.3	2635.3	5	4	1	0	1	-	-	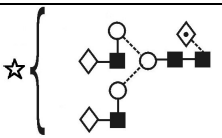	-	0.8 (±0.21)	MALDI-TOF MS
2389.8	2389.8	2966.4	2966.4	5	4	1	2		b	1	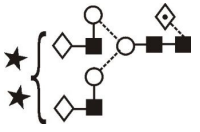	17.6	9.8 (±0.12)	MALDI-TOF MS ESI-MS/MS
1183.4	1183.4								c	0				
-	-	2996.5	2996.5	5	4	1	1	1	-	-	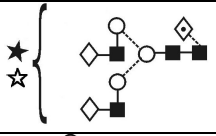	-	1.3 (±0.09)	MALDI-TOF MS
1924.6	1924.6	2285.1	2285.1	4	5	1	0		a	0	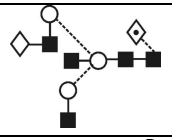	0.3	0.6 (±0.06)	MALDI-TOF MS ESI-MS/MS
2117.8	2117.8	-	-	4	5	1	1		b	0	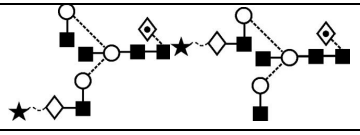	0.1		ESI-MS/MS

1940.6	1940.6	2315.1	2315.1	5	5	0	0		a	0	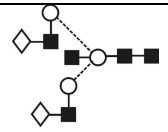	0.1	0.5 (±0.18)	MALDI-TOF MS ESI-MS/MS
2133.8	2133.8	-	-	5	5	0	1		b	0	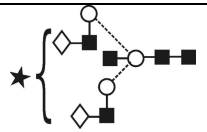	0.1		ESI-MS/MS
1979.6	1979.6	-	-	9	2	0	0		a	0	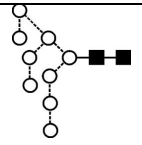	0.3		ESI-MS/MS
2086.7	2086.7	2489.2	2489.2	5	5	1	0		a	0	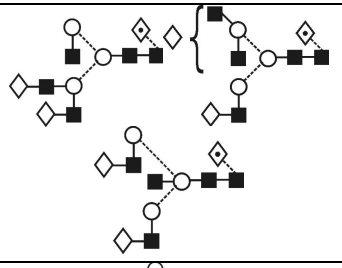	0.3	1.3 (±0.02)	MALDI-TOF MS ESI-MS/MS
2279.8	2279.8	2850.4	2850.4	5	5	1	1		b	0	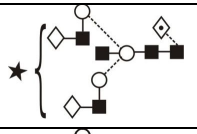	0.2	1.0 (±0.02)	MALDI-TOF MS ESI-MS/MS
1284.9	1284.9	3211.5	3211.6	5	5	1	2		c	0	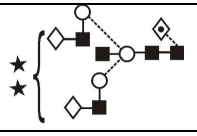	trace	0.9 (±0.08)	MALDI-TOF MS ESI-MS/MS

2102.7	2102.7	2519.2	2519.2	6	5	0	0		a	0	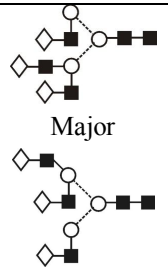 Major	0.3	1.7 (±0.18)	MALDI-TOF MS ESI-MS/MS
2295.8	2295.8	2880.4	2880.4				1		b	0	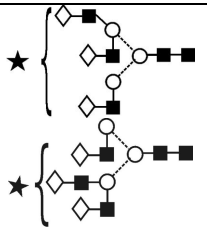	0.2	1.6 (±0.02)	MALDI-TOF MS ESI-MS/MS
1292.9	1292.9	3241.6	3241.6				2		c	0	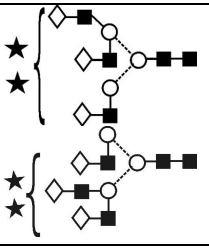	3.1	1.3 (±0.04)	MALDI-TOF MS ESI-MS/MS
-	-	3602.7	3602.8				3		-	-	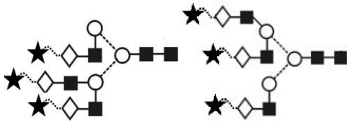	-	1.1 (±0.18)	MALDI-TOF MS

2248.8	2248.8	2693.4	2693.4			1	0		a	0	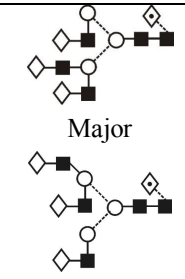 Major	0.5	5.2 (±0.08)	MALDI-TOF MS ESI-MS/MS
2441.9	2441.9	3054.5	3054.5				1	0	b	0	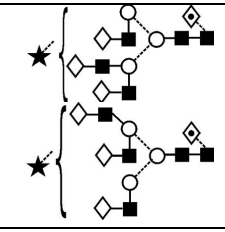	0.3	5.5 (±0.28)	MALDI-TOF MS ESI-MS/MS
-	-	3084.5	3084.5				0	1			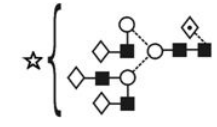	-	0.7 (±0.19)	MALDI-TOF MS MALDI-QIT-TOF MS/MS
1366.0	1366.0	3415.6	3415.7				2	0	c	0	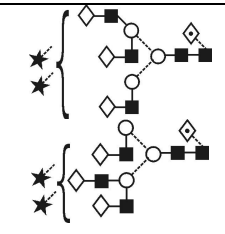 Major	10.3	6.5 (±0.32)	MALDI-TOF MS ESI-MS/MS

-	-	3445.6	3445.7				1	1			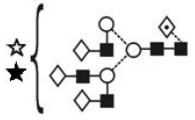	-	0.9 (±0.10)	MALDI-TOF MS MALDI-QIT-TOF MS/MS
1511.5	1511.5	3776.8	3776.9				3	0	d	0	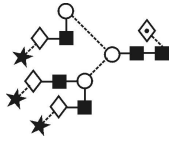 Major	5.5	6.0 (±0.03)	MALDI-TOF MS ESI-MS/MS
1522.5	1522.5							0	c	1	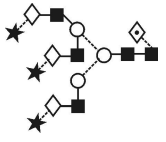			
-	-	3806.8	3806.9				2	1	-	-	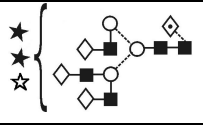	-	1.0 (±0.08)	MALDI-TOF MS

-	-	2764.4	2764.4	6	6	0	0	0	-	-	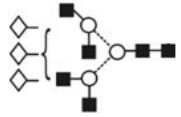	-	0.6 (±0.09)	MALDI-TOF MS
-	-	2938.5	2938.5	6	6	1	0	0	-	-	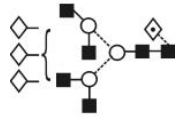	-	1.2 (±0.13)	MALDI-TOF MS
2467.8	2467.8	-	-	7	6	0	0		a	0	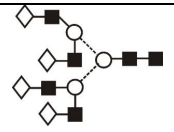	trace	-	ESI-MS/MS
-	-	3329.6	3329.7				1	0	-	-	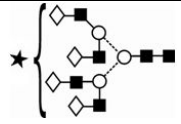	-	1.1 (±0.02)	MALDI-TOF MS
1475.5	1475.5	3690.7	3690.8				2	0	c	0	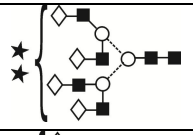	2.0	0.9 (±0.07)	MALDI-TOF MS ESI-MS/MS
1080.4	1080.4	-	-				3		c	0	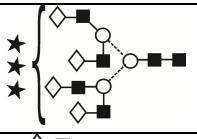	trace		ESI-MS/MS
2613.9	2613.9	3142.6	3142.6			1	0		a	0	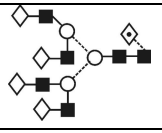	0.1	2.8 (±0.05)	MALDI-TOF MS ESI-MS/MS

		3503.6	3503.7				1				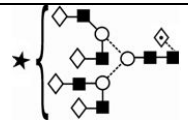		2.9 (±0.14)	
1548.5	1548.5	3864.8	3864.9				2		c	0	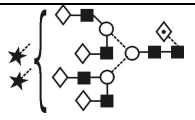	4.0	2.4 (±0.23)	MALDI-TOF MS ESI-MS/MS
1694.1	1694.1	-	-				3		c	0	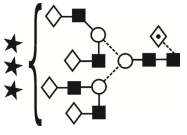	4.3		ESI-MS/MS
1149.1	1129.1	-	-				3		d	0				
1705.1	1705.1	-	-				3		c	1				
1226.1	1226.1	-	-				4		d	0	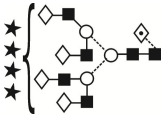	0.7		ESI-MS/MS
1850.6	1850.6	-	-				4		c	1				
1861.6	1861.6	-	-				4		c	2				
1731.1	1731.1	3952.8	3953.0	8	7	1	1 2		c	0	-	0.4 0.8		MALDI-TOF MS ESI-MS/MS
1250.8	1250.8	-	-				3		d	0		0.7		ESI-MS/MS
1372.5	1372.5	-	-	9	8	1	3		d	0	-	0.5		ESI-MS/MS
1469.6	1469.5	-	-				4		d	0		0.1		ESI-MS/MS
1477.1	1476.8	-	-						d	1				

[a]Ions detected on ESI-MS: (a) $[M+(H_2PO_4)]^-$, (b) $[M-H]^-$, (c) $[M-H_2]^{2-}$, (d) $[M-H_3]^{3-}$ (e) $[M+Na]^+$

profile of the GalT-KO pig kidney from the MALDI-TOF MS and ESI-MS results. The oligosaccharide compositions of hexoses (H), *N*-acetylhexosamines (HN), fucoses (F), N-acetylneuraminic acids (NA), and N-glycolylneuraminic acids (NG) were proposed based on their *m/z* values including adduct molecules. N-linked glycan profile of GalT-KO pig kidney revealed remarkable diverse N-linked glycan repertoire which is composed of both high-mannose type glycans and complex/hybrid type glycans as shown in **Table 3.2**. Many of complex type glycans were sialic acid or/and fucose-containing glycans. However, α-Gal antigen as a major carbohydrate antigen in xenotransplantation was not observed indicating that the α-Gal-containing N-glycan was not expressed on GalT-KO kidney. On the other hand, eight NeuGc-containing N-glycans [observed at *m/z* 2186.2 2635.2 2880.3 2996.3 3026.4 3084.4 3445.4 3806.5 ($[M + Na]^+$)] were found in this study, which has been considered as one of non-Gal antigens. This result indicated that there are still NeuGc antigens present on the pig tissues after knockout of α1,3-galactosyltransferase gene.

3.2.3 Structural analysis of N-linked glycans by exoglycosidase sequencing and ESI-MS/MS

To validate the structure of N-linked glycans in GalT-KO pig kidney, enzymatic analysis using exoglycosidases was used in this study. First, it was confirmed the absence of α-Gal antigen on GalT-KO pig kidney using α-galactosidase from green coffee bean. It was reported that a contaminating activity of β-galactosidase was not detected in the α-galactosidase according to the

manufacturer. Despite the treatment with this exoglycosidase, MALDI-TOF mass spectrum showed no mass shifts of oligosaccharide peaks **(Figure 3.9)**, and thus indicated that the Galα1,3Gal residue of N-linked glycan was not expressed on GalT-KO pig kidney. In contrast to the α-galactosidase, β-galactosidase from bovine testis removed all non-reducing Gal residues from N-linked glycans (complex type glycans). β-hexosaminidase from *S. pneumoniae* reduced all oligosaccharides to the core structure of N-linked glycan with and without fucose ($Man_3GlcNAc_2Fuc_1$ or $Man_3GlcNAc_2$). In contrast to the complex type glycans, there remained high-mannose type glycans which are resistant to activities of exoglycosidases used. This sequential exoglycosidase digestion with sialidase, with sialidase and β-galactosidase, and with sialidase, β-galactosidase, and β-hexosaminidase allowed confirming the chemical structure of total N-linked glycans in GalT-KO pig kidney **(Figure 3.10)**.

The tandem mass spectrometry analysis using ESI-MS provides direct support for the enzymatic sequencing of oligosaccharide. Ion mobility was used to separate ions in different charged states and to reduce remaining contamination [116, 117]. Negative ion MS/MS spectra were recorded in the transfer cell and interpreted according to previous studies [118-121]. Fragments were formed by proton extraction from hydroxyl groups by the phosphate anion to give a $[M-H]^-$ ion which then fragments further to give the diagnostic ions. Unlike neutral glycans, sialylated glycans was less informative because ionization is mainly by direct loss of a proton from the carboxylic group of the sialic acid. Thus, for structural determination, an additional experiment was performed in which the sialic acids were hydrolyzed and the resulting neutral glycans were fragmented. Sample was

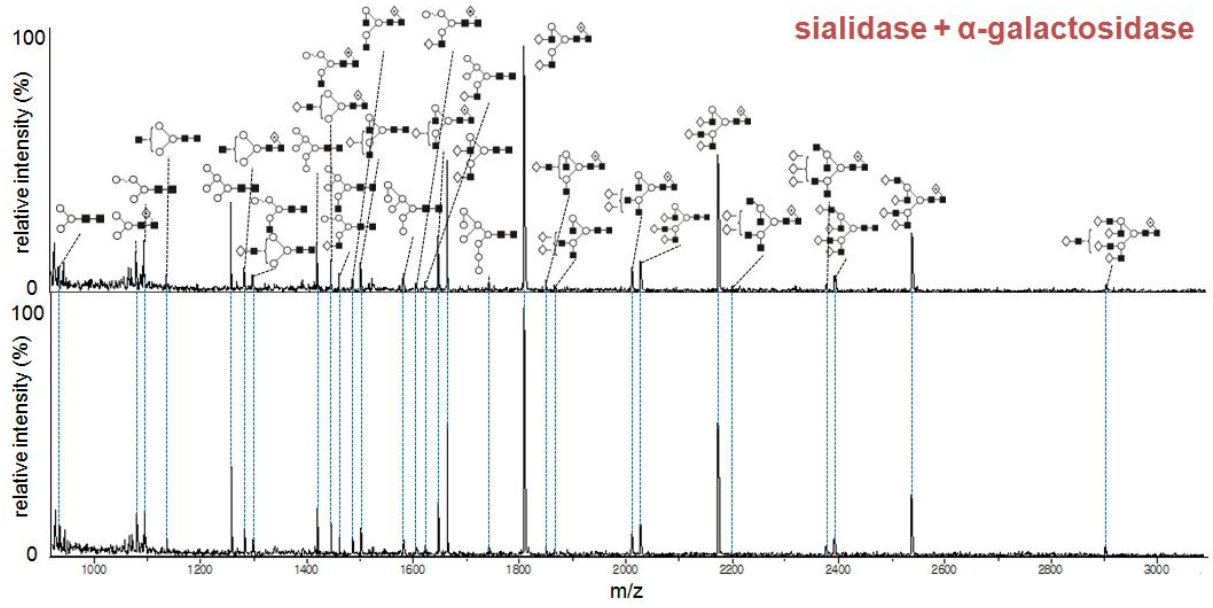

Figure 3.9 Confirmation of the absence of α-Gal antigen on GalT-KO pig kidney by α-galactosidase digestion

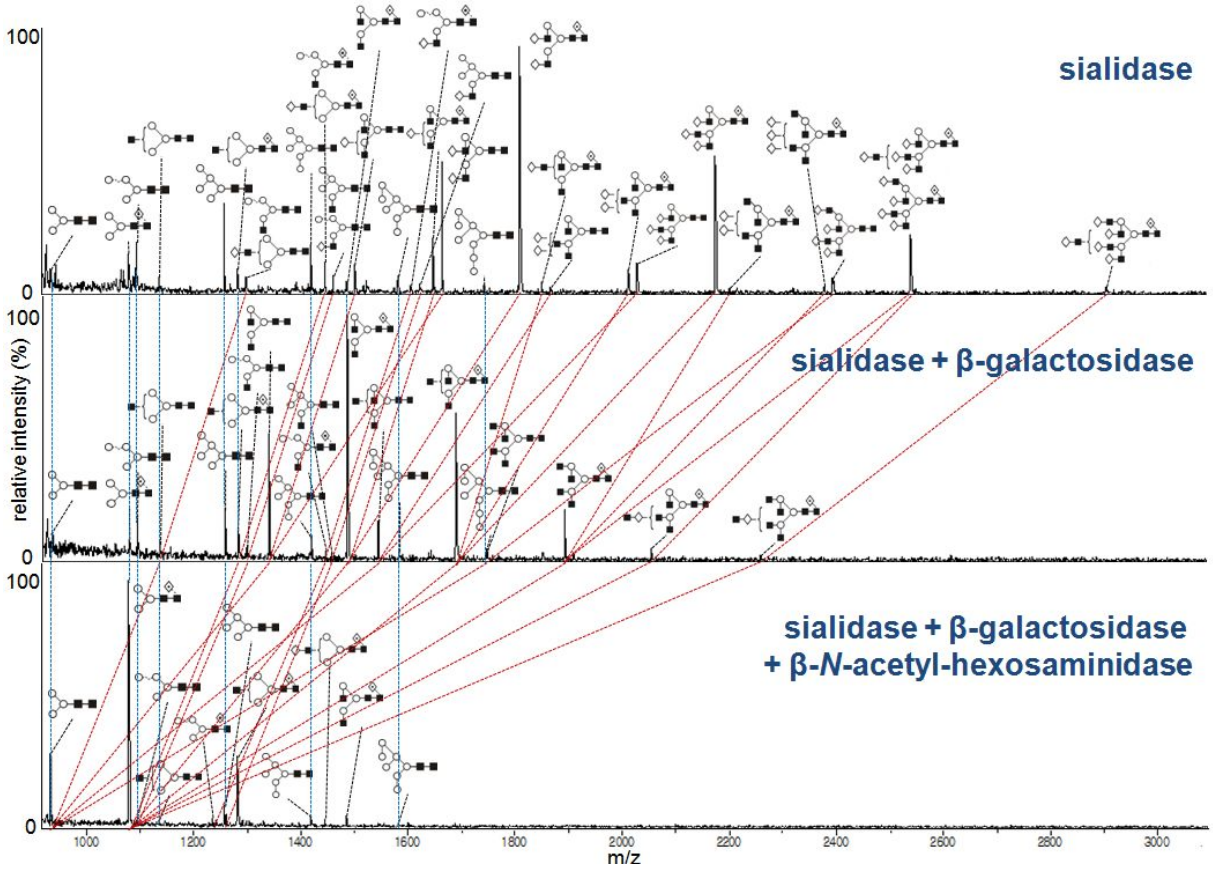

Figure 3.10 Validation of N-linked glycan structures on GalT-KO pig kidney by exoglycosidase sequencing

treated with acetic acid to remove sialic acids and the neutral glycans were examined by ESI-MS/MS. Neutral glycans were the same as in untreated sample showing that sialylated glycans were all derivatives of these compounds. As a result, mass fragmentation patterns of high-mannose type and complex/hybrid type glycans are consistent with our previous MS/MS results on WT pig kidney [106, 107] except for α-Gal-terminated glycans. In the present study, there are no $^{1,3}A_4$ ions at *m/z* 586.4, which is the representative (or typical) α-Gal fragment ion ($Hex_2HexNAc\text{-}OCH{=}CHO^-$) [122], indicating that α-Gal residue of N-linked glycans was not presented on GalT-KO pig kidney. **Table 3.2** represents N-linked glycan structures identified by MS/MS analysis.

3.2.4 Structural validation of non-Gal antigens using MALDI-QIT-TOF MS/MS and ESI-MS/MS

The structures of NeuGc antigens were confirmed in GalT-KO pig kidney using tandem mass spectrometric analyses. The mass fragmentation pattern represents predominant b- and y-ions [nomenclature proposed by Domon and Costello [75]], which were produced from glycosidic bond cleavage, while cross ring fragment ions (a- and x-ions) are weak or absent in MALDI-QIT-TOF MS/MS. The representative MS/MS spectra are shown in **Figure 3.11**. The presence of NeuGc residue was validated by a diagnostic fragment b-ion at *m/z* 877.4 corresponding to non-reducing NeuGcHexHexNAc. In addition, this MS/MS analysis revealed that there are apparently mono-NeuGc- containing N-linked oligosaccharides expressed on the pig kidney tissue. ESI-MS analysis provides

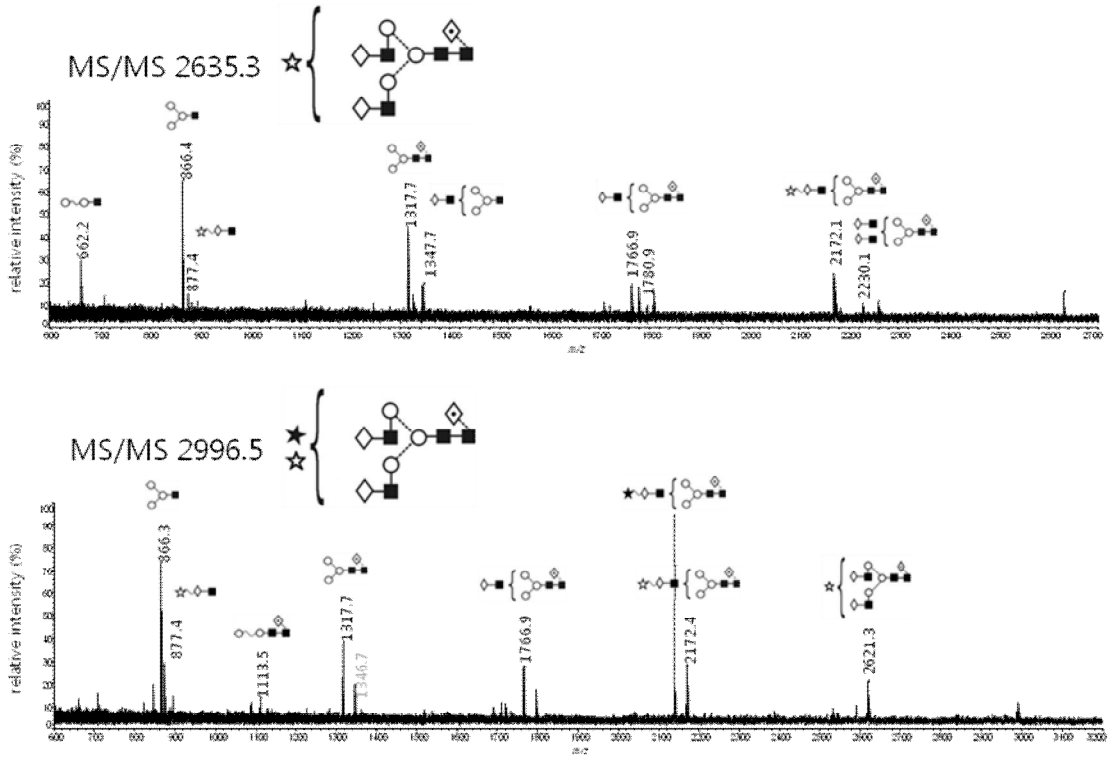
MS/MS 2635.3
relative intensity (%)
662.2
866.4
877.4
1317.7
1347.7
1766.9
1780.9
2172.1
2230.1
MS/MS 2996.5
relative intensity (%)
866.3
877.4
1113.5
1317.7
1346.7
1766.9
2172.4
2621.3

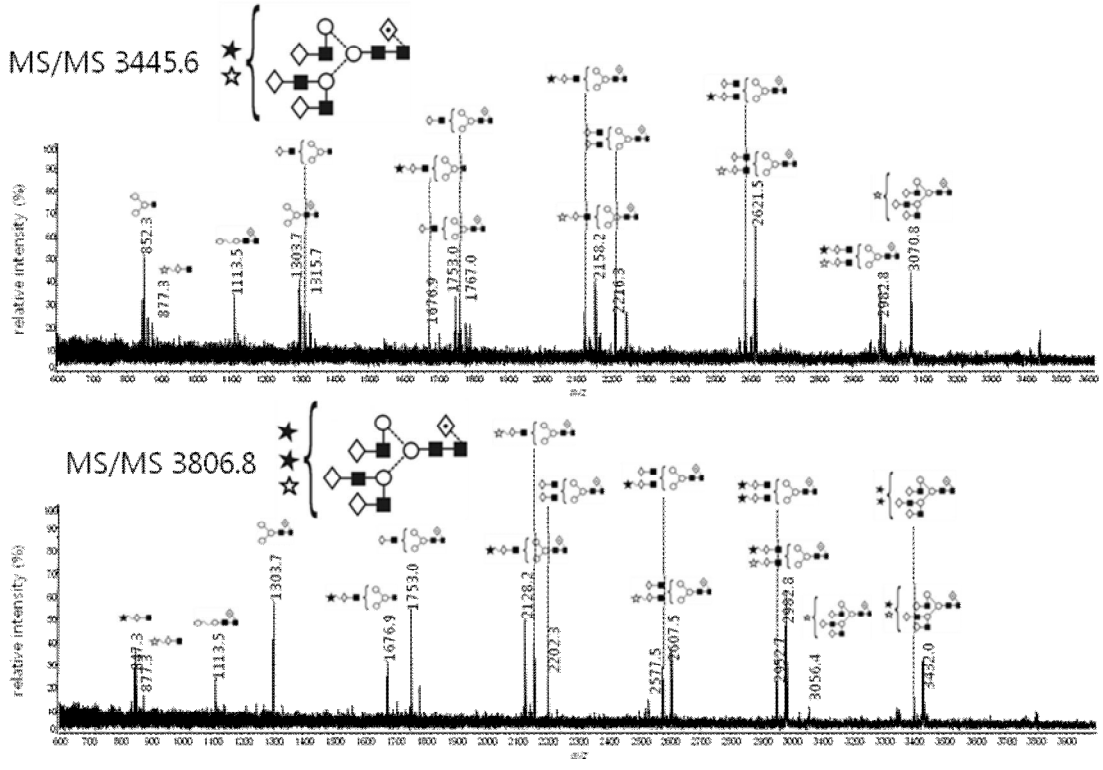

Figure 3.11 Structural identification of NeuGc-containing N-glycans (*m/z* 2635.3, 2996.5, 3445.6, and 3806.8) by MALDI-QIT-TOF MS/MS

direct support for MALDI-TOF MS analysis.

3.2.5 Quantitation of N-linked glycans using MALDI-TOF MS coupled with solid-phase permethylation and ESI-MS

MALDI-TOF MS analysis combined with permethylation was previously reported as a good quantitative methodology [113]. Moreover, solid-phase permethylation was demonstrated to be more quantitative than the traditional permethylation [93]. Therefore, MALDI-TOF MS analysis combined with this derivatization method was used for pig N-glycome quantitation in this study. For more accurate quantitation, the relative level of oligosaccharides was measured from peak intensities of each oligosaccharide among peak intensities of total oligosaccharides. By integrating from the first to the third isotopic peak intensities, the peak intensity of each oligosaccharide was obtained. To identify glycosylation change by the deletion of α1,3-galactosyltransferase gene, N-glycan profiles on GalT-KO pig kidney was compared with our previous results on WT [106]. In contrast to WT, which showed a large array of α-Gal-containing glycans (35.2-42.0% total N-linked glycans) **(Table 3.3)**, the GalT-KO showed extensive sialic acid-containing glycan expression (58.0% total N-linked glycans) in **Figure 3.12a**. The previous analysis on WT identified sialic acid-containing N-glycans including NeuGc antigens, but failed to quantitatively measure the abundance of sialic acid-terminated glycans because desialylated glycans were quantified. The present study made up for the direct comparison of sialylation between WT and GalT-KO by quantifying both sialylated glycans. As a result, the relative abundances of

Table 3.3 Relative quantitation of N-linked glycan types on GalT-KO pig kidney compared with a previous study on WT [55]

	relative quantity (%)	
	W.T	GT-KO
α-Gal type	43.9 (35.3)	0.0
high-mannose type	16.2 (32.2)	9.1
others (including sialylation)	39.9 (32.5)	79.3
fucosylation	37.9 (30.7)	71.9

(): quantified by ESI-MS

sialylated glycans in GalT-KO were higher than those in WT (41.4% total N-linked glycans). MS analysis also revealed a slightly higher level of NeuGc-terminated N-glycans on GalT-KO (7.9%) relative to the WT (3.7%) as shown in **Figure 3.12b**. In addition, the result revealed that the relative quantity of fucose-containing glycans increased in the GalT-KO (71.9% total N-linked glycans) compared to WT results [106].

3.2.6 Discussion

In xenotransplantation, the carbohydrate antigen as well as the protein antigen has been an important factor to induce immune rejections, and thus to overcome this xenograft failure. However, it is difficult to extensively profile the cellular glycome array expressed on the surface of non-human primates (e.g., pigs) due to structural diversity and complexity of the glycome. The present study reported on a qualitative and quantitative N-glycome analysis of GalT-KO pig kidney using MS-based approaches. In addition, by integrating this study with our previous results regarding the WT pig [55], an in-depth comparison of N-glycomes between WT and GalT-KO pigs was carried out. Considering that cellular glycomes are complex and diverse repertoire as mentioned above, this comprehensive glycomic analysis would be an important approach for further glycobiology studies.

Although GalT-KO non-human primates were produced for preventing HAR, there has been a controversy over the elimination of α-Gal antigens. A previous study demonstrated that the GalT-KO pig expressed low levels of α-Gal antigen, and other α1,3-galactosyltransferase, GGTA2 was reported to synthesize

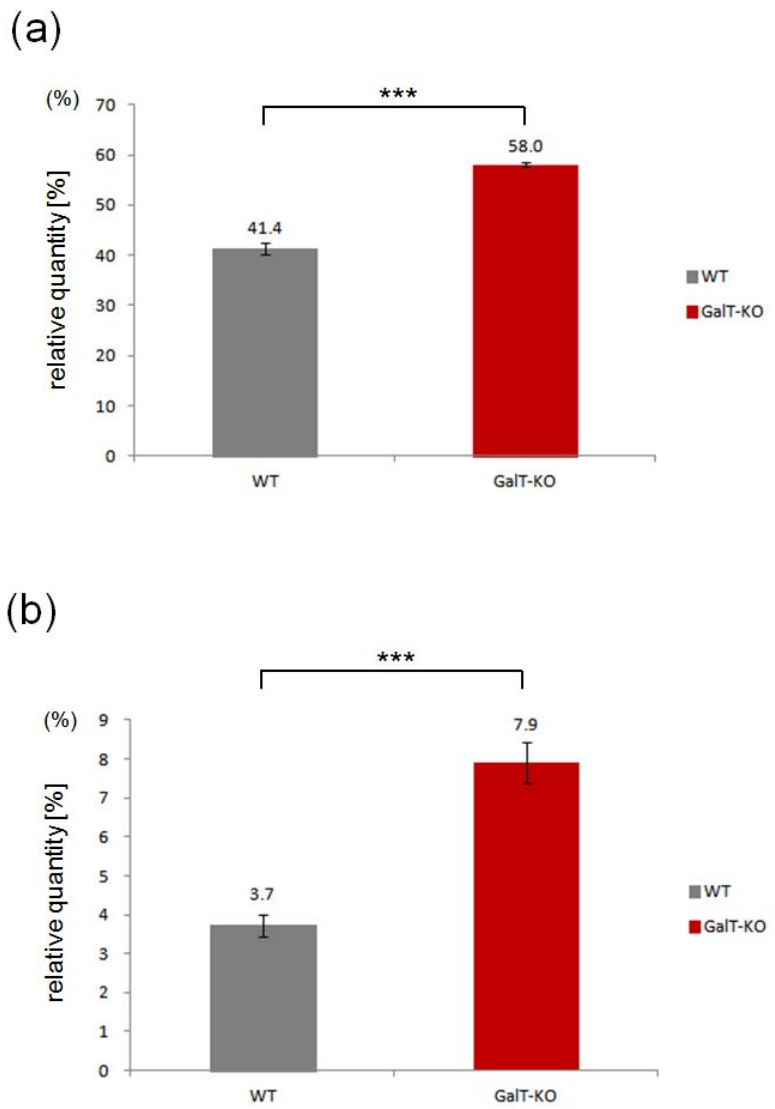

Figure 3.12 Comparative quantitation of (a) sialic acids and (b) NeuGc-containing N-glycans derived from WT and GalT-KO pig kidney tissues. The annotation with asterisks in this figure is as follows: ***: $p < 0.001$

isoglobotriaosylceramide (iGb3; Galα1,3Galβ1,4Glcβ1Ceramid) as an alternative α-Gal antigen candidate in GalT-KO non-human primates [43, 44], suggesting that there are two different glycan processing pathway for the synthesis of Galα1,3Gal disaccharide [45]. Therefore, it is important to confirm the absence of terminal Galα1,3Gal residues in GalT-KO pig kidney. The current analysis showed here the complete absence of α-Gal antigens on GalT-KO pig kidney. The iGb3 glycolipid antigen was not observed as well because oligosaccharide release method was used to release N-linked glycans from proteins by PNGase F digestion.

The increase or decrease of specific oligosaccharides is a significant consideration of oligosaccharide processing as well as presence or absence of them. This study enabled MS-based quantitative analyses of N-linked glycans derived from WT and GalT-KO pig kidneys as well as the identification of carbohydrate antigens. The current analysis revealed that abundance of sialic acid-terminated glycans is higher in GalT-KO relative to WT, and is there consistent with previous studies [29, 123]. However, due to limitations of lectin-based assay used, the previous studies did not explain the correlation of oligosaccharide structure with the oligosaccharide quantitative alteration. Here, the chemical structures of total N-linked glycans in pig kidneys were identified, and were quantified relatively as shown in **Table 3.2**. The present study suggested that both α1,3-galactosyltransferase and sialyltransferase competitively recognize an identical acceptor substrate which contains galactose of N-acetyllactosamine, and the activity of α1,3-galactosyltransferase is relatively higher than that of sialyltransferase in WT pigs. In contrast to the WT, sialyltransferases in GalT-KO may predominantly participate in the transfer of a sialic acid to a terminal exposed

galactose of N-acetyllactosamine because of the abolishment of α1,3-galactosyltransferase activity, and therefore more sialic acid-linked glycans are present on GalT-KO. Interestingly, the current analysis also revealed that fucose level of N-linked glycans in GalT-KO is higher than WT. However, in contrast to the increase of sialic acid-linked glycans, it is less obvious that the relative quantity of N-linked glycans with a core fucose is increased in GalT-KO. This aberrant glycosylation, which is likely to be affected by perturbed oligosaccharide synthetic pathways, was observed in previous studies on GalT-KO pig organs [63, 115]. In addition, recent proteomics studies on GalT-KO primates showed that a wide variety of proteins changed their expression levels [30, 124]. Taken together, this study suggested that the deletion of α1,3-galactosyltransferase gene may influence the expression of other carbohydrate antigens including non-Gal antigens as well as the elimination of Galα1,3Gal residue.

Another xenoantigenic carbohydrate, NeuGc (e.g., H-D antigen), has been regarded as one of non-Gal antigens participating in immune rejections. As noted above, although GalT-KO pigs were produced, there still remain NeuGc-containing oligosaccharides presented on pig cell surfaces, and the aberrant glycosylation on GalT-KO pig raises the possibility that the NeuGc level may change. This study, showed these NeuGc-containing N-glycans on GalT-KO pig kidney using MS. After α1,3-galactosyltransferase deficiency in pigs, some studies have progressed and reported to delineate GalT-KO pig glycome using lectin-based array, but failed to detect NeuGc antigen because there is no available lectin which is specific for the NeuGc residue [63, 115].`Recently, NeuGc residues, which used chemical reagent fluorescence labeling, were detected on GalT-KO pig organs [29]. However,

mass spectrometric analysis allowed for structural identification of these NeuGc antigens compared to the fluorescence detection. In addition, quantitative analysis revealed here that the level of NeuGc was higher in GalT-KO pig kidney relative to WT, and is therefore consistent with a previous study on GalT-KO pig tissues [29]. In the context of NeuGc biosynthesis, GalT-KO pigs showed a higher expression of NAD^+-isocitrate dehydrogenase (IDH) [30], which is cytidine monophosphate-N-acetylneuraminic acid hydroxylase (CMAH) cofactor. This CMAH enzyme is absent on humans and responsible for NeuGc biosynthesis [125]. Moreover, Saethre et al. demonstrated that the anti-HD antibodies specific for the NeuGc antigen accounted for a large proportion of anti-non-Gal antibodies in human sera, and these anti-HD antibody levels correlated with activation of GalT-KO pig endothelial cell [28]. Therefore, it should be emphasized that the NeuGc antigen is an important carbohydrate antigen to overcome xenograft failures in GalT-KO pig era.

Chapter 4. Development of the database of qualitative and quantitative pig glycome repertoire

4.1 Pig glycome database and query in the database

The relational pig glycome database was built up from specific pathogen-free Chicago Medical School miniature pig [126] glycan profiles, which have been qualitatively and quantitatively characterized by various mass spectrometry-based techniques. It includes N-glycomes from pig kidney [55], endothelial cells, islets [56], corneal endothelial cells, keratocytes [127], heart and glycosphingolipid-derived glycans from pig endothelial cells and islets [54]. The O-glycomes from pig kidney, endothelial cells [58] and heart [57] are also included.

Two major query options are implemented in the pig glycome database, namely, 'pig tissue/cell specific glycans' and 'mass spectrometry-based glycan searching'. The 'pig tissue/cell specific glycans' option allows the retrieval of glycans derived from a specific pig tissue/cell. Users can obtain the full lists of glycans by clicking a specific pig organ or cell icon. It is also possible to set parameters including glycan epitope. On the other hand, the 'mass spectrometry-based glycan searching' is a way to look for a specific glycan information from a mass-to-charge ratio (m/z). If the users input the experimental mass value (m/z), the program enables the users to gather the possible glycan structures and organs. In addition, the pig glycome database allows users to set a mass tolerance that can be specified in Daltons ± of the measured value to avert no search result found because of instrumental variations. The users can also narrow down the list of the glycans by specifying several factors. It includes the followings: mass spectrometry instrument, glycan derivatization method, glycan type, ion mode, ion adducts and origin, but it will be updated continuously.

4.2 Database content

The search result from the pig glycome database contains mass value (m/z), derivatization, glycan type, structure, antigen, quantity and origin. The mass value is an experimental value of the corresponding glycan mass (mono-isotopic) analyzed using matrix-assisted laser desorption/ionization time-of-flight mass spectrometry or electrospray ionization mass spectrometry. The derivatization indicates the chemical derivatization for glycan analysis using mass spectrometry. All the glycans in the XDB are classified into three types: N-linked glycans (at the side chain of Asn), O-linked glycans (at the Ser/Thr residues) in glycoproteins and glycosphingolipid-derived glycans. Especially, the α-galactosylated glycans are labeled with 'α-Gal antigen' in the column of 'Antigen type'. The chemical structures were drawn with Oxford glycan nomenclature [128]. The relative quantity of glycans, which was measured by NP-HPLC or quantitative MS analysis, was incorporated in the result table as well. Additionally, pie graphs represent the relative quantities of each type of glycans (e.g. high-mannose glycans, α-Gal glycans, sialylated glycans and so on).

4.3 Use of the database program

Examples of using pig glycome database

There are two ways of searching for specific glycan information in XDB. One is a query on 'Pig tissue/cell specific glycans' and the other is on 'Mass spectrometry-

based glycan search'.

(1) The following describes how to searching all *N*-glycans derive from pig endothelial cells using a query on 'Pig tissue/cell specific glycans'.

The user can set 4 parameters (species, glycan type, cell type and glycan epitope) before submitting a query or click a picture of pig endothelial cells for viewing the result. In this case, 'pig', '*N*-linked glycan', 'endothelial cells' and 'all' were selected in species, glycan type, cell/tissue type and glycan epitope section, respectively. Next, the user can click 'submit' button. Please refer to **Figure 4.1**. Once the query is submitted, the search result page is displayed **(Figure 4.2)**. The search result page displays a table list and a pie graph. The table list contains mass to charge ratio value (*m/z*), derivatization, glycan type, structure, antigen, quantity and origin. The pie graph represents relative quantities of each type of glycans such α-Gal glycans, sialylated glycans

(2) The following describes how to searching *N*-glycans having *m/z* 1809.6 from pig organs using a query on 'Mass spectrometry-based glycan search'.

There are a number of parameters that have to be set before submitting a query **(Figure 4.3)**.

a. The user can enter a single mass to charge ratio (*m/z*) value to search against the database.

b. The user can specify a mass tolerance threshold in Daltons +/- based on the mass accuracy of the user's instrument. Entering a number from 0.5 to 1.0 is recommended for an appropriate result.

c. The user has the option to search for mass spectrometry instruments, namely,

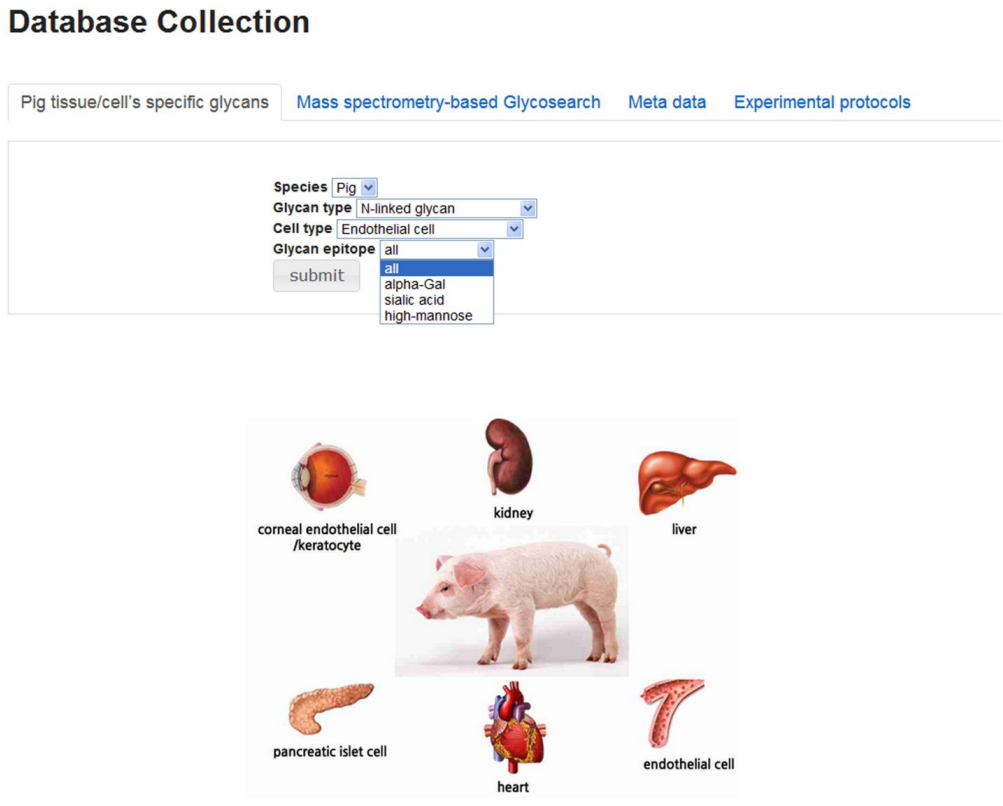

Figure 4.1 Pig glycome database interface displaying the entered parameters for searching pig endothelial cells *N*-glycans

Search Result

MALDI-TOF MS [M+Na]+	ESI-MS [M+H2PO4]- or [M-H]-	Derivatization	Glycan	Composition	Structure	Antigen type	Quantity	Organ	Origin
933.4	1007.3	underivatised	N-glycan	(Hex)3 (HexNAc)2			1.6	endothelial cell	pig
1079.4	1153.3	underivatised	N-glycan	(Hex)3 (HexNAc)2 (Deoxyhexose)1			0.6	endothelial cell	pig
1095.4	1169.3	underivatised	N-glycan	(Hex)4 (HexNAc)2			0.3	endothelial cell	pig
1136.4	1210.3	underivatised	N-glycan	(HexNAc)1 + (Man)3(GlcNAc)2			0.6	endothelial cell	pig
1257.5	1331.4	underivatised	N-glycan	(Hex)2 + (Man)3(GlcNAc)2			3.4	endothelial cell	pig
1282.5	1356.4	underivatised	N-glycan	(HexNAc)1 (Deoxyhexose)1 + (Man)3(GlcNAc)2			0.5	endothelial cell	pig
1298.5	1372.4	underivatised	N-glycan	(Hex)1 (HexNAc)1 + (Man)3(GlcNAc)2			1.4	endothelial cell	pig
1339.5	1413.4	underivatised	N-glycan	(HexNAc)2 + (Man)3(GlcNAc)2			0.3	endothelial cell	pig
1419.5	1493.4	underivatised	N-glycan	(Hex)3 + (Man)3(GlcNAc)2			9.3	endothelial cell	pig
1444.6	1518.5	underivatised	N-glycan	(Hex)1 (HexNAc)1 (Deoxyhexose)1 + (Man)3(GlcNAc)2				endothelial cell	pig

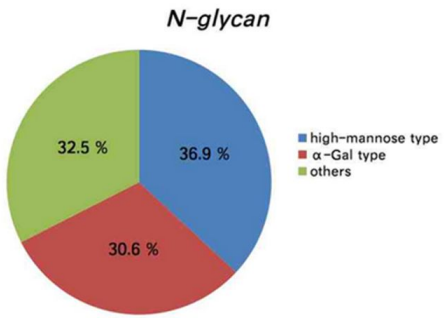

Figure 4.2 The search result page displaying pig endothelial cells *N*-glycans information in the pig glycome database

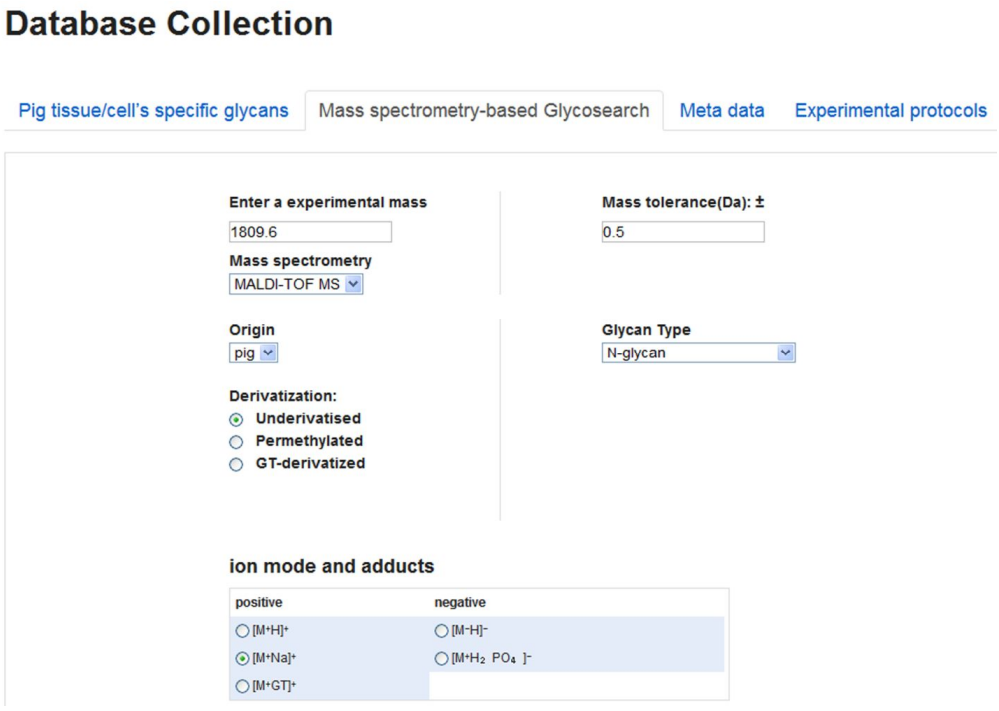

Figure 4.3 Pig glycome database interface showing the entered parameters for searching glycans having *m/z* 1809.6 (adducted to sodium ion) analyzed by MALDI-TOF MS

MALDI-TOF MS and ESI-MS.

d. The user can select one of three glycan types: *N*-glycan, *O*-glycan and glycolipid-derived glycan

e. The user also can choose a derivatization method for analysis of glycans. If any derivatization methods were not used, 'underivatised' can be selected.

f. Finally, The user has the option to search for ion mode (positive or negative) and the most common adducts (e.g. $[M+Na]^+$ or $[M+H_2PO_4]^-$) obtained by ionization process in the mass spectrometer.

g. After all parameters have been set, the user click 'search' button.

In this case, *m/z* value entered was 1809.6, the mass tolerance was set to 0.5 and MALDI-TOF MS in mass spectrometry was selected. Finally, the glycan type, derivatization and ion adduct selected were N-glycan, underivatization and $[M+Na]^+$, respectively.

Once the query is submitted, the search result page is displayed **(Figure 4.4)**. The search result contains specified mass to charge ratio value (*m/z*), derivatization, glycan type, structure, antigen, quantity and origin.

4.4 Discussion

Although many of the well-established glycan databases offer the detailed glycan structures, it is difficult to solely collect the pig glycans according to the specific organ or cell, which is a promising candidate for xenotransplantation. Therefore, in this study, an unique and specialized database have been built to provide reliable information on glycans, which are derived from tissues and cells of

Search Result

MALDI-TOF MS [M+Na]+	ESI-MS [M+H2PO4]- or [M-H]-	Derivatization	Glycan	Composition	Structure	Quantity	Organ	Origin
1809.6	1883.6	underivatised	N-glycan	(Hex)2 (HexNAc)2 (Deoxyhexose)1 + (Man)3(GlcNAc)2		5.2	kidney	pig
1809.7		underivatised	N-glycan	(Hex)2 (HexNAc)2 (Deoxyhexose)1 + (Man)3(GlcNAc)2		10.3	corneal endothelial cell	pig
1809.4		underivatised	N-glycan	(Hex)2 (HexNAc)2 (Deoxyhexose)1 + (Man)3(GlcNAc)2		5.4	keratocyte	pig
1809.6	1883.6	underivatised	N-glycan	(Hex)2 (HexNAc)2 (Deoxyhexose)1 + (Man)3(GlcNAc)2		7.0	endothelial cell	pig
1809.6	1883.6	underivatised	N-glycan	(Hex)2 (HexNAc)2 (Deoxyhexose)1 + (Man)3(GlcNAc)2	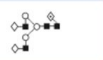	4.2	pancreatic islet cell	pig

Figure 4.4 The search result page displaying glycan, having *m/z* 1809.6 (adducted to sodium ion) analyzed by MALDI-TOF MS, information in the pig glycome database

pigs. Moreover, it contains both qualitative and quantitative information on xenoantigenic glycans, which play an important role in immune-rejection response. Taken together, this database is potentially promising and facilitates xenotransplantation research as well as basic carbohydrate research. The pig glycome database will allow users to use hyperlink the human glycan database with Consortium for Functional Glycomics (CFG), which contains glycan profiles in human cells and tissues for pig-to-human xenotransplantation research. In the near future, this pig glycome database will be updated with a list of glycans from α1,3-galactosyltransferase gene-knock out pig samples as well. It will represent the quantitative visualization of WT and GalT-KO pig glycans according to some structural features. It includes the followings: glycan types (high-mannose type and complex/hybrid type), specific residue-containing glycans (sialylated glycan and fucosylated glycan), and xenoantigenic glycans (α-Gal-terminated glycan and NeuGc-terminated glycan).

Chapter 5. Pig glycan and human immune cell interaction study

5.1 Assay for human immune cell activity against pig glycomes

The N-linked glycans isolated from WT and GalT-KO pig kidney tissues were prepared, and then confirmed by using MALDI-TOF MS as described above. For detection of human cell activity against the pig N-linked glycans, expression levels of seven surface markers (CD86, CD80, CD40, CD11b, CD11c, CD14, and MHCII) on monocytes were assessed by FACS analysis **(Figure 5.1)**. CD86, CD80, CD40 which was present on the surface of antigen-presenting cells (APCs) such as monocyte and dendritic cell, induce co-stimulatory signals for T-cell activation. CD11c is found at high levels on human dendritic cells, and thus serves as a human dendritic cell marker as well as MHCII, while CD11b acts as a macrophage marker. CD14 plays a role as a co-receptor against bacterial lipopolysaccharide (LPS). Expression levels of these surface markers on monocytes were compared after the treatment with N-linked glycans of WT and GalT-KO, respectively. The results represent no difference of the expression levels of the surface markers between WT and GalT-KO N-linked glycan treatments as shown in **Figure 5.2**.

5.2 Screening of human immune cell proteins using pig glycan-immobilized beads

For the high-throughput screening for human immune cell surface proteins interacting with pig glycans **(Figure 5.3)**, a glycan immobilization method described previously [106] were used in this study. N-linked glycans derived from WT and GalT-KO pig kidneys were purified according to an N-linked glycan

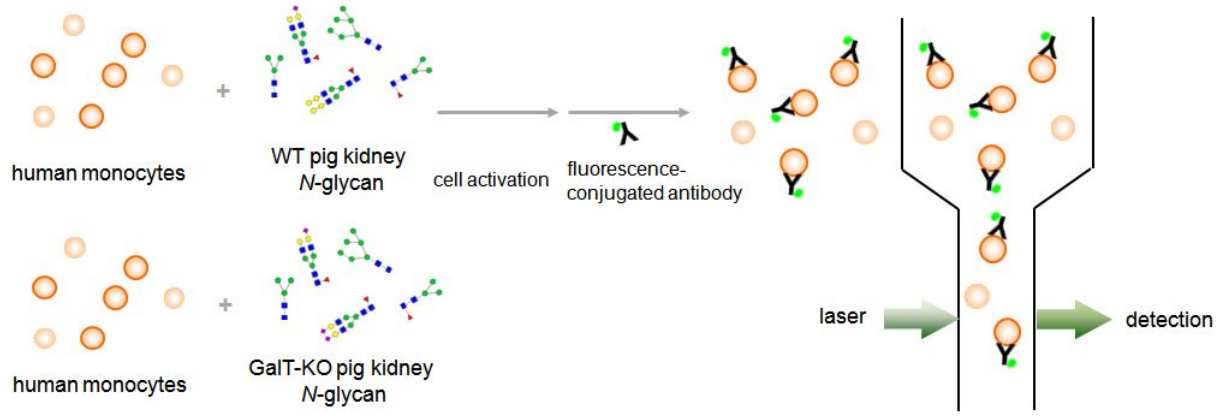

surface marker	function	Antibody (Ab)
CD86	co-stimulatory molecules for T cell activation	anti CD86 Ab-FITC
CD80		anti CD80 Ab-PE
CD40		anti CD40 Ab-FITC
CD11b	macrophage marker	anti CD11b Ab-APC
CD11c	dendritic cell marker	anti CD11c Ab-APC
CD14	microbial LPS receptor	anti CD14 Ab-PerCP
MHCII	dendritic cell marker	anti MHCII Ab-PE

FITC: Fluorescein isothiocyanate
PE: Phycoerythrin
APC: Allophycocyanin
PerCP: Peridinin chlorophyll protein

Figure 5.1 Scheme for human immune cell activation against WT and GalT-KO pig glycans using FACS analysis

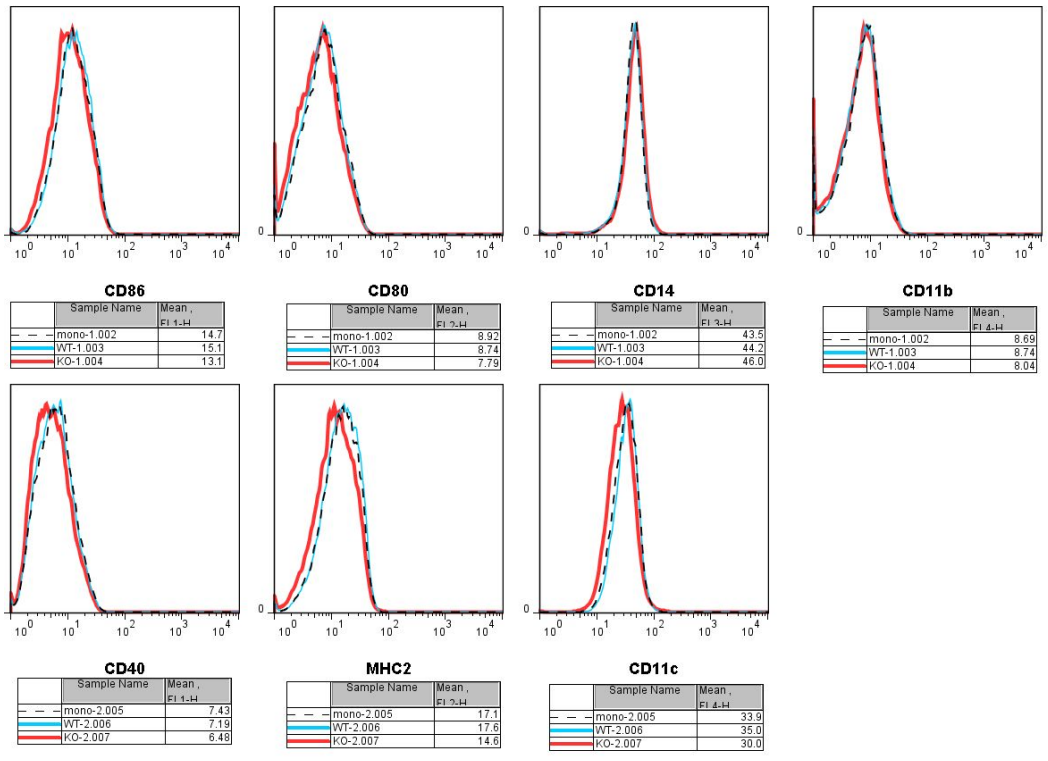

Figure 5.2 FACS analysis for expression levels of surface marker after the treatment of WT and GalT-KO pig glycans

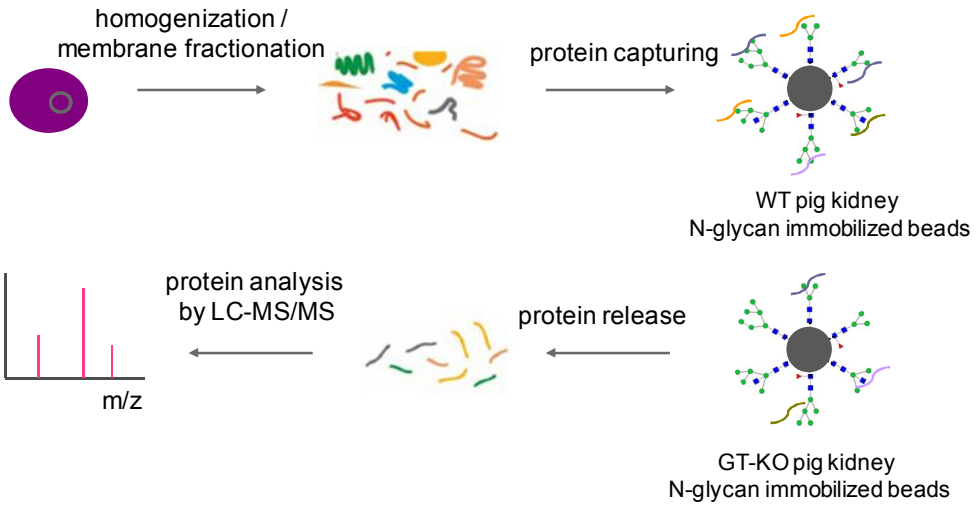

Figure 5.3 A strategy for screening and identification of human immune cell surface proteins interaction with pig glycans

purification procedure as mentioned above, and were immobilized with 4-hydrazinobenzoic acid (HBA)-functionalized HiCore beads by Schiff base formation, respectively. It was previously reported that the HiCore resin structure as a core-shell-type minimized non-specific protein binding [103]. Because the free reducing end of N-linked glycans formed as an aldehyde group was covalently conjugated with hydrazide group onto beads, this glycan-immobilization system allowed directional conjugation which enables the carbohydrate epitope to properly bind to the its protein receptor. In addition, the introduction of β-alanine-ε-aminocaproic acid-β-alanine-ε-aminocaproic acid (BEBE) non-natural amino acid spacer between the glycan-HBA and the bead plays a role in preventing the steric hindrance in their interactions. Thus, this glycan-immobilized bead can be cell-mimetic system covered by heterogeneous glycoconjugates. To investigate the interaction between pig glycan and human cell surface proteins, the human cell membrane fraction and pig glycan-immobilized beads were incubated and then the specific-binding tryptic-digested fraction was analyzed by LC-ESI-MS/MS. The results showed the some proteins were identified from human dendritic cells through NCBI human database **(Table 5.1)**, but almost proteins are not membrane proteins.

5.3 Discussion

Understanding the interactions between pig xeno-carbohydrates and human immune cells can be approached from different perspective and is important for the advancement of basic science and drug development. A previous study reported on

Table 5.1 Identification of pig glycan-binding proteins from human dendritic cell using LTQ-FT MS. Max. XCorr is the highest XCorr value (>1.7, 2.5, and 3.0 for singly-, doubly-, and triply-charged ions respectively) for the detected peptides.

Protein	**WT**			**GalT-KO**		
	coverage (%)	Max.Xcorr	charge	coverage (%)	Max.Xcorr	charge
Serum albumin	36.12			28.90		
KVPQVSTPTLVEVS.R		4.21	3		4.06	3
RHPYFYAPELLFFA.K		3.65	3		3.73	3
RHPDYSVVLLL.R		3.04	3		3.46	3
QTALVELV.K		2.76	2			
LVNEVTEFA.K		2.63	2		2.59	2
DVFLGmFLYEYA.R					2.81	2
Apolipoprotein A-I	52.06			44.94		
LLDNWDSVTSTFS.K		3.80	2			
QGLLPVLESF.K		3.64	2		3.40	2
DYVSQFEGSALG.K		3.17	2		2.94	2
DSGRDYVSQFEGSALG.K					3.69	3

VSFLSALEEYT.K					3.21	2
Fibrinogen beta chain	34.62			24.85		
HQLYIDETVNSNIPTNL.R		3.69	3		3.73	3
QGFGNVATNTDG.K		2.93	2		2.71	2
DNENVVNEYSSELE.K		2.83	2			
Isoform Gamma-A of Fibrinogen gamma chain	32.27			24.71		
IHLISTQSAIPYAL.R		4.26	3		4.16	3
YLQEIYNSNNQ.K		2.66	2			
Isoform 2 of Fibrinogen alpha chain	16.61			13.20		
VQHIQLLQ.K		3.16	2		2.90	2
GLIDEVNQDFTN.R					2.83	2
Tektin-2	6.05					
LQADIACKANSMLLDTKCmDT.R		3.52	3			
PR domain-containing protein 11	8.61					
MLKMAEPIASLMIVEcRACL.R		3.09	2			
Ras-related protein Rab-44				3.04		
DALQQDLHATGSEPRLGTQRA.R					2.87	2

the fishing-out of glycan-binding proteins in human serum using pig glycan-immobilized beads [106]. The study developed a novel GBP screening technique combined with MS analysis, and these results showed identification of potential GBPs associated with pig-to-xenograft rejection, such as antibodies, cytokines, and complement components, etc. But, this approach has a minor limitation for GalT-KO pig glycan study because of the use of alpha1,3-galactosidase on WT. Here, the present study tried to access to the interaction between GalT-KO pig glycome and human immune cells. However, a previous study demonstrated that enrichment of membrane proteins by conventional subcellular fractionation lead to identification of only a small amount of membrane proteins [129]. Moreover, these membrane proteins are largely contaminated with other subcellular proteins in cytosol and nucleus fractions etc. It may be also needed that sufficient human immune cells are provided from cell-line culture for the successful experiment. Therefore the identification of human cell surface proteins interacting with pig glycome remains challenge, and the complete characterization of pig glycan-specific interaction with human immune cells still remained to be solved in xenotransplantation researches.

Chapter 6. Conclusion & Further Suggestions

In xenotransplantation, although GalT-KO pigs have been produced as donors, there are still other xenoantigenic carbohydrates present on the surface of pig cells and tissues. These non-Gal antigens such as H-D antigen trigger AVR or DXR, and subsequence lead to the xenograft failure. Moreover, the targeted deletion of α1,3-galactosyltransferase gene results in the perturbation of many other genes regardless of the α1,3-galactosyltransferase gene, and thereby leading to unknown phenotype effects such as an increase or decrease of other xenoantigen levels. Therefore, the identification of cellular glycome including non-Gal antigens is important to overcome the above mentioned obstacle.

MS has recently become a powerful analytical tool for characterizing the oligosaccharide structures through tandem exoglycosidase digestion or mass spectrometric analysis. Moreover, MS approaches combined with diverse chemical derivatization of the oligosaccharides enabled to achieve reliable quantitation of the oligosaccharide. Both qualitative and quantitative analyses of glycans have results in a great number of glycome data, and thus it is essential to develop data repositories and software tools, which facilitate the annotation and interpretation of the big glycome data.

This study presents an MS-based analysis for delineating of N-glycome repertoire derived from both WT and GalT-KO pig cells and tissues, and the comparison of the total N-glycomic profiles between WT and GalT-KO. In case of pig cells, total 47 N-glycan isolated from WT and GalT-KO pig fibroblasts was identified using MALDI-TOF MS analysis. In addition, MALDI-TOF MS analysis coupled with solid-phase permethylation allowed comparatively quantifying these N-linked glycans between WT and GalT-KO. The results showed that the relative

abundance of sialic acid-containing glycans increased in GalT-KO pig fibroblasts (92.3%) compared to WT (69.9%). MALDI-QIT-TOF MS/MS analysis indicated that $Hex_5HexNAc_4Fuc_1NeuAc_2$ bi-antennary N-glycan of sialylated glycans leads to an increase of total sialylated glycan level in GalT-KO pig fibroblasts. The current analysis showed NeuGc level was slightly higher in GalT-KO pig (6.1%) relative to WT (4.5%), suggesting that the deletion of α1,3-galactosyltransferase gene may not only remove construction of Galα1,3Gal residue but also increase sialylated glycans including NeuGc antigen.

In case of pig kidney tissues, this study present the integrated MS-based approaches for the identification and quantitation of total N-linked glycans derived from GalT-KO pig kidney, and the comparative profiling of the N-glycans between WT and GalT-KO. N-linked glycans of GalT-KO pig kidney identified by complementary MS analyses using MALDI-TOF MS and ESI-MS instruments, showing remarkable complex N-linked glycan diversity including both high-mannose type glycans and complex/hybrid type glycans. Most of complex type glycans were composed of sialylated or/and fucosylated glycans. Among the diverse glycan array on the GalT-KO pig kidney, it was confirmed that α-Gal antigen as a major carbohydrate antigen was absent by MALDI-TOF MS analysis coupled with α-galactosidase digestion. Total N-linked glycan structures are elucidated using ESI-MS/MS and MALDI-TOF MS combined with sequential exoglycosidase sequencing. Moreover, NeuGc-linked glycan structures regarded as a non-Gal antigen present on the pig GalT-KO pig kidney were initially validated by MALDI-QIT-TOF MS/MS analysis. For relative quantitation of N-linked glycans on GalT-KO, MALDI-TOF MS analysis combined with solid-phase

permethylation method was used. Unlike WT, which showed abundant α-Gal-containing glycans (35.2-42.0% total N-linked glycans), the results showed that showed a large array of sialic acid-linked glycan expression (58.0% total N-linked glycans). The present analysis also revealed that the NeuGc level was higher in GalT-KO pig (7.9%) relative to WT (3.7%). This comprehensive glycomic analysis highlighted the unique total *N*-glycosylation characteristics of pig kidney tissues.

Pig glycome database was developed here, which curates WT pig glycomes derived from various cells/tissues on pig. This database was designed as a user-friendly web-based interface and is now available on the web (www.bioinformatics.snu.ac.kr/xdb) However, despite the importance of GalT-KO pig description for further xenotransplantation study in GalT-KO pig era, the pig glycome database has not yet included GalT-KO pig glycomes. Based on our present database platform, an advanced database will be present which contains structural and quantitative information on both WT and GalT-KO pig glycomes. In addition, this database allowed the relative comparison of glycome quantities between the WT and GalT-KO. In the near future, this database will be updated with other GalT-KO cells or/and tissues (e.g. GalT-KO fibroblasts) on pig as well as GalT-KO kidney.

Furthermore, for understanding of interactions between pig carbohydrates and human immune cells, human immune cell activation against WT and GalT-KO pig glycans respectively, was measured by FACS analysis, and their proteins were screened and identified using glycan-immobilized beads and LC-MS/MS analysis. The results showed no difference of surface marker expression and pig glycan-specific proteins associated with human immune cells between WT and GalT-KO

pig. The complete identification of interaction between pig glycans and human immune cells still remained to be solved for xenotransplantation studies.

This work would like to emphasize on (1) establishment of the MS-based quantitative analysis as well as structural analysis of glycans (2) in-depth investigation for pig glycosylation on the WT and GalT-KO pig cell and tissue (3) the development of pig glycome database for comprehensive understanding of pig-to-human xenotransplantation. Taken together, I anticipate that MS-based glycomic analysis and the relational pig glycome database will contribute in important information to pre-clinical xenotransplantation trials as well as glycobiology.

References

[1] Kornfeld, R., Kornfeld, S., Assembly of asparagine-linked oligosaccharides. *Annu Rev Biochem* 1985, *54*, 631-664.

[2] Shakin-Eshleman, S. H., Remaley, A. T., Eshleman, J. R., Wunner, W. H., Spitalnik, S. L., N-linked glycosylation of rabies virus glycoprotein. Individual sequons differ in their glycosylation efficiencies and influence on cell surface expression. *J Biol Chem* 1992, *267*, 10690-10698.

[3] Varki, A., *Essentials of glycobiology*, Cold Spring Harbor Laboratory Press, Cold Spring Harbor, N.Y. 2009.

[4] Marino, K., Bones, J., Kattla, J. J., Rudd, P. M., A systematic approach to protein glycosylation analysis: a path through the maze. *Nat Chem Biol*, *6*, 713-723.

[5] Crocker, P. R., Feizi, T., Carbohydrate recognition systems: functional triads in cell-cell interactions. *Curr Opin Struct Biol* 1996, *6*, 679-691.

[6] Edelman, G. M., Cell adhesion molecules. *Science* 1983, *219*, 450-457.

[7] Roseman, S., Reflections on glycobiology. *J Biol Chem* 2001, *276*, 41527-41542.

[8] Marth, J. D., Grewal, P. K., Mammalian glycosylation in immunity. *Nat Rev Immunol* 2008, *8*, 874-887.

[9] Haslam, S. M., Julien, S., Burchell, J. M., Monk, C. R.*, et al.*, Characterizing the glycome of the mammalian immune system. *Immunol Cell Biol* 2008, *86*, 564-573.

[10] Dennis, J. W., Granovsky, M., Warren, C. E., Glycoprotein glycosylation and cancer progression. *Biochim Biophys Acta* 1999, *1473*, 21-34.

[11] Ohtsubo, K., Marth, J. D., Glycosylation in cellular mechanisms of health and disease. *Cell* 2006, *126*, 855-867.

[12] Feinberg, H., Castelli, R., Drickamer, K., Seeberger, P. H., Weis, W. I., Multiple modes of binding enhance the affinity of DC-SIGN for high mannose N-linked glycans found on viral glycoproteins. *J Biol Chem* 2007, *282*, 4202-4209.

[13] Appelmelk, B. J., van Die, I., van Vliet, S. J., Vandenbroucke-Grauls, C. M.*, et al.*, Cutting edge: carbohydrate profiling identifies new pathogens that interact with dendritic cell-specific ICAM-3-grabbing nonintegrin on dendritic cells. *J Immunol* 2003, *170*, 1635-1639.

[14] van Vliet, S. J., Saeland, E., van Kooyk, Y., Sweet preferences of MGL: carbohydrate specificity and function. *Trends Immunol* 2008, *29*, 83-90.

[15] Robinson, M. J., Sancho, D., Slack, E. C., LeibundGut-Landmann, S., Reis e Sousa, C., Myeloid C-type lectins in innate immunity. *Nat Immunol* 2006, *7*, 1258-1265.

[16] van Kooyk, Y., Geijtenbeek, T. B., DC-SIGN: escape mechanism for pathogens. *Nat Rev Immunol* 2003, *3*, 697-709.

[17] Leffler, H., Carlsson, S., Hedlund, M., Qian, Y., Poirier, F., Introduction to galectins. *Glycoconj J* 2004, *19*, 433-440.

[18] Hirabayashi, J., Hashidate, T., Arata, Y., Nishi, N.*, et al.*, Oligosaccharide specificity of galectins: a search by frontal affinity chromatography. *Biochim Biophys Acta* 2002, *1572*, 232-254.

[19] Rabinovich, G. A., Toscano, M. A., Jackson, S. S., Vasta, G. R., Functions of cell surface galectin-glycoprotein lattices. *Curr Opin Struct Biol* 2007, *17*, 513-520.

[20] Liu, F. T., Rabinovich, G. A., Galectins as modulators of tumour progression.

Nat Rev Cancer 2005, *5*, 29-41.

[21] Crocker, P. R., Paulson, J. C., Varki, A., Siglecs and their roles in the immune system. *Nat Rev Immunol* 2007, *7*, 255-266.

[22] Kolarich, D., Lepenies, B., Seeberger, P. H., Glycomics, glycoproteomics and the immune system. *Curr Opin Chem Biol*, *16*, 214-220.

[23] Dai, Y., Vaught, T. D., Boone, J., Chen, S. H.*, et al.*, Targeted disruption of the alpha1,3-galactosyltransferase gene in cloned pigs. *Nat Biotechnol* 2002, *20*, 251-255.

[24] Lai, L., Kolber-Simonds, D., Park, K. W., Cheong, H. T.*, et al.*, Production of alpha-1,3-galactosyltransferase knockout pigs by nuclear transfer cloning. *Science* 2002, *295*, 1089-1092.

[25] Kolber-Simonds, D., Lai, L., Watt, S. R., Denaro, M.*, et al.*, Production of alpha-1,3-galactosyltransferase null pigs by means of nuclear transfer with fibroblasts bearing loss of heterozygosity mutations. *Proc Natl Acad Sci U S A* 2004, *101*, 7335-7340.

[26] Miyagawa, S., Yamamoto, A., Matsunami, K., Wang, D.*, et al.*, Complement regulation in the GalT KO era. *Xenotransplantation*, *17*, 11-25.

[27] Platt, J. L., New directions for organ transplantation. *Nature* 1998, *392*, 11-17.

[28] Saethre, M., Baumann, B. C., Fung, M., Seebach, J. D., Mollnes, T. E., Characterization of natural human anti-non-gal antibodies and their effect on activation of porcine gal-deficient endothelial cells. *Transplantation* 2007, *84*, 244-250.

[29] Park, J. Y., Park, M. R., Bui, H. T., Kwon, D. N.*, et al.*, alpha1,3-galactosyltransferase deficiency in germ-free miniature pigs increases N-

glycolylneuraminic acids as the xenoantigenic determinant in pig-human xenotransplantation. *Cell Reprogram*, *14*, 353-363.

[30] Kim, D. H., Lee, H. Y., Kim, H., Lee, Y. S., Park, S. B., Quantitative evaluation of HiCore resin for the nonspecific binding of proteins by on-bead colorimetric assay. *J Comb Chem* 2006, *8*, 280-285.

[31] Yang, Y. G., Sykes, M., Xenotransplantation: current status and a perspective on the future. *Nat Rev Immunol* 2007, *7*, 519-531.

[32] Li, S., Waer, M., Billiau, A. D., Xenotransplantation: role of natural immunity. *Transpl Immunol* 2009, *21*, 70-74.

[33] Li, S., Yan, Y., Lin, Y., Bullens, D. M.*, et al.*, Rapidly induced, T-cell independent xenoantibody production is mediated by marginal zone B cells and requires help from NK cells. *Blood* 2007, *110*, 3926-3935.

[34] Xu, X. C., Goodman, J., Sasaki, H., Lowell, J., Mohanakumar, T., Activation of natural killer cells and macrophages by porcine endothelial cells augments specific T-cell xenoresponse. *Am J Transplant* 2002, *2*, 314-322.

[35] Jin, R., Greenwald, A., Peterson, M. D., Waddell, T. K., Human monocytes recognize porcine endothelium via the interaction of galectin 3 and alpha-GAL. *J Immunol* 2006, *177*, 1289-1295.

[36] Cardozo, L. A., Rouw, D. B., Ambrose, L. R., Midulla, M.*, et al.*, The neutrophil: the unnoticed threat in xenotransplantation? *Transplantation* 2004, *78*, 1721-1728.

[37] al-Mohanna, F., Collison, K., Parhar, R., Kwaasi, A.*, et al.*, Activation of naive xenogeneic but not allogeneic endothelial cells by human naive neutrophils: a potential occult barrier to xenotransplantation. *Am J Pathol* 1997, *151*, 111-120.

[38] al-Mohanna, F. A., Collison, K. S., Allen, S. P., Stern, D., Yacoub, M. H., Naive neutrophils and xenotransplantation. *Lancet* 1996, *348*, 1246.

[39] Sheikh, S., Parhar, R., Al-Mohanna, F., Rapid static adhesion of human naive neutrophil to naive xenoendothelium under physiologic flow is independent of Galalpha1,3-gal structures. *J Leukoc Biol* 2002, *71*, 932-940.

[40] Perper, R. J., Najarian, J. S., Experimental renal heterotransplantation. I. In widely divergent species. *Transplantation* 1966, *4*, 377-388.

[41] Giles, G. R., Boehmig, H. J., Lilly, J., Amemiya, H., *et al.*, Mechanism and modification of rejection of heterografts between divergent species. *Transplant Proc* 1970, *2*, 522-538.

[42] Galili, U., Interaction of the natural anti-Gal antibody with alpha-galactosyl epitopes: a major obstacle for xenotransplantation in humans. *Immunol Today* 1993, *14*, 480-482.

[43] Milland, J., Christiansen, D., Lazarus, B. D., Taylor, S. G., *et al.*, The molecular basis for galalpha(1,3)gal expression in animals with a deletion of the alpha1,3galactosyltransferase gene. *J Immunol* 2006, *176*, 2448-2454.

[44] Keusch, J. J., Manzella, S. M., Nyame, K. A., Cummings, R. D., Baenziger, J. U., Expression cloning of a new member of the ABO blood group glycosyltransferases, iGb3 synthase, that directs the synthesis of isoglobo-glycosphingolipids. *J Biol Chem* 2000, *275*, 25308-25314.

[45] Taylor, S. G., McKenzie, I. F., Sandrin, M. S., Characterization of the rat alpha(1,3)galactosyltransferase: evidence for two independent genes encoding glycosyltransferases that synthesize Galalpha(1,3)Gal by two separate glycosylation pathways. *Glycobiology* 2003, *13*, 327-337.

[46] Asaoka, H., Nishinaka, S., Wakamiya, N., Matsuda, H., Murata, M., Two chicken monoclonal antibodies specific for heterophil Hanganutziu-Deicher antigens. *Immunol Lett* 1992, *32*, 91-96.

[47] Schauer, R., Srinivasan, G. V., Coddeville, B., Zanetta, J. P., Guerardel, Y., Low incidence of N-glycolylneuraminic acid in birds and reptiles and its absence in the platypus. *Carbohydr Res* 2009, *344*, 1494-1500.

[48] Varki, A., N-glycolylneuraminic acid deficiency in humans. *Biochimie* 2001, *83*, 615-622.

[49] Kamerling, J. P., Vliegenthart, J. F., Identification of O-cetylated N-acylneuraminic acids by mass spectrometry. *Carbohydr Res* 1975, *41*, 7-17.

[50] Morozumi, K., Kobayashi, T., Usami, T., Oikawa, T.*, et al.*, Significance of histochemical expression of Hanganutziu-Deicher antigens in pig, baboon and human tissues. *Transplant Proc* 1999, *31*, 942-944.

[51] Muchmore, E. A., Milewski, M., Varki, A., Diaz, S., Biosynthesis of N-glycolyneuraminic acid. The primary site of hydroxylation of N-acetylneuraminic acid is the cytosolic sugar nucleotide pool. *J Biol Chem* 1989, *264*, 20216-20223.

[52] Kawano, T., Kozutsumi, Y., Kawasaki, T., Suzuki, A., Biosynthesis of N-glycolylneuraminic acid-containing glycoconjugates. Purification and characterization of the key enzyme of the cytidine monophospho-N-acetylneuraminic acid hydroxylation system. *J Biol Chem* 1994, *269*, 9024-9029.

[53] Bouhours, D., Pourcel, C., Bouhours, J. E., Simultaneous expression by porcine aorta endothelial cells of glycosphingolipids bearing the major epitope for human xenoreactive antibodies (Gal alpha 1-3Gal), blood group H determinant and N-glycolylneuraminic acid. *Glycoconj J* 1996, *13*, 947-953.

[54] Kim, Y. G., Harvey, D. J., Yang, Y. H., Park, C. G., Kim, B. G., Mass spectrometric analysis of the glycosphingolipid-derived glycans from miniature pig endothelial cells and islets: identification of NeuGc epitope in pig islets. *J Mass Spectrom* 2009, *44*, 1489-1499.

[55] Kim, Y. G., Gil, G. C., Harvey, D. J., Kim, B. G., Structural analysis of alpha-Gal and new non-Gal carbohydrate epitopes from specific pathogen-free miniature pig kidney. *Proteomics* 2008, *8*, 2596-2610.

[56] Kim, Y. G., Gil, G. C., Jang, K. S., Lee, S.*, et al.*, Qualitative and quantitative comparison of N-glycans between pig endothelial and islet cells by high-performance liquid chromatography and mass spectrometry-based strategy. *J Mass Spectrom* 2009, *44*, 1087-1104.

[57] Jeong, H. J., Adhya, M., Park, H. M., Kim, Y. G., Kim, B. G., Detection of Hanganutziu-Deicher antigens in O-glycans from pig heart tissues by matrix-assisted laser desorption/ionization time-of-flight mass spectrometry. *Xenotransplantation*, *20*, 407-417.

[58] Park, H. M., Yang, Y. H., Kim, B. G., Kim, Y. G., Structural characterization of alpha-galactosylated O-glycans from miniature pig kidney and endothelial cells. *Carbohydr Res*, *369*, 48-53.

[59] Malykh, Y. N., Shaw, L., Schauer, R., The role of CMP-N-acetylneuraminic acid hydroxylase in determining the level of N-glycolylneuraminic acid in porcine tissues. *Glycoconj J* 1998, *15*, 885-893.

[60] Breimer, M. E., Gal/non-Gal antigens in pig tissues and human non-Gal antibodies in the GalT-KO era. *Xenotransplantation*, *18*, 215-228.

[61] Swanson, J. L., Cooling, L., Porcine red blood cells express a polyagglutinable

red blood cell phenotype. *Transfusion* 2005, *45*, 1035-1036; author reply 1036-1037.

[62] Kirkeby, S., Mikkelsen, H. B., Distribution of the alphaGal- and the non-alphaGal T-antigens in the pig kidney: potential targets for rejection in pig-to-man xenotransplantation. *Immunol Cell Biol* 2008, *86*, 363-371.

[63] Miyagawa, S., Takeishi, S., Yamamoto, A., Ikeda, K.*, et al.*, Survey of glycoantigens in cells from alpha1-3galactosyltransferase knockout pig using a lectin microarray. *Xenotransplantation*, *17*, 61-70.

[64] Itzkowitz, S. H., Yuan, M., Montgomery, C. K., Kjeldsen, T.*, et al.*, Expression of Tn, sialosyl-Tn, and T antigens in human colon cancer. *Cancer Res* 1989, *49*, 197-204.

[65] Springer, G. F., Immunoreactive T and Tn epitopes in cancer diagnosis, prognosis, and immunotherapy. *J Mol Med (Berl)* 1997, *75*, 594-602.

[66] Leduc, E. H., Tanaka, N., A study of the cellular distribution of Forssman antigen in various species. *J Immunol* 1956, *77*, 198-212.

[67] Hakomori, S., Wang, S. M., Young, W. W., Jr., Isoantigenic expression of Forssman glycolipid in human gastric and colonic mucosa: its possible identity with "A-like antigen" in human cancer. *Proc Natl Acad Sci U S A* 1977, *74*, 3023-3027.

[68] Kawanami, J., The appearance of Forssman hapten in human tumor. *J Biochem* 1972, *72*, 783-785.

[69] Young, W. W., Jr., Hakomori, S. I., Levine, P., Characterization of anti-Forssman (anti-Fs) antibodies in human sera: their specificity and possible changes in patients with cancer. *J Immunol* 1979, *123*, 92-96.

[70] Rudd, P. M., Guile, G. R., Kuster, B., Harvey, D. J., *et al.*, Oligosaccharide sequencing technology. *Nature* 1997, *388*, 205-207.

[71] Iourin, O., Mattu, T. S., Mian, N., Keir, G., *et al.*, The identification of abnormal glycoforms of serum transferrin in carbohydrate deficient glycoprotein syndrome type I by capillary zone electrophoresis. *Glycoconj J* 1996, *13*, 1031-1042.

[72] Guile, G. R., Rudd, P. M., Wing, D. R., Prime, S. B., Dwek, R. A., A rapid high-resolution high-performance liquid chromatographic method for separating glycan mixtures and analyzing oligosaccharide profiles. *Anal Biochem* 1996, *240*, 210-226.

[73] Bigge, J. C., Patel, T. P., Bruce, J. A., Goulding, P. N., *et al.*, Nonselective and efficient fluorescent labeling of glycans using 2-amino benzamide and anthranilic acid. *Anal Biochem* 1995, *230*, 229-238.

[74] Campbell, M. P., Royle, L., Radcliffe, C. M., Dwek, R. A., Rudd, P. M., GlycoBase and autoGU: tools for HPLC-based glycan analysis. *Bioinformatics* 2008, *24*, 1214-1216.

[75] Domon, B., Costello, C. E., A Systematic Nomenclature for Carbohydrate Fragmentations in Fab-Ms Ms Spectra of Glycoconjugates. *Glycoconjugate Journal* 1988, *5*, 397-409.

[76] Cooper, H. J., Hakansson, K., Marshall, A. G., The role of electron capture dissociation in biomolecular analysis. *Mass Spectrom Rev* 2005, *24*, 201-222.

[77] Hakansson, K., Chalmers, M. J., Quinn, J. P., McFarland, M. A., *et al.*, Combined electron capture and infrared multiphoton dissociation for multistage MS/MS in a Fourier transform ion cyclotron resonance mass spectrometer. *Anal*

Chem 2003, *75*, 3256-3262.

[78] Wu, S. L., Huhmer, A. F., Hao, Z., Karger, B. L., On-line LC-MS approach combining collision-induced dissociation (CID), electron-transfer dissociation (ETD), and CID of an isolated charge-reduced species for the trace-level characterization of proteins with post-translational modifications. *J Proteome Res* 2007, *6*, 4230-4244.

[79] Adamson, J. T., Hakansson, K., Electron detachment dissociation of neutral and sialylated oligosaccharides. *J Am Soc Mass Spectrom* 2007, *18*, 2162-2172.

[80] Adamson, J. T., Hakansson, K., Electron capture dissociation of oligosaccharides ionized with alkali, alkaline Earth, and transition metals. *Anal Chem* 2007, *79*, 2901-2910.

[81] Hirabayashi, J., Concept, strategy and realization of lectin-based glycan profiling. *J Biochem* 2008, *144*, 139-147.

[82] Gupta, G., Surolia, A., Sampathkumar, S. G., Lectin microarrays for glycomic analysis. *OMICS*, *14*, 419-436.

[83] Hirabayashi, J., Yamada, M., Kuno, A., Tateno, H., Lectin microarrays: concept, principle and applications. *Chem Soc Rev*, *42*, 4443-4458.

[84] Anumula, K. R., Dhume, S. T., High resolution and high sensitivity methods for oligosaccharide mapping and characterization by normal phase high performance liquid chromatography following derivatization with highly fluorescent anthranilic acid. *Glycobiology* 1998, *8*, 685-694.

[85] Royle, L., Dwek, R. A., Rudd, P. M., Determining the structure of oligosaccharides N- and O-linked to glycoproteins. *Curr Protoc Protein Sci* 2006, *Chapter 12*, Unit 12 16.

[86] Domann, P. J., Pardos-Pardos, A. C., Fernandes, D. L., Spencer, D. I.*, et al.*, Separation-based glycoprofiling approaches using fluorescent labels. *Proteomics* 2007, *7 Suppl 1*, 70-76.

[87] Rakus, J. F., Mahal, L. K., New technologies for glycomic analysis: toward a systematic understanding of the glycome. *Annu Rev Anal Chem (Palo Alto Calif)*, *4*, 367-392.

[88] Pilobello, K. T., Slawek, D. E., Mahal, L. K., A ratiometric lectin microarray approach to analysis of the dynamic mammalian glycome. *Proc Natl Acad Sci U S A* 2007, *104*, 11534-11539.

[89] Diswall, M., Angstrom, J., Karlsson, H., Phelps, C. J.*, et al.*, Structural characterization of alpha1,3-galactosyltransferase knockout pig heart and kidney glycolipids and their reactivity with human and baboon antibodies. *Xenotransplantation*, *17*, 48-60.

[90] Puga Yung, G. L., Li, Y., Borsig, L., Millard, A. L.*, et al.*, Complete absence of the alphaGal xenoantigen and isoglobotrihexosylceramide in alpha1,3galactosyltransferase knock-out pigs. *Xenotransplantation*, *19*, 196-206.

[91] Gil, G. C., Kim, Y. G., Kim, B. G., A relative and absolute quantification of neutral N-linked oligosaccharides using modification with carboxymethyl trimethylammonium hydrazide and matrix-assisted laser desorption/ionization time-of-flight mass spectrometry. *Anal Biochem* 2008, *379*, 45-59.

[92] Ciucanu, I., Kerek, F., A Simple and Rapid Method for the Permethylation of Carbohydrates. *Carbohydrate Research* 1984, *131*, 209-217.

[93] Kang, P., Mechref, Y., Novotny, M. V., High-throughput solid-phase permethylation of glycans prior to mass spectrometry. *Rapid Commun Mass*

Spectrom 2008, *22*, 721-734.

[94] Kang, P., Mechref, Y., Kyselova, Z., Goetz, J. A., Novotny, M. V., Comparative glycomic mapping through quantitative permethylation and stable-isotope labeling. *Anal Chem* 2007, *79*, 6064-6073.

[95] Alvarez-Manilla, G., Warren, N. L., Abney, T., Atwood, J., 3rd*, et al.*, Tools for glycomics: relative quantitation of glycans by isotopic permethylation using 13CH3I. *Glycobiology* 2007, *17*, 677-687.

[96] Jang, K. S., Kim, Y. G., Gil, G. C., Park, S. H., Kim, B. G., Mass spectrometric quantification of neutral and sialylated N-glycans from a recombinant therapeutic glycoprotein produced in the two Chinese hamster ovary cell lines. *Anal Biochem* 2009, *386*, 228-236.

[97] Toyoda, M., Ito, H., Matsuno, Y. K., Narimatsu, H., Kameyama, A., Quantitative derivatization of sialic acids for the detection of sialoglycans by MALDI MS. *Anal Chem* 2008, *80*, 5211-5218.

[98] Gil, G. C., Iliff, B., Cerny, R., Velander, W. H., Van Cott, K. E., High throughput quantification of N-glycans using one-pot sialic acid modification and matrix assisted laser desorption ionization time-of-flight mass spectrometry. *Anal Chem*, *82*, 6613-6620.

[99] Campbell, M. P., Hayes, C. A., Struwe, W. B., Wilkins, M. R.*, et al.*, UniCarbKB: putting the pieces together for glycomics research. *Proteomics*, *11*, 4117-4121.

[100] Cooper, C. A., Joshi, H. J., Harrison, M. J., Wilkins, M. R., Packer, N. H., GlycoSuiteDB: a curated relational database of glycoprotein glycan structures and their biological sources. 2003 update. *Nucleic Acids Res* 2003, *31*, 511-513.

[101] Kameyama, A., Kikuchi, N., Nakaya, S., Ito, H., *et al.*, A strategy for identification of oligosaccharide structures using observational multistage mass spectral library. *Anal Chem* 2005, *77*, 4719-4725.

[102] Raman, R., Venkataraman, M., Ramakrishnan, S., Lang, W., *et al.*, Advancing glycomics: implementation strategies at the consortium for functional glycomics. *Glycobiology* 2006, *16*, 82R-90R.

[103] von der Lieth, C. W., Freire, A. A., Blank, D., Campbell, M. P., *et al.*, EUROCarbDB: An open-access platform for glycoinformatics. *Glycobiology*, *21*, 493-502.

[104] Ahn, K. S., Kim, Y. J., Kim, M., Lee, B. H., *et al.*, Resurrection of an alpha-1,3-galactosyltransferase gene-targeted miniature pig by recloning using postmortem ear skin fibroblasts. *Theriogenology*, *75*, 933-939.

[105] Fujimura, T., Takahagi, Y., Shigehisa, T., Nagashima, H., *et al.*, Production of alpha 1,3-galactosyltransferase gene-deficient pigs by somatic cell nuclear transfer: a novel selection method for gal alpha 1,3-Gal antigen-deficient cells. *Molecular reproduction and development* 2008, *75*, 1372-1378.

[106] Kim, Y. G., Shin, D. S., Yang, Y. H., Gil, G. C., *et al.*, High-throughput screening of glycan-binding proteins using miniature pig kidney N-glycan-immobilized beads. *Chem Biol* 2008, *15*, 215-223.

[107] Kim, Y. G., Kim, S. Y., Hur, Y. M., Joo, H. S., *et al.*, The identification and characterization of xenoantigenic nonhuman carbohydrate sequences in membrane proteins from porcine kidney. *Proteomics* 2006, *6*, 1133-1142.

[108] Börnsen, K. O., Mohr, M. D., Widmer, H. M., Ion exchange and purification of carbohydrates on a Nafion(R) membrane as a new sample pretreatment for

matrix-assisted laser desorption-ionization mass spectrometry. *Rapid Commun. Mass Spectrom.* 1995, *9*, 1031-1034.

[109] Giles, K., Pringle, S. D., Worthington, K. R., Little, D.*, et al.*, Applications of a travelling wave-based radio-frequency-only stacked ring ion guide. *Rapid Commun. Mass Spectrom.* 2004, *18*, 2401-2414.

[110] Domon, B., Costello, C. E., A systematic nomenclature for carbohydrate fragmentations in FAB-MS/MS spectra of glycoconjugates. *Glycoconj. J.* 1988, *5*, 397-409.

[111] Harvey, D. J., Merry, A. H., Royle, L., Campbell, M. P.*, et al.*, Proposal for a standard system for drawing structural diagrams of *N*- and *O*-linked carbohydrates and related compounds. *Proteomics* 2009, *9*, 3796-3801.

[112] Lehtonen, A., Matikainen, S., Miettinen, M., Julkunen, I., Granulocyte-macrophage colony-stimulating factor (GM-CSF)-induced STAT5 activation and target-gene expression during human monocyte/macrophage differentiation. *J Leukoc Biol* 2002, *71*, 511-519.

[113] Wada, Y., Azadi, P., Costello, C. E., Dell, A.*, et al.*, Comparison of the methods for profiling glycoprotein glycans--HUPO Human Disease Glycomics/Proteome Initiative multi-institutional study. *Glycobiology* 2007, *17*, 411-422.

[114] Kang, P., Mechref, Y., Klouckova, I., Novotny, M. V., Solid-phase permethylation of glycans for mass spectrometric analysis. *Rapid Commun Mass Spectrom* 2005, *19*, 3421-3428.

[115] Miyagawa, S., Maeda, A., Takeishi, S., Ueno, T.*, et al.*, A lectin array analysis for wild-type and alpha-Gal-knockout pig islets versus healthy human islets. *Surg*

Today, *43*, 1439-1447.

[116] Harvey, D. J., Sobott, F., Crispin, M., Wrobel, A.*, et al.*, Ion mobility mass spectrometry for extracting spectra of *N*-glycans directly from incubation mixtures following glycan release: Application to glycans from engineered glycoforms of intact, folded HIV gp120. *J. Am. Soc. Mass Spectrom.* 2011, *22*, 568-581.

[117] Harvey, D. J., Scarff, C. A., Edgeworth, M., Crispin, M.*, et al.*, Travelling wave ion mobility and negative ion fragmentation for the structural determination of *N*-linked glycans. *Electrophoresis* 2013, *In Press*.

[118] Harvey, D. J., Fragmentation of negative ions from carbohydrates: Part 2, Fragmentation of high-mannose *N*-linked glycans. *J. Am. Soc. Mass Spectrom.* 2005, *16*, 631-646.

[119] Harvey, D. J., Fragmentation of negative ions from carbohydrates: Part 1; Use of nitrate and other anionic adducts for the production of negative ion electrospray spectra from *N*-linked carbohydrates. *J. Am. Soc. Mass Spectrom.* 2005, *16*, 622-630.

[120] Harvey, D. J., Fragmentation of negative ions from carbohydrates: Part 3, Fragmentation of hybrid and complex *N*-linked glycans. *J. Am. Soc. Mass Spectrom.* 2005, *16*, 647-659.

[121] Harvey, D. J., Royle, L., Radcliffe, C. M., Rudd, P. M., Dwek, R. A., Structural and quantitative analysis of *N*-linked glycans by MALDI and negative ion nanospray mass spectrometry. *Anal. Biochem.* 2008, *376*, 44-60.

[122] Harvey, D. J., Fragmentation of negative ions from carbohydrates: part 3. Fragmentation of hybrid and complex N-linked glycans. *J Am Soc Mass Spectrom* 2005, *16*, 647-659.

[123] Park, J. Y., Park, M. R., Kwon, D. N., Kang, M. H.*, et al.*, Alpha 1,3-galactosyltransferase deficiency in pigs increases sialyltransferase activities that potentially raise non-gal xenoantigenicity. *J Biomed Biotechnol*, *2011*, 560850.

[124] Thorlacius-Ussing, L., Ludvigsen, M., Kirkeby, S., Vorum, H., Honore, B., Proteomic analysis of tissue from alpha1,3-galactosyltransferase knockout mice reveals that a wide variety of proteins and protein fragments change expression level. *PLoS One*, *8*, e80600.

[125] Varki, A., Loss of N-glycolylneuraminic acid in humans: Mechanisms, consequences, and implications for hominid evolution. *Am J Phys Anthropol* 2001, *Suppl 33*, 54-69.

[126] Setcavage, T. M., Kim, Y. B., Variability of the immunological state of germfree colostrum-deprived Minnesota miniature piglets. *Infect Immun* 1976, *13*, 600-607.

[127] Kim, Y. G., Oh, J. Y., Gil, G. C., Kim, M. K.*, et al.*, Identification of alpha-Gal and non-Gal epitopes in pig corneal endothelial cells and keratocytes by using mass spectrometry. *Curr Eye Res* 2009, *34*, 877-895.

[128] Harvey, D. J., Merry, A. H., Royle, L., Campbell, M. P.*, et al.*, Proposal for a standard system for drawing structural diagrams of N- and O-linked carbohydrates and related compounds. *Proteomics* 2009, *9*, 3796-3801.

[129] Wollscheid, B., Bausch-Fluck, D., Henderson, C., O'Brien, R.*, et al.*, Mass-spectrometric identification and relative quantification of N-linked cell surface glycoproteins. *Nat Biotechnol* 2009, *27*, 378-386.

Appendix. Pig glycome database source code

1. Processing of logic algorism source code

```
class User < ActiveRecord::Base
   has_secure_password

   attr_accessible :login_id, :password, :password_confirmation

   validates_uniqueness_of :login_id
end


class Molecule < ActiveRecord::Base

attr_accessible :image,:ESImpz, :MALDImpzNa, :MALDImpzGT, :derivatiz
ation,
     :glycan, :m_type, :quantity, :organ, :origin
  mount_uploader :image, ImageUploader

  def Mass()
    if self.MALDImpzGT != 0
      return self.MALDImpzGT
    elsif self.MALDImpzNa != 0
      return self.MALDImpzNa
    elsif self.ESImpzNa != 0
      return self.ESImpzNa
    elsif self.ESImpzPO != 0
      return self.ESImpzPO
    end
    return 0
  end

  def maldi_image
    path = 'structure/'
    path << self.Mass.to_s << '.png'
```

```
  end

  def maldi_image_path
    rails_path = "/xdb/assets/"
    rails_path << maldi_image
  end

  def self.search(param)
      search = {}
      result = []
      if param[:search]
         p 'Molecule\'s Search'
         p param
         if param[:Mass]
            maldi  =  (param[:Mass_select]  ==  'MALDI-TOF  MS')  &&
(param[:ion_mode_tag] == 'MPNAP')
            esi_PO       =   (param[:Mass_select]   ==   'ESI-MS')   &&
(param[:ion_mode_tag] == 'H2PO4')
            esi_Na    =    (param[:Mass_select]    ==    'ESI-MS')    &&
(param[:ion_mode_tag] == 'MPNAP')


            gt = (param[:Mass_select] == 'MALDI-TOF MS') &&
              (param[:ion_mode_tag] == 'MPGTP')

            unless maldi or esi_PO or esi_Na or gt
               return result, nil
            end

            mass_sel = :MALDImpzNa if maldi
            mass_sel = :ESImpzPO if esi_PO
            mass_sel = :ESImpzNa if esi_Na
            mass_sel = :MALDImpzGT if gt
            search[     mass_sel     ]     =     (param[:Mass].to_f-
param[:tolerance].to_f)..
               (param[:Mass].to_f+param[:tolerance].to_f)
```

```
        end
        search[:origin] = param[:origin] if param[:origin]
        search[:derivatization]    =    param[:derivatization]    if
param[:derivatization]
        search[:glycan] = param[:glycan] if param[:glycan]
        search[:organ] = param[:organ] if param[:organ]

        p 'Molecule\'s Search'
        p search
        if search.empty? then return result end
        result = Molecule.where(search)
     else
        result = find(:all)
     end
     return result, mass_sel
  end

  def self.old_search(param)
    if param[:search]
     result = []
#     if param[:Mass_select].to_sym == :MALDImpzNa
     if( param[:Mass_select] == 'MALDI-TOF MS')
        unless ( param[:ion_mode_tag] == 'MPNAP')
           return result;
        end
        mass_sel = :MALDImpzNa
     elsif (param[:Mass_select] == 'ESI-MS')
        unless ( param[:ion_mode_tag] == 'H2PO4')
           return result;
        end
        mass_sel = :ESImpz
     end
     result = Molecule.where(mass_sel=>
                          (param[:Mass].to_f-param[:tolerance].to_f)..

(param[:Mass].to_f+param[:tolerance].to_f),
```

```
                        :origin => param[:origin],
                        :derivatization => param[:derivatization],
                        :glycan => param[:glycan])
#     if param[:Mass_select] == 'MALDI-TOF MS'
#       result = Molecule.where(:MALDImpz =>
#         (param[:Mass].to_f-param[:tolerance].to_f)..
#         (param[:Mass].to_f+param[:tolerance].to_f))
#
##     elsif param[:Mass_select].to_sym == :ESImpz
#     elsif param[:Mass_select]== 'ESI-MS'
#       result =
#         Molecule.where(:ESImpz =>
#         (param[:Mass].to_f-param[:tolerance].to_f)..
#         (param[:Mass].to_f+param[:tolerance].to_f))
#
#     end
       result
   else
     find(:all)
   end
  end

  def self.checkTolerance(data, _input, _tolerance)
    input = BigDecimal.new(_input)
    tolerance = BigDecimal.new(_tolerance)

    if( -tolerance <= input - data && input - data <= tolerance)
      return true
    else
      return false
    end

  end
end
```

```
class Static::ExperimentalProtocolsController < ApplicationController

  def document_id
    :experimental_protocols
  end

  def kidney_n
  end

  def endo_islet_n
  end

  def endo_islet_g
  end

  def corneal_kerato_n
  end

  def kidney_endo_o
  end

  def heart_n
  end
end


class ApplicationController < ActionController::Base
  protect_from_forgery

  before_filter do |controller|
    @current_document = nil
    @current_document = controller.send(:document_id) if controller.respond_to?(:document_id)
    @is_db_page = controller.respond_to?(:document_id)
  end
```

```
  def db_page?
    return @is_db_page
  end

  private
  def current_user
     @current_user      ||=      User.find(session[:user_id])      if
session[:user_id]
  end

  def current_document
    @current_document ||= nil
  end
  def current_document=(cu)
    @current_document = cu
  end
  helper_method :current_user, :current_document, :db_page?
end


class FlashImagesController < ApplicationController
  def document_id
    :glyco_profile
  end
  def index
  end
  def search
  end
end


class MoleculesController < ApplicationController

  def document_id
    :glyco_base
```

```
  end

  def search

    if params[:search]

            @molecules, @mass_sel = Molecule.search(params)
    else
            @molecules = Molecule.all
    end
    #redirect_to :action => :index
#    render :index
    respond_to do |format|
      format.html
      format.json {render json: @molecules }
    end
  end

  # GET /molecules
  # GET /molecules.json
  def index
    #@molecules = Molecule.all

    if params[:search]

            @molecules = Molecule.search(params)
    else
            @molecules = Molecule.all
    end
    #@molecules = Molecule.search(params)

    respond_to do |format|
      format.html # index.html.erb
      format.json { render json: @molecules }
    end
  end
```

```
# GET /molecules/1
# GET /molecules/1.json
def show
  @molecule = Molecule.find(params[:id])

  respond_to do |format|
    format.html # show.html.erb
    format.json { render json: @molecule }
  end
end

# GET /molecules/new
# GET /molecules/new.json
def new
  unless current_user
      redirect_to root_url
      return
  end
  @molecule = Molecule.new

  respond_to do |format|
    format.html # new.html.erb
    format.json { render json: @molecule }
  end
end

# GET /molecules/1/edit
def edit
  unless current_user
      redirect_to root_url
      return
  end
  @molecule = Molecule.find(params[:id])
end
```

```
  # POST /molecules
  # POST /molecules.json
  def create
    unless current_user
        redirect_to root_url
        return
    end
    @molecule = Molecule.new(params[:molecule])
    p params[:molecule]
    p @molecule

    respond_to do |format|
      if @molecule.save
        format.html { redirect_to @molecule, notice: 'Molecule was
successfully created.' }
        format.json { render json: @molecule, status: :created,
location: @molecule }
      else
        format.html { render action: "new" }
        format.json { render json: @molecule.errors,
status: :unprocessable_entity }
      end
    end
  end

  # PUT /molecules/1
  # PUT /molecules/1.json
  def update
    unless current_user
        redirect_to root_url
        return
    end
    @molecule = Molecule.find(params[:id])

    respond_to do |format|
      if @molecule.update_attributes(params[:molecule])
```

```
      format.html { redirect_to @molecule, notice: 'Molecule was
successfully updated.' }
      format.json { head :ok }
    else
      format.html { render action: "edit" }
      format.json { render json: @molecule.errors,
status: :unprocessable_entity }
    end
  end
 end

 # DELETE /molecules/1
 # DELETE /molecules/1.json
 def destroy
  unless current_user
      redirect_to root_url
      return
  end
  @molecule = Molecule.find(params[:id])
  @molecule.destroy

  respond_to do |format|
    format.html { redirect_to molecules_url }
    format.json { head :ok }
  end
 end
end


class SessionsController < ApplicationController
 def new
 end

 def create
    user = User.find_by_login_id(params[:email])
    if user && user.authenticate(params[:password])
```

```
        session[:user_id] = user.id
        redirect_to root_url, notice: "Logged in!"
    else
        flash.now.alert = "Email or password is invalid"
         render action: "new"
    end
  end

  def destroy
    session[:user_id] = nil
    redirect_to root_url, notice: "logged out!"
  end

end


class StaticPagesController < ApplicationController
  def index
  end
  def about
  end
end


class UsersController < ApplicationController


end


class MetaDataController < ApplicationController
  def document_id
    :meta_data
  end

  def meta_data
```

```
  end

  def default
    @doc_name = params[:doc_name]
  end

#  def kidneyN
#  end
#
#  def endoNisletN
#  end
#
#  def endoGisletG
#  end
#
#  def corNkeraN
#  end
#
#  def kidneyOendoO
#  end
#
#  def heartN
#  end
end


module Static::ExperimentalProtocolsHelper
end


module ApplicationHelper
end


module FlashImagesHelper
end
```

```
module MetaDataHelper
end


module MoleculesHelper
    def custom_humanize( string )
      string[0] = string[0].capitalize
      return string
    end
    def zero_to_empty( int )
        if int == 0.0
            return ''
        else
            return int
        end
    end
end


module SessionsHelper
end


module UsersHelper
end


# encoding: utf-8

class ImageUploader < CarrierWave::Uploader::Base

  # Include RMagick or MiniMagick support:
   include CarrierWave::RMagick
  # include CarrierWave::MiniMagick
```

```
  # Choose what kind of storage to use for this uploader:
  storage :file
  # storage :fog

  # Override the directory where uploaded files will be stored.
  # This is a sensible default for uploaders that are meant to be
mounted:
  def store_dir

"uploads/#{model.class.to_s.underscore}/#{mounted_as}/#{model.id}"
  end

  # Provide a default URL as a default if there hasn't been a file
uploaded:
  # def default_url
  #                   "/images/fallback/"      +      [version_name,
"default.png"].compact.join('_')
  # end

  # Process files as they are uploaded:
  # process :scale => [200, 300]
  #
  # def scale(width, height)
  #   # do something
  # end

  # Create different versions of your uploaded files:
   version :thumb do
     #process :scale => [50, 50]
     process :resize_to_limit => [50,50]
   end

  # Add a white list of extensions which are allowed to be uploaded.
  # For images you might use something like this:
  # def extension_white_list
```

```
  #   %w(jpg jpeg gif png)
  # end

  # Override the filename of the uploaded files:
  # Avoid using model.id or version_name here, see uploader/store.rb
for details.
  # def filename
  #   "something.jpg" if original_filename
  # end

end
```

2. Construction of web page

```
<%= form_for @molecule, :html => {:multipart => true} do |f| %>
  <% if @molecule.errors.any? %>
    <div id="error_explanation">
      <h2><%=    pluralize(@molecule.errors.count,    "error")    %>
prohibited this molecule from being saved:</h2>

      <ul>
      <% @molecule.errors.full_messages.each do |msg| %>
        <li><%= msg %></li>
      <% end %>
      </ul>
    </div>
  <% end %>

  <div class="field">
    <%= f.label :MALDImpz %><br />
    <%= f.text_field :MALDImpz %>
  </div>
  <div class="field">
    <%= f.label :ESImpz %><br />
    <%= f.text_field :ESImpz %>
  </div>
  <div class="field">
    <%= f.label :derivatization %><br />
        <%=
f.select(:derivatization,options_for_select(%w(underivatised
permethylated
        peracetylate),@molecule.derivatization))%>
    <%#= f.check_box :derivatization %>
  </div>
  <div class="field">
    <%= f.label :glycan %><br />
        <%= f.select(:glycan, options_for_select(
```

```
      %w(N-glycan    O-glycan    glycan\    from\    glycolipid),
@molecule.glycan))%>
  </div>
  <div class="field">
    <%= f.label :type %><br />
    <%= f.text_field :m_type %>
  </div>
  <div class="field">
    <%= f.label :quantity %><br />
    <%= f.text_field :quantity %>
  </div>
  <div class="field">
        <%= f.label :origin%><br />
        <%= f.select(:origin, options_for_select(
        %w(human    pig    other\    mammalia    plant    fungi),
@molecule.origin))%>
  </div>
  <div class="field">
    <%= f.label :organ %><br />
        <%= f.text_field :organ %>
  </div>
  <div class="field">
      <%= f.file_field :image %>
  </div>
  <div class="actions">
    <%= f.submit %>
  </div>
<% end %>


<!-- <h2 class='alt'> -->
<!--h3>
Pig Glycan Database is a tool that can receive pig glycan
information (glycan type, predicted structure, and so on) from their
experimentally determined masses. The program can be used for free
or derivatized glycans.
```

```
</h3-->
<hr />


<% if current_user %>
       <%= button_to 'New Molecule', new_molecule_path%>
<%end%>


h1>Editing molecule</h1>

<%= render 'form' %>

<%= link_to 'Show', @molecule %> |
<%= link_to 'Back', molecules_path %>


<div class="container db">

<div class="span22 prepend-1">
       <%= render "glycan_header"%>
</div>


<div class="span22 prepend-1" style="font-size:120%">
       <%= render "search_form"%>
       <br class="space"/>
       <br class="space"/>
       <br class="space"/>
</div>

<div class="span22 prepend-1">
       <%= render 'new_molecule'%>
       <br class="space"/>
       <br class="space"/>
       <br class="space"/>
```

```
</div>

</div>


<h1>New molecule</h1>

<%= render 'form' %>

<%= link_to 'Back', molecules_path %>


<div class="container">



        <div class="span-22 prepend-1 append-1">
              <a name='search-result'></a>
                <h3>Search Result</h3>
        </div>

        <div class="span-24">
                <div class="border">
                <%= render "search_result"%>
                </div>
                <br class="space"/><br class="space"/>
        </div>



        <div class="span-22 prepend-1 append-1">
                <h3>Search</h3>
                <%= render "search_form" %>
                <br class="space">    <br class="space">
        </div>
```

```
        <div class="span-22 prepend-1 append-1">
               <br class="space">    <br class="space">
               <%= render "new_molecule"%>
        </div>

        <div class="span-22">
        <br class="space"/>   <br class="space"/>   <br
class="space"/>
        </div>
</div>


<% content_for :stylesheets do %>
    img.structure {
        width: 132px;
        height: 60px;
        max-width: none;
    }
<% end %>


<p id="notice"><%= notice %></p>

<p>
  <b>Maldimpz:</b>
  <%= @molecule.MALDImpz %>
</p>

<p>
  <b>Esimpz:</b>
  <%= @molecule.ESImpz %>
</p>

<p>
```

```
  <b>Derivatization:</b>
  <%= @molecule.derivatization %>
</p>

<p>
  <b>Glycan:</b>
  <%= @molecule.glycan %>
</p>

<p>
  <b>Type:</b>
  <%= @molecule.m_type %>
</p>

<p>
  <b>Quantity:</b>
  <%= @molecule.quantity %>
</p>

<p>
  <b>Organ:</b>
  <%= @molecule.organ %>
</p>

<p>
  <b>Origin:</b>
  <%= @molecule.origin %>
</p>

<p>
    <%= image_tag @molecule.image_url if @molecule.image? %>
</p>

<%= link_to 'Edit', edit_molecule_path(@molecule) %> |
<%= link_to 'Back', molecules_path %>
```

```
<div id='mother_image'>

  <%= image_tag 'pig.jpg', :id => 'pig' %>
  <div id='kidney'     class='clickable' > </div>
  <div id='liver'      class='clickable' > </div>
  <div id='islet'      class='clickable' > </div>
  <div id='heart'      class='clickable' > </div>
  <div id='eye'        class='clickable' > </div>
  <div id='endothelial' class='clickable' > </div>

</div>


<div id="eye_dialog" title="choose one">
  <button id='b_corneal'>corneal endothelial cell</button>
  </br> </br>
  <button id='b_kerato'>keratocyte</button>
</div>
<div id="heart_dialog" title="choose one">
  <button id='b_aortic_valve'>aortic valve</button>
  </br> </br>
  <button id='b_pulmunary_valve'>pulmonary valve</button>
  </br> </br>
  <button id='b_aortic_wall'>aortic wall</button>
  </br> </br>
  <button id='b_pulmunary_wall'>pulmonary wall</button>
  </br> </br>
  <button id='b_muscle'>muscle</button>
  </br> </br>
  <button id='b_pericardium'>pericardium</button>
</div>


<select name="effects" id="effectTypes">
  <option value="blind">Blind</option>
```

```
  <option value="bounce">Bounce</option>
  <option value="clip">Clip</option>
  <option value="drop">Drop</option>
  <option value="explode">Explode</option>
  <option value="fold">Fold</option>
  <option value="highlight">Highlight</option>
  <option value="puff">Puff</option>
  <option value="pulsate">Pulsate</option>
  <option value="scale">Scale</option>
  <option value="shake">Shake</option>
  <option value="size">Size</option>
  <option value="slide">Slide</option>
</select>

<!--  a  href="#"  id="button"  class="ui-state-default  ui-corner-
all">Run Effect</a-->


<div class="span-22 prepend-1" >
        <br /><br /><br />

  <%= image_tag 'graph/kidney_n.jpg',
    :class => 'g_hidden graph g_kidney'%>

  <%= image_tag 'graph/corneal_endothelial_cell_n.jpg',
    :class => 'g_hidden graph g_corneal' %>

  <%= image_tag 'graph/keratocyte_n.jpg',
    :class => 'g_hidden graph g_keratocyte' %>

  <%= image_tag 'graph/pancreatic_islet_cell_n.jpg',
    :class => 'g_hidden graph g_islet' %>
  <%= image_tag 'graph/pancreatic_islet_cell_glycolipid.jpg',
    :class => 'g_hidden graph g_islet' %>

  <%= image_tag 'graph/heart_pericandium_n.jpg',
```

```
    :class => 'g_hidden graph g_pericardium' %>

  <%= image_tag 'graph/heart_pulmunary_valve_n.jpg',
    :class => 'g_hidden graph g_pul_valve' %>

  <%= image_tag 'graph/heart_pulmunary_wall_n.jpg',
    :class => 'g_hidden graph g_pul_wall' %>

  <%= image_tag 'graph/heart_muscle_n.jpg',
    :class => 'g_hidden graph g_muscle' %>

  <%= image_tag 'graph/heart_aortic_valve_n.jpg',
    :class => 'g_hidden graph g_aortic_valve' %>

  <%= image_tag 'graph/heart_aortic_wall_n.jpg',
    :class => 'g_hidden graph g_aortic_wall' %>

  <%= image_tag 'graph/endothelial_cell_n.jpg',
    :class => 'g_hidden graph g_endothelial'%>
  <%= image_tag 'graph/endothelial_cell_glycolipid.jpg',
    :class => 'g_hidden graph g_endothelial'%>
        <br /><br /><br />

</div>


<div class='span-22'>
  <p>
    <h5>
      1. Key to structural symbols in this and other figures: ■
GlcNAc, ○ mannose, ◊ galactose, ◈ fucose. The angles of the lines
joining the symbols denote linkage: | 1-2, ⟋ 1-3, — 1-4, and
\  1-6. Full line beta-linkage, broken lines alpha-linkage.
      <br />
      2. Some of these glycans have isomeric structures or different
structures. Additional information can be found in our previous
```

```
reports.
     <br />
     3. The ions of GT-derivatized glycans are [M+GT]+ in MALDI-TOF
MS.
     <br />
     4. The ions (< m/z 1727.0) of sialic acids are doublet charged
([M-2H]2-) in ESI-MS within our dataset.
     <br />
   </h5>
  </p>
</div>


<div class="container db">

  <div class="span-10 prepend-6">
    <div class="field" style="font-size: 120%">
      <%= label_tag :species %>
      <%= select_tag("species", options_for_select(
        [%w(Pig pig)], params[:species]))%>

      </br>
      <%= label_tag :glycan_type%>
      <%= select_tag("glycan", options_for_select(
        [%w(N-linked\ glycan N-glycan),
        %w(O-linked\ glycan O-glycan),
        %w(Glycolipid-derived\ glycan glycolipid-derived\ glycan)],
        params[:glycan_type]))%>

      </br>
      <%= label_tag :cell_type%>
      <%= select_tag("cell type", grouped_options_for_select(
        {
          'Tissue' => [%w(Kidney kidney),
                       %w(Heart heart),
                       %w(-aortic\ valve aortic\ valve),
```

```
                    %w(-pulmonary\ valve pulmonary\ valve),
                    %w(-pulmonary\ wall pulmonary\ wall),
                    %w(-aortic\ wall aortic\ wall),
                    %w(-muscle muscle),
                    %w(-pericardium pericardium),
                  ],
        'Cell'   => [
                     %w(Endothelial\ cell endothelial\ cell),
                     %w(Pancreatic\            islet\            cell
pancreatic\ islet\ cell),
                     %w(Keratocytes keratocyte),
                     %w(Corneal\ endothelial\ cell
                        corneal\ endothelial\ cell),
                   ]
      }
    ))%>

  </br>
    <%= label_tag :glycan_epitope %>
    <%= select_tag("glycan epitope", options_for_select(
          [%w(all),
          %w(alpha-Gal antigen),
          %w(sialylation),
          %w(-N-acetylneuraminic\ acid-terminated),
          %w(-Hanganutziu-Deicher\ antigen),
          %w(high-mannose),
          %w(fucosylation),
          %w(-core\ fucosylation),
          %w(-outer-arm\ fucosylation)]
    )) %>
  </br>
  <%=button_tag(:type => 'button', :id => 'search_button') do %>
    <% 'submit' %>
  <% end %>
  </br> </br>
  </div>
```

```
  </div>

  <div class="span-24 image_description">
    <p>
      <h5>Key to structural symbols in this and other figures: ★
NeuAc, ☆ NeuGc, ■ GlcNAc, ○ mannose, ◊ galactose, ◈ fucose. The
angles of the lines joining the
       symbols denote linkage: l 1-2, / 1-3, — 1-4, and \ 1-6.
      </h5>
    </p>
  </div>

  <div>
    <%= render "ajax_table"%>
  </div>

  <div class="demo span-22">

      <%#= render :partial => 'effect' %>

  </div><!-- End demo -->

  <%= render 'dialogs' %>

</div>

<div class="span-24 image_description">
  <p>
    <h5>
       1. Some of these glycans have isomeric structures or
different structures. Additional information can be found in our
previous reports.
    </h5>


    <h5>
```

```
      2. The ions of GT-derivatized glycans are [M+GT]+ + in MALDI-
TOF MS.
   </h5>


   <h5>
     3. The ions (< m/z 1727.0) of sialic acids are doublet charged
([M-2H]2-) in ESI-MS within our dataset.
   </h5>
  </p>
</div>

<div class="span-22 support_link ">
  <h5>
    Access to supporting experimental
    <ul>
      <li><a      href='http://www.ncbi.nlm.nih.gov/pubmed/18546155'>
Kidney N-glycan</a></li>
      <li><a      href='http://www.ncbi.nlm.nih.gov/pubmed/19373860'>
Endothelial and islet cell (N-glycan)</a></li>
      <li><a
href='http://www.ncbi.nlm.nih.gov/pubmed/19760646'>Endothelial   and
islet cell (glycolipid-derived glycan) </a></li>
      <li><a
href='http://www.ncbi.nlm.nih.gov/pubmed/19895316'>Corneal
endothelial cell and keratocytes (N-glycan)</a></li>
      <li><a
href='http://www.ncbi.nlm.nih.gov/pubmed/23399746'>Kidney        and
endothelial cell (O-glycan)</a></li>
      <li><a href='http://www.ncbi.nlm.nih.gov/pubmed/22808845'>Heart
(N-glycan) </a></li>
    </ul>
    <!--<a         href='http://www.ncbi.nlm.nih.gov/pubmed/18546155'
class='support_link   Kidney   N-glycan'>   Access   to   supporting
experimental data Kidney (N-glycan)<br /></a>-->
    <!--<a         href='http://www.ncbi.nlm.nih.gov/pubmed/19373860'
```

```
class='support_link endothelial islet N-glycan' >Access to supporting experimental data Endothelial and islet cell (N-glycan)<br /></a>-->
   <!--<a href='http://www.ncbi.nlm.nih.gov/pubmed/19760646' class='support_link endothelial islet' >Access to supporting experimental data Endothelial and islet cell (glycolipid-derived glycan)<br /></a>-->
   <!--<a href='http://www.ncbi.nlm.nih.gov/pubmed/19895316' class='support_link corneal keratocytes N-glycan' >Access to supporting experimental data Corneal endothelial cell and keratocytes (N-glycan)<br /></a>-->
   <!--<a href='http://www.ncbi.nlm.nih.gov/pubmed/23399746' class='support_link endothelial Kidney O-glycan' >Access to supporting experimental data Kidney and endothelial cell (O-glycan)<br /></a>-->
   <!--<a href='http://www.ncbi.nlm.nih.gov/pubmed/22808845' class='support_link heart N-glycan' >Access to supporting experimental data Heart (N-glycan)</a>-->
  </h5>
</div>

<%= render 'graphs' %>

<div class="span-22">

   <div class='span-22'>
      <%= render 'clickable_images' %>
   </div>

   <div class="span-22">
      <br class="space"/>
      <br class="space"/>
      <br class="space"/>
      <br class="space"/>
      <br class="space"/>
      <br class="space"/>
```

```
        <br class="space"/>
        <br class="space"/>
        <br class="space"/>
        <br class="space"/>
        <br class="space"/>
        <br class="space"/>
    </div>
</div>

<% content_for :stylesheets do %>
    .support_link {
        display:none;
    }
    .image_description {
        display: none;
    }
    .composition {
        width: 250px;
    }
    img.structure {
        width: 132px;
        height: 60px;
        max-width: none;
    }
    .graph {
        width: 60%;
        margin: 0 auto;
    }
        #mother_image {
                position:relative;
              margin-bottom:7px;
              width: 505px;
              height: 386px;
                margin: 0 auto;
        }
        #pig {
```

```
        position:absolute;
        top:0px;
width: 100%;
z-index:-1;
 }
 #kidney {
        position:absolute;
        top:0%;
        left:45%;
width: 20%;
height: 30%;
 }
 #liver {
        position:absolute;
        top:8%;
        left:76%;
width: 24%;
height: 29%;
 }
 #heart {
        position:absolute;
        top:69%;
        left:45%;
width: 21%;
height: 33%;
 }
 #islet {
        position:absolute;
        top:67%;
        left:5%;
width: 25%;
height: 28%;
 }
 #eye {
        position:absolute;
        top:6%;
```

```
                left:1%;
        width: 30%;
        height: 30%;
         }
    #endothelial {
    position:absolute;
    top:68%;
    left:76%;
    width: 24%;
    height: 29%;
    }

    .alpha_antigen {
           color: #FF2020;
    }

    .neu_antigen {
           color: #2020F0;
    }

        #draggable { width: 150px; height: 150px; padding: 0.5em;
color: #ccc;}
        #feedback { font-size: 1.4em; }
        #selectable .ui-selecting { background: #FECA40; }
        #selectable  .ui-selected  {  background:  #F39814;  color:
white; }
        #selectable { list-style-type: none; margin: 0; padding: 0;
width: 60%; }
        #selectable  li  {  margin:  3px;  padding:  0.4em;  font-size:
1.4em; height: 18px; }

  <!-- #top_menu {display: none}
  #right_menu {float: right; background-color: yellow; color: black}
-->
<% end %>
```

```
<div class="container">
<h1>Log In</h1>


<div class="span-22">
<%= form_tag sessions_path do %>
    <div class="field">
        <%= label_tag :login_id %><br />
        <%= text_field_tag :email, params[:email] %>
    </div>
    <div class="field">
        <%= label_tag :password %><br />
        <%= password_field_tag :password %>
    </div>

    <div class="actions"><%= submit_tag "Log In" %>
<% end %>

</div>
</div>
```

국문 초록

본 연구에서는, 인간으로 이종장기이식의 유망한 기증동물로 여겨지고 있는 α-Gal 당질항원의 합성효소 유전자를 제거한 돼지 (α1,3-galactosyltransferase gene-knockout, GalT-KO) 의 세포와 조직을 대상으로 면역거부반응과 관련된 당에 대한 질량 분석기 기반의 정성 및 정량적 분석 연구를 수행하였다.

첫째, 야생주 돼지와 GalT-KO 돼지 세포 표면에 발현된 N-글라이칸들의 구조와 양을 비교하였다. 고체 상태 완전메틸화 방법을 결합한 매트릭스 보조 레이저 탈착 이온화 (MALDI) 질량 분석 기법을 이용하여 야생주 돼지와 GalT-KO 돼지의 섬유아세포 표면의 N-글라이칸의 구조 및 정량적 차이를 규명할 수 있었다. 이 결과를 통해 α-Gal 당질항원의 합성효소 유전자 제거는 돼지 세포 표면의 α-Gal 당질항원의 제거뿐만 아니라, 돼지 다른 당질항원을 포함한 전체적인 당의 발현 정도에 영향을 준다는 것을 확인할 수 있었다.

둘째, GalT-KO 돼지에서 실제 인간으로 이종이식의 직접적 대상이 되는 간 조직으로부터 N-글라이칸들의 구조 및 정량 분석을 통해 야생주 돼지의 간 표면의 N-글라이칸들과 비교하였다. MALDI 질량 분석기와 전기분사 이온화 (ESI) 질량 분석기의 상호보완적 분석기법을 이용하여 GalT-KO 돼지 표면의 당들에서 α-Gal 당질항원이 제거된 것을 확인하였고, 면역거부반응을 일으키는 non-Gal 당질항원으로 알려진 N-

글라이코릴뉴라미닉산이 존재하는 것을 확인하였다. 말단당 가수분해효소를 이용한 시퀀싱과 ESI 질량 분석기를 이용한 텐덤 질량분석 기법을 통해 이들 GalT-KO 돼지 간 조직 표면에 발현된 모든 N-글라이칸들의 구조를 규명하였다. 특히, MALDI-quadropole 이온 트랩 질량 분석기법을 통해 N-글라이코릴뉴라미닉산들의 구조를 새롭게 규명할 수 있었다. 그리고 당의 구조적 분석과 더불어 고체 상태 완전메틸화를 결합한 MALDI 및 ESI 질량 분석기법을 통해 GalT-KO 돼지 N-글라이칸들의 정량 분석을 함으로써 야생주 돼지와의 N-글라이코릴뉴라미닉산을 포함한 모든 N-글라이칸의 정량적 차이를 밝혀내었다. 이 결과는 GalT-KO 이후의 이종장기이식 면역거부반응 제어를 위한 연구에 중요한 정보를 제시할 수 있다.

더 나아가 돼지의 다양한 부위의 세포 및 조직들에 존재하는 당을 데이터화한 데이터베이스 프로그램을 개발하였다. 질량 분석 기반의 분석을 통해 얻은 당의 구조 및 정량적 정보를 바탕으로, 돼지 세포 및 조직별 또는 질량 정보 중심의 검색을 통해 이용자들이 원하는 돼지 당의 정보를 찾을 수 있도록 하였다. 그리고 전체적인 프로그램의 틀은 이용자 친화적인 웹 기반의 인터페이스로 설계하였다. 그리고 돼지 조직 표면에 발현된 당과 인간 면역세포들과의 상호작용을 탐색하기 위해서 돼지 N-글라이칸에 대한 인간 면역세포의 활성화 측정 및 N-글라이칸들과 결합하는 인간 수지상 면역세포 표면단백질을 규명하고자 하였다.

본 연구를 통해 분석한 GalT-KO 돼지의 세포와 조직 표면에 발현된 당의 구조 및 정량적 정보는 이종장기이식 분야에서 이종당질항원에 대한 면역거부반응을 제어하기 위한 중요한 연구 자료가 될 수 있을 것으로 기대한다.

주요어: 이종장기이식, 면역거부반응, GalT-KO 돼지, 질량분석기법, 당, 돼지 당 데이터베이스

학번: 2007-21191